



York, C.B. (2017) On bending-twisting coupled laminates. *Composite Structures*, 160, pp. 887-900. (doi:[10.1016/j.compstruct.2016.10.063](https://doi.org/10.1016/j.compstruct.2016.10.063))

This is the author's final accepted version.

There may be differences between this version and the published version. You are advised to consult the publisher's version if you wish to cite from it.

<http://eprints.gla.ac.uk/130308/>

Deposited on: 18 October 2016

Enlighten – Research publications by members of the University of Glasgow
<http://eprints.gla.ac.uk>

On Bending-Twisting Coupled Laminates

C B York*

*Aerospace Sciences, School of Engineering, University of Glasgow, University Avenue,
G12 8QQ, Glasgow, Scotland.*

Abstract

The definitive list of stacking sequences is presented for *Bending-Twisting* coupled ($\mathbf{A}_s\mathbf{B}_0\mathbf{D}_F$) laminates, with up to 21 plies. This class of laminate arises from the ubiquitous balanced and symmetric design rule, but symmetry is shown to be a sufficient rather than a necessary constraint. Each stacking sequence configuration is derived in symbolic form together with dimensionless parameters from which the extensional and bending stiffness terms are readily calculated for any fibre/matrix system and angle-ply orientation. Expressions for ply orientation dependent lamination parameters are also given, together with graphical representations, which demonstrate the extent of the design space. Pseudo Quasi-Homogeneous ($\mathbf{A}_s\mathbf{B}_0\mathbf{D}_F$) laminates are introduced as an important laminate sub-set, **since** such laminates have concomitant orthotropic properties, i.e. matching orthotropic or isotropic stiffnesses in extension and bending, from which the isolated effects of *Bending-Twisting coupling* can be studied. These **coupling** effects are quantified for **compression** buckling of Angle-ply and Quasi-Isotropic laminated plates with simply supported and clamped edges.

* Corresponding author:

Tel: +44 (0)141 3304345, E-mail address: Christopher.York@Glasgow.ac.uk

Keywords

Bending-Twisting coupling; Buckling; Non-dimensional Stiffness Parameters; Lamination Parameters; Laminate Stacking Sequences.

Nomenclature

\mathbf{A}, A_{ij}	= extensional stiffness matrix and its elements ($i, j = 1, 2, 6$)
\mathbf{B}, B_{ij}	= coupling stiffness matrix and its elements ($i, j = 1, 2, 6$)
\mathbf{D}, D_{ij}	= bending stiffness matrix and its elements ($i, j = 1, 2, 6$)
$E_{1,2}, G_{12}$	= in-plane Young's moduli and shear modulus
H	= laminate thickness (= number of plies, $n \times$ ply thickness, t)
k_x	= non-dimensional buckling load factor in compression
\mathbf{M}	= vector of moment resultants ($= \{M_x, M_y, M_{xy}\}^T$)
\mathbf{N}	= vector of force resultants ($= \{N_x, N_y, N_{xy}\}^T$)
n	= number of plies in laminate stacking sequence
Q_{ij}	= reduced stiffness ($i, j = 1, 2, 6$)
Q'_{ij}	= transformed reduced stiffness ($i, j = 1, 2, 6$)
t	= ply thickness
U_i	= laminate invariant ($i = 1, 2, 3, 4, 5$)
x, y, z	= principal axes
z_k	= layer k interface distance from laminate mid-plane
$\boldsymbol{\varepsilon}$	= vector of in-plane strains ($= \{\varepsilon_x, \varepsilon_y, \gamma_{xy}\}^T$)
$\boldsymbol{\kappa}$	= vector of curvatures ($= \{\kappa_x, \kappa_y, \kappa_{xy}\}^T$)
λ	= buckling half-wave

ν_{ij}	= Poisson ratio ($i, j = 1, 2$)
θ_k	= ply orientation for layer k
ξ_{1-2}	= lamination parameters for extensional stiffness
ξ_{9-12}	= lamination parameters for bending stiffness
ζ	= bending stiffness parameter for laminate ($= n^3$)
ζ_{\pm}	= bending stiffness parameter for angle-ply sub-sequence
ζ_+, ζ_-	= bending stiffness parameter for positive/negative angle-ply sub-sequence
ζ_o, ζ_{\bullet}	= bending stiffness parameter for cross-ply sub-sequences
$+, -, \pm$	= angle plies, used in stacking sequence definition
o, \bullet	= cross-ply, used in stacking sequence definition

Matrix sub-scripts

0	= All elements zero
F	= All elements <u>F</u> inite
I	= <u>I</u> otropic form
S	= <u>S</u> pecially orthotropic or <u>S</u> imple form

1. Introduction

This article is one in a series, investigating unique forms of thermo-mechanically coupling behaviour. These are described collectively in an original article [1],

identifying all 24 possible coupling interactions between *Extension*, *Shearing*, *Bending* and *Twisting*.

Here, attention is focussed on the identification of laminated composite materials possessing isolated mechanical *Bending-Twisting* coupling, i.e., with no other coupling present. It complements a previous article on isolated mechanical *Extension-Shearing* coupling [2].

Stacking sequence listings are derived for *Bending-Twisting* coupled laminates with up to 21 plies; or 42 plies if the data is interpreted as the symmetric half of the laminate stacking sequence definition.

Symmetric stacking sequences are ubiquitous in composite laminate design practice, for the simple reason that their use guarantees the laminate will remain flat, or warp free, after high temperature curing. Non-symmetric laminates are commonly associated with, or often (incorrectly) used to describe [4], configurations that warp extensively after high temperature curing. However, non-symmetric stacking sequence configurations will be shown to provide the same thermo-mechanical properties as their symmetric counterpart, but are part of a much larger and generally unexplored design space. Balanced stacking sequences guarantee that *Extension-Shearing* coupling is eliminated by using matching pairs of angle-ply layers [5].

With very few exceptions, composite designs for aircraft construction are currently certified only for balanced and symmetric laminates [6], which may possess fully uncoupled stiffness properties [3] as well as *Bending-Twisting* coupling and therefore this common design rule is by no means the panacea for characterisation of mechanical behaviour.

In this article, laminate stacking sequence configurations are derived in symbolic form together with dimensionless parameters from which the extensional and bending stiffness terms are readily calculated; solutions are therefore independent of the fibre/matrix system and angle-ply orientation. Expressions relating the dimensionless parameters to the well-known ply orientation dependent lamination parameters are also given, together with graphical representations of feasible domains for a range of ply number groupings (n) including typical fuselage skin thicknesses, i.e., with between ($n \Rightarrow$) 12 and 16 plies.

Quasi-Isotropic laminates are presented as an important sub-set of *Bending-Twisting* coupled laminates. Pseudo Quasi-Homogeneous laminates are also introduced, since such laminates have concomitant orthotropic properties, i.e. matching orthotropic stiffness in extension and bending, from which the isolated effects of *Bending-Twisting* can be studied; especially where concomitant properties are isotropic in nature. Quasi-Homogeneous designs permit ply percentage and buckling strength contours to be mapped onto the same lamination parameter design space, and thus serve to demonstrate the effect on buckling strength of ignoring the presence of *Bending-Twisting* coupling; examples, including Pseudo Quasi-Homogeneous Quasi-Isotropic laminate designs, are given.

Bending-Twisting coupling is generally known to result in weaker compression buckling strength compared to the equivalent fully uncoupled laminate, i.e., with matching stiffness properties, although there is evidence that this continues to be ignored in design practice as well as in the recent literature [7], leading to potentially unsafe design predictions, despite the guidance provided in long standing articles [8] and the availability of approximate closed form solutions with a high degree of accuracy

[9]. Some new insights into the relative buckling strength with respect to lamination parameter design spaces are provided, by way of an introduction to an accompanying article [10], which explores in detail the effect of *Bending-Twisting* coupling on compression and shear buckling strength, and is applicable to the data presented here, as well as to data for *Extension-Shearing* and *Bending-Twisting* coupled laminates.

The remainder of this article is arranged as follows. Section 3 provides an overview of mechanical coupling behaviour before details of the derivation of definitive listings of *Bending-Twisting* coupled laminate configurations are presented, including non-dimensional and angle-ply dependent parameters and examples calculations. Section 4 provides information on the extent of the feasible design space for *Bending-Twisting* coupled laminates, with comparison to *Simple* laminates, including the dominant forms of sub-sequence symmetries. Lamination parameters are also introduced to allow the available design space to be visually interrogated. The use of ply percentage mapping, as an approach to design for bending stiffness, is also discussed in the context of Quasi-Homogenous and Pseudo Quasi-Homogeneous laminates. Section 5 describes the association between ply percentages and compression buckling strength, through a similar mapping procedure. Classical Garland curves are then presented in a form that permits an assessment of the bounds on the buckling strength of *Bending-Twisting* coupled laminates subject to compression load. Finally, a note on laminate selection is given in Section 6 before conclusions are drawn in Section 7.

2. Mechanical Coupling

Laminated composite materials are characterized in terms of their response to mechanical (and/or thermal) loading, which is associated with a description of the

coupling behaviour, unique to this type of material, i.e. coupling between in-plane (i.e. extension or membrane) and out-of-plane (i.e. bending or flexure) responses when $B_{ij} \neq 0$ in Eq. (1), coupling between in-plane shearing and extension when $A_{16} = A_{26} \neq 0$, and coupling between bending and twisting when $D_{16} = D_{26} \neq 0$.

$$\begin{Bmatrix} N_x \\ N_y \\ N_{xy} \end{Bmatrix} = \begin{bmatrix} A_{11} & A_{12} & A_{16} \\ & A_{22} & A_{26} \\ \text{Sym.} & & A_{66} \end{bmatrix} \begin{Bmatrix} \varepsilon_x \\ \varepsilon_y \\ \tau_{xy} \end{Bmatrix} + \begin{bmatrix} B_{11} & B_{12} & B_{16} \\ & B_{22} & B_{26} \\ \text{Sym.} & & B_{66} \end{bmatrix} \begin{Bmatrix} \kappa_x \\ \kappa_y \\ \kappa_{xy} \end{Bmatrix} \quad (1)$$

$$\begin{Bmatrix} M_x \\ M_y \\ M_{xy} \end{Bmatrix} = \begin{bmatrix} B_{11} & B_{12} & B_{16} \\ & B_{22} & B_{26} \\ \text{Sym.} & & B_{66} \end{bmatrix} \begin{Bmatrix} \varepsilon_x \\ \varepsilon_y \\ \tau_{xy} \end{Bmatrix} + \begin{bmatrix} D_{11} & D_{12} & D_{16} \\ & D_{22} & D_{26} \\ \text{Sym.} & & D_{66} \end{bmatrix} \begin{Bmatrix} \kappa_x \\ \kappa_y \\ \kappa_{xy} \end{Bmatrix}$$

Whilst Eq. (1) describes the well-known **ABD** relation from classical laminate plate theory, it is more often expressed using compact notation:

$$\begin{Bmatrix} \mathbf{N} \\ \mathbf{M} \end{Bmatrix} = \begin{bmatrix} \mathbf{A} & \mathbf{B} \\ \mathbf{B} & \mathbf{D} \end{bmatrix} \begin{Bmatrix} \boldsymbol{\varepsilon} \\ \boldsymbol{\kappa} \end{Bmatrix} \quad (2)$$

The coupling behaviour, which is dependent on the form of the elements in each of the extensional **[A]**, coupling **[B]** and bending **[D]** stiffness matrices, is now described by an extended subscript notation, defined previously by the Engineering Sciences Data Unit, or ESDU [5] and subsequently augmented for the purposes of this series of articles. Hence, laminates with coupling between bending and twisting, are referred to by the designation **A_SB₀D_F**, signifying that the elements of the extensional stiffness matrix **[A]** are simple or specially orthotropic in nature, i.e.:

$$\begin{bmatrix} A_{11} & A_{12} & 0 \\ & A_{22} & 0 \\ \text{Sym.} & & A_{66} \end{bmatrix} \quad (3)$$

the coupling matrix $[\mathbf{B}]$ is null, whilst all elements of the bending stiffness matrix $[\mathbf{D}]$ are finite, i.e.:

$$\begin{bmatrix} D_{11} & D_{12} & D_{16} \\ & D_{22} & D_{26} \\ \text{Sym.} & & D_{66} \end{bmatrix} \quad (4)$$

where the elements of the stiffness matrices are derived from the well know relationships:

$$A_{ij} = \sum Q'_{ij}(z_k - z_{k-1}) \quad (6)$$

$$B_{ij} = \sum Q'_{ij}(z_k^2 - z_{k-1}^2)/2 = 0$$

$$D_{ij} = \sum Q'_{ij}(z_k^3 - z_{k-1}^3)/3$$

Note that the term *fully uncoupled orthotropic* laminate is synonymous with *specialty orthotropic* or *Simple* laminate. Such laminates possess none of the coupling characteristics described above and are represented by the designation $\mathbf{A}_s\mathbf{B}_0\mathbf{D}_s$, since the elements of the bending stiffness matrix $[\mathbf{D}]$ are also *Simple* or specially orthotropic in nature, i.e.:

$$\begin{bmatrix} D_{11} & D_{12} & 0 \\ & D_{22} & 0 \\ \text{Sym.} & & D_{66} \end{bmatrix} \quad (7)$$

Extensionally Isotropic laminates, with the designation $\mathbf{A}_I\mathbf{B}_0\mathbf{D}_s$ and Fully Isotropic laminates, with the designation $\mathbf{A}_I\mathbf{B}_0\mathbf{D}_I$, represent sub-sets of *Simple* laminates and are useful for benchmarking purposes. In the former case, the extensional stiffness matrix with designation \mathbf{A}_s is replaced with \mathbf{A}_I to indicate extensional isotropy, given that:

$$A_{11} = A_{22} \quad (8)$$

$$A_{66} = (A_{11} - A_{12})/2 \quad (9)$$

In the latter case, the bending stiffness matrix with designation \mathbf{D}_S is replaced with \mathbf{D}_I to indicate bending isotropy, and hence full isotropy, given that, in addition to the Eqs (8) and (9):

$$D_{ij} = A_{ij}H^2/12 \quad (10)$$

where H is the laminate thickness.

Extensionally Isotropic laminates should be differentiated from the more common Quasi-Isotropic laminates, with designation $\mathbf{A}_I\mathbf{B}_0\mathbf{D}_F$, possessing *Bending-Twisting* coupling.

Quasi-Homogeneous laminates possess concomitant stiffness properties, i.e. matching stiffness in extension and bending, as described by Eq. (10) and are presented elsewhere for *Simple* laminates [1]. For laminates with *Bending-Twisting* coupling, only the orthotropic stiffness properties are concomitant, since $A_{16} = A_{26} = 0$, whereas $D_{16}, D_{26} \neq 0$. Hence such laminates are referred to as Pseudo Quasi-Homogeneous. This special laminate class is used to study the isolated effects of *Bending-Twisting* coupling; and highlight the problem associated with the use of ply percentages in design practice. Note that the term *Pseudo* is used here as an important caveat, since the properties described are present only when the structural and material axes are coincident.

This article presents therefore the definitive list of cross-ply and/or angle-ply stacking sequences for *Bending-Twisting* (or **B-T**) coupling, with the designation $\mathbf{A}_S\mathbf{B}_0\mathbf{D}_F$, together with the dimensionless stiffness parameters from which the elements of the extensional $[\mathbf{A}]$ and bending stiffness $[\mathbf{D}]$ matrices are readily calculated. These new

stacking sequences complement the definitive list of Fully Orthotropic (or *Simple*) laminates, with the designation $\mathbf{A}_S\mathbf{B}_0\mathbf{D}_S$, for up to 21 plies [3] and those with *Extension-Shearing* (or $E-S$) coupling, with the designation $\mathbf{A}_F\mathbf{B}_0\mathbf{D}_S$, also for up to 21 plies [2]. The related mechanical coupling designations in this series are summarized in Table 1.

3. Derivation of stacking sequences

In the derivation of the stacking sequences that follow, the general rule of symmetry is relaxed. For compatibility with the previously published data [11], similar symbols have been adopted for defining all stacking sequences that follow. However, additional symbols and parameters are necessarily included to differentiate between cross plies (0° and 90°), given that symmetry about the laminate mid-plane is no longer assumed.

The resulting sequences are characterized by sub-sequence symmetry using a double prefix notation, the first character of which relates to the form of the angle-ply sub-sequence and the second character to the cross-ply sub-sequence. The double prefix contains combinations of the following characters: *A* to indicate Anti-symmetric form; *N* for Non-symmetric; and *S* for Symmetric. Additionally, for cross-ply sub-sequences only, *C* is used to indicate Cross-symmetric form.

To avoid the trivial solution of a stacking sequence with cross plies only, all sequences have an angle-ply (+) on one outer surface of the laminate. As a result, the other surface ply may have an angle-ply of equal (+) or opposite (−) orientation or a cross ply (○ or ●), which may be either 0 or 90° .

Non-dimensional parameters are derived with each stacking sequence, which provide a compact data set allowing the extensional and bending stiffness properties to be readily calculated for any fibre/matrix system and angle-ply orientation.

3.1 Development of non-dimensional parameters

The development of non-dimensional parameters is demonstrated, by way of an example for a 16-ply symmetric laminate stacking sequence $[+/\circ/\bullet/+/ \bullet/-_2/\circ]_s$, in Table 2. The first two columns of Table 2 provide the ply number and orientation, respectively, whilst subsequent columns illustrate the summations, for each ply orientation, of $(z_k - z_{k-1})$, $(z_k^2 - z_{k-1}^2)$ and $(z_k^3 - z_{k-1}^3)$, relating to the **A**, **B** and **D** matrices, respectively. Here, the distance from the laminate mid-plane, z , is expressed in terms of ply thickness t ; assumed to be unit value.

The non-dimensional parameters arising from the tabular summations are as follows.

For the extension stiffness matrix **[A]**: the number of ($0^\circ = 90^\circ$) cross plies

$$n_\circ = n_\bullet, (= {}_A\Sigma_\circ) = 4,$$

the number of negative angle plies

$$n_-, (= {}_A\Sigma_-) = 4,$$

the number of positive angle plies

$$n_+, (= {}_A\Sigma_+) = 4.$$

Due to the balanced nature of this class of laminate, angle ply results may be conveniently combined to a single parameter

$$n_\pm = n_+ + n_-.$$

The coupling stiffness matrix **[B]** summations confirm that $B_{ij} = 0$ for this laminate.

For the bending stiffness matrix **[D]**: the bending stiffness parameter for (0° and 90°) cross plies

$$\zeta_{\circ} = \zeta_{\bullet} (= 4 \times {}_D\Sigma_{\circ} = 4 \times 256 = {}_D\Sigma_{\bullet} = 4 \times 256) = 1024,$$

the bending stiffness parameter for negative angle plies

$$\zeta_{-} (= 4 \times {}_D\Sigma_{-} = 4 \times 52) = 208,$$

and the bending stiffness parameter for positive angle plies

$$\zeta_{+} (= 4 \times {}_D\Sigma_{+} = 4 \times 460) = 1840,$$

$$\text{where } n^3 = 16^3 = \zeta = \zeta_{\circ+} + \zeta_{\bullet} + \zeta_{-} + \zeta_{+} = 4096.$$

Bending-Twisting coupled ($\mathbf{A}_S\mathbf{B}_0\mathbf{D}_F$) laminates satisfy the following non-dimensional parameter criteria:

$$\begin{aligned} n_{+} &= n_{-} \\ \zeta_{+} &\neq \zeta_{-} \end{aligned} \tag{11}$$

whilst $n_{+} = n_{-}$ and $\zeta_{+} = \zeta_{-}$ are the conditions giving rise to the *Simple* laminate classes.

3.2 Extensional and Bending stiffness relations

Inserting the non-dimension parameters into Eqs (6) for the extensional $[\mathbf{A}]$ and bending $[\mathbf{D}]$ stiffness matrices gives the following relations:

$$\mathbf{A}_{ij} = \{n_{+}\mathbf{Q}'_{ij+} + n_{-}\mathbf{Q}'_{ij-} + n_{\circ}\mathbf{Q}'_{ij\circ} + n_{\bullet}\mathbf{Q}'_{ij\bullet}\} \times t \tag{12}$$

$$\mathbf{D}_{ij} = \{\zeta_{+}\mathbf{Q}'_{ij+} + \zeta_{-}\mathbf{Q}'_{ij-} + \zeta_{\circ}\mathbf{Q}'_{ij\circ} + \zeta_{\bullet}\mathbf{Q}'_{ij\bullet}\} \times t^3/12 \tag{13}$$

The transformed reduced stiffness terms in Eqs. (12) and (13) are given by:

$$\begin{aligned} \mathbf{Q}'_{11} &= \mathbf{Q}_{11}\cos^4\theta + 2(\mathbf{Q}_{12} + 2\mathbf{Q}_{66})\cos^2\theta\sin^2\theta + \mathbf{Q}_{22}\sin^4\theta \\ \mathbf{Q}'_{12} &= \mathbf{Q}'_{21} = (\mathbf{Q}_{11} + \mathbf{Q}_{22} - 4\mathbf{Q}_{66})\cos^2\theta\sin^2\theta + \mathbf{Q}_{12}(\cos^4\theta + \sin^4\theta) \end{aligned} \tag{14}$$

$$Q'_{16} = Q'_{61} = \{(Q_{11} - Q_{12} - 2Q_{66})\cos^2\theta + (Q_{12} - Q_{22} + 2Q_{66})\sin^2\theta\}\cos\theta\sin\theta$$

$$Q'_{22} = Q_{11}\sin^4\theta + 2(Q_{12} + 2Q_{66})\cos^2\theta\sin^2\theta + Q_{22}\cos^4\theta$$

$$Q'_{26} = Q'_{62} = \{(Q_{11} - Q_{12} - 2Q_{66})\sin^2\theta + (Q_{12} - Q_{22} + 2Q_{66})\cos^2\theta\}\cos\theta\sin\theta$$

$$Q'_{66} = (Q_{11} + Q_{22} - 2Q_{12} - 2Q_{66})\cos^2\theta\sin^2\theta + Q_{66}(\cos^4\theta + \sin^4\theta)$$

and the reduced stiffness terms by:

$$Q_{11} = E_1/(1 - \nu_{12}\nu_{21})$$

$$Q_{12} = \nu_{12}E_2/(1 - \nu_{12}\nu_{21}) = \nu_{21}E_1/(1 - \nu_{12}\nu_{21}) \quad (15)$$

$$Q_{22} = E_2/(1 - \nu_{12}\nu_{21})$$

$$Q_{66} = G_{12}$$

For compactness of the data presented in the definitive listing of laminate stacking sequences that follow, for each ply number grouping, n , Eqs. (13) are re-cast as:

$$A_{ij} = \{n_{\pm}Q'_{ij+} + n_oQ'_{ij\bullet} + (n - n_{\pm} - n_o)Q'_{ij\bullet}\} \times t \quad (16)$$

$$D_{ij} = \{\zeta_{\pm}(\zeta_+/\zeta_{\pm})Q'_{ij+} + \zeta_{\pm}(1 - \zeta_+/\zeta_{\pm})Q'_{ij-} + \zeta_oQ'_{ij\bullet} + (\zeta - \zeta_{\pm} - \zeta_o)Q'_{ij\bullet}\} \times t^3/12$$

to account for missing parameters n_{\bullet} and ζ_{\bullet} , the fact that $n_+ = n_-$ in balanced laminates and the inclusion of the ratio ζ_+/ζ_{\pm} , indicating the degree of *Bending-Twisting* coupling.

3.3 Lamination parameters relations

Lamination parameters facilitate the graphical inspection of feasible design space for Bending-Twisting coupled laminates, which are presented in Section 4. They also facilitate the formulation of a simple proof for the non-dimensional parameter criteria for this class of laminate, given in Eqs (11); this is provided in the electronic annex. In

the context of the non-dimensional parameters presented in the current article, the necessary lamination parameters are related through the following ply orientation dependent expressions:

$$\xi_1 = \{n_{\pm}(n_{+}/n_{\pm})\cos(2\theta_{+}) + n_{\pm}(1 - n_{+}/n_{\pm})\cos(2\theta_{-}) + n_{\circ}\cos(2\theta_{\circ}) + n_{\bullet}\cos(2\theta_{\bullet})\}/n \quad (17)$$

$$\xi_2 = \{n_{\pm}(n_{+}/n_{\pm})\cos(4\theta_{+}) + n_{\pm}(1 - n_{+}/n_{\pm})\cos(4\theta_{-}) + n_{\circ}\cos(4\theta_{\circ}) + n_{\bullet}\cos(4\theta_{\bullet})\}/n$$

relating to extensional stiffness, and

$$\begin{aligned} \xi_9 &= \{\zeta_{\pm}(\zeta_{+}/\zeta_{\pm})\cos(2\theta_{+}) + \zeta_{\pm}(1 - \zeta_{+}/\zeta_{\pm})\cos(2\theta_{-}) + \zeta_{\circ}\cos(2\theta_{\circ}) + \zeta_{\bullet}\cos(2\theta_{\bullet})\}/n^3 \\ \xi_{10} &= \{\zeta_{\pm}(\zeta_{+}/\zeta_{\pm})\cos(4\theta_{+}) + \zeta_{\pm}(1 - \zeta_{+}/\zeta_{\pm})\cos(4\theta_{-}) + \zeta_{\circ}\cos(4\theta_{\circ}) + \zeta_{\bullet}\cos(4\theta_{\bullet})\}/n^3 \\ \xi_{11} &= \{\zeta_{\pm}(\zeta_{+}/\zeta_{\pm})\sin(2\theta_{+}) + \zeta_{\pm}(1 - \zeta_{+}/\zeta_{\pm})\sin(2\theta_{-}) + \zeta_{\circ}\sin(2\theta_{\circ}) + \zeta_{\bullet}\sin(2\theta_{\bullet})\}/n^3 \\ \xi_{12} &= \{\zeta_{\pm}(\zeta_{+}/\zeta_{\pm})\sin(4\theta_{+}) + \zeta_{\pm}(1 - \zeta_{+}/\zeta_{\pm})\sin(4\theta_{-}) + \zeta_{\circ}\sin(4\theta_{\circ}) + \zeta_{\bullet}\sin(4\theta_{\bullet})\}/n^3 \end{aligned} \quad (18)$$

relating to bending stiffness.

Note that the extensional stiffness parameter $n_{+} = n_{-} = n_{\pm}/2$ for $(\mathbf{A}_S\mathbf{B}_0\mathbf{D}_F)$ laminates contained in this article, hence Eqs. (17) reduce to:

$$\xi_1 = \{n_{\pm}\cos(2\theta_{\pm}) + n_{\circ}\cos(2\theta_{\circ}) + n_{\bullet}\cos(2\theta_{\bullet})\}/n \quad (19)$$

$$\xi_2 = \{n_{\pm}\cos(4\theta_{\pm}) + n_{\circ}\cos(4\theta_{\circ}) + n_{\bullet}\cos(4\theta_{\bullet})\}/n$$

Elements of the *Simple* or uncoupled extensional stiffness matrix $[\mathbf{A}]$ are related to the lamination parameters [12] by:

$$\mathbf{A}_{11} = \{U_1 + \xi_1 U_2 + \xi_2 U_3\} \times H \quad (20)$$

$$\mathbf{A}_{12} = \mathbf{A}_{21} = \{-\xi_2 U_3 + U_4\} \times H$$

$$A_{22} = \{U_1 - \xi_1 U_2 + \xi_2 U_3\} \times H$$

$$A_{66} = \{-\xi_2 U_3 + U_5\} \times H$$

and the fully populated bending stiffness matrix $[\mathbf{D}]$ by:

$$D_{11} = \{U_1 + \xi_9 U_2 + \xi_{10} U_3\} \times H^3/12$$

$$D_{12} = \{U_4 - \xi_{10} U_3\} \times H^3/12$$

$$D_{16} = D_{61} = \{\xi_1 U_2/2 + \xi_{12} U_3\} \times H^3/12$$

(21)

$$D_{22} = \{U_1 - \xi_9 U_2 + \xi_{10} U_3\} \times H^3/12$$

$$D_{26} = D_{62} = \{\xi_{11} U_2/2 - \xi_{12} U_3\} \times H^3/12$$

$$D_{66} = \{-\xi_{10} U_3 + U_5\} \times H^3/12$$

where the laminate invariants are given in terms of the reduced stiffnesses of Eqs (15) by:

$$U_1 = \{3Q_{11} + 3Q_{22} + 2Q_{12} + 4Q_{66}\}/8$$

$$U_2 = \{Q_{11} - Q_{22}\}/2$$

$$U_3 = \{Q_{11} + Q_{22} - 2Q_{12} - 4Q_{66}\}/8$$

(22)

$$U_4 = \{Q_{11} + Q_{22} + 6Q_{12} - 4Q_{66}\}/8$$

$$U_5 = \{Q_{11} + Q_{22} - 2Q_{12} + 4Q_{66}\}/8$$

3.4 Numerical Example

For IM7/8552 carbon-fiber/epoxy material with Young's moduli $E_1 = 161.0\text{GPa}$ and $E_2 = 11.38\text{GPa}$, shear modulus $G_{12} = 5.17\text{GPa}$ and Poisson ratio $\nu_{12} = 0.38$, lamina thickness $t = 0.1397\text{mm}$ the 16-ply symmetric laminate stacking sequence $[+/\textcircled{O}/\bullet/+\bullet/-2/\textcircled{O}]_s$, for which the non-dimensional parameters were developed in Section 3.1 and Table 2, where $\zeta_{\pm} = (1840 + 208) = 2048$ and $\zeta_{+}/\zeta_{\pm} = 1840/(1840 + 208) = 0.898$ or 89.8%. For standard fibre angles $\theta = \pm 45^\circ, 0^\circ$ and 90° in place of symbols \pm , \textcircled{O} and \bullet , respectively, the transformed reduced stiffnesses are given in Table 7.

The A_{ij} and D_{ij} follow from Eqs (16):

$$A_{ij} = \{n_{\pm}Q'_{ij+} + n_{\textcircled{O}}Q'_{ij\textcircled{O}} + (n - n_{\pm} - n_{\textcircled{O}})Q'_{ij\bullet}\} \times t$$

$$A_{11} = \{8 \times 50,894 + 4 \times 162,660 + (16 - 8 - 4) \times 0\} \times 0.1397 = 154,198 \text{ N/mm}$$

$$D_{ij} = \{\zeta_{\pm}(\zeta_{+}/\zeta_{\pm})Q'_{ij+} + \zeta_{\pm}(1 - \zeta_{+}/\zeta_{\pm})Q'_{ij-} + \zeta_{\textcircled{O}}Q'_{ij\textcircled{O}} + (\zeta - \zeta_{\pm} - \zeta_{\textcircled{O}})Q'_{ij\bullet}\} \times t^3/12$$

$$D_{16} = \{2048 \times 0.898 \times 37,791 + 2048 \times (1 - 0.898) \times -37,791 + 1024 \times 0$$

$$+ (4096 - 2048 - 1024) \times 0\} \times 0.1397^3/12 = 14,012 \text{ N.mm}$$

The final stiffness matrices for the laminate follow:

$$\begin{bmatrix} A_{11} & A_{12} & A_{16} \\ & A_{22} & A_{26} \\ \text{Sym.} & & A_{66} \end{bmatrix} = \begin{bmatrix} 154,198 & 50,206 & 0 \\ & 154,198 & 0 \\ \text{Sym.} & & 51,996 \end{bmatrix} \text{ N/mm}$$

$$\begin{bmatrix} D_{11} & D_{12} & D_{16} \\ & D_{22} & D_{26} \\ \text{Sym.} & & D_{66} \end{bmatrix} = \begin{bmatrix} 64,199 & 20,903 & 14,012 \\ & 64,199 & 14,012 \\ \text{Sym.} & & 21,648 \end{bmatrix} \text{ N.mm}$$

The form of these stiffness matrices has special significance since $A_{11} = A_{22}$ by inspection, and calculation reveals that $A_{66} = (A_{11} - A_{12})/2$, indicating that this laminate

is extensionally isotropic, as defined in Eqs (8) and (9). Further calculation reveals that $D_{ij} = A_{ij}H^2/12$, hence the properties are quasi-homogeneous, as defined in Eq. (10). Of course only the orthotropic stiffness properties are concomitant, since $A_{16} = A_{26} = 0$, whereas $D_{16}, D_{26} \neq 0$. Hence this laminate is described as Pseudo Quasi-Homogeneous Quasi-Isotropic.

The extensional (ξ_1, ξ_2) and bending ($\xi_9, \xi_{10}, \xi_{11}$) lamination parameters are calculated from Eqs. (19):

$$\xi_1 = \{n_{\pm}\cos(2\theta_{\pm}) + n_o\cos(2\theta_o) + n_{\bullet}\cos(2\theta_{\bullet})\}/n$$

$$\xi_1 = \{8 \times \cos(90^\circ) + 4 \times \cos(0^\circ) + 4 \times \cos(180^\circ)\}/16 = 0.00$$

$$\xi_2 = \{n_{\pm}\cos(4\theta_{\pm}) + n_o\cos(4\theta_o) + n_{\bullet}\cos(4\theta_{\bullet})\}/n$$

$$\xi_2 = \{8 \times \cos(180^\circ) + 4 \times \cos(0^\circ) + 4 \times \cos(360^\circ)\}/16 = 0.00$$

which signify that this laminate is extensionally isotropic.

The bending lamination parameters from Eqs. (18):

$$\xi_9 = \{\zeta_{\pm}(\zeta_{+}/\zeta_{\pm})\cos(2\theta_{+}) + \zeta_{\pm}(1 - \zeta_{+}/\zeta_{\pm})\cos(2\theta_{-}) + \zeta_o\cos(2\theta_o) + \zeta_{\bullet}\cos(2\theta_{\bullet})\}/n^3$$

$$\xi_9 = \{2048 \times (0.898)\cos(90^\circ) + 2048 \times (1 - 0.898)\cos(90^\circ) + 1024 \times \cos(0^\circ) + 1024 \times \cos(180^\circ)\}/4096 = 0.00$$

$$\xi_{10} = \{\zeta_{\pm}(\zeta_{+}/\zeta_{\pm})\cos(4\theta_{+}) + \zeta_{\pm}(1 - \zeta_{+}/\zeta_{\pm})\cos(4\theta_{-}) + \zeta_o\cos(4\theta_o) + \zeta_{\bullet}\cos(4\theta_{\bullet})\}/n^3$$

$$\xi_{10} = \{2048 \times (0.898)\cos(180^\circ) + 2048 \times (1 - 0.898)\cos(180^\circ) + 1024 \times \cos(0^\circ) + 1024 \times \cos(0^\circ)\}/4096 = 0.00$$

$$\xi_{11} = \{\zeta_{\pm}(\zeta_{+}/\zeta_{\pm})\sin(2\theta_{+}) + \zeta_{\pm}(1 - \zeta_{+}/\zeta_{\pm})\sin(2\theta_{-}) + \zeta_o\sin(2\theta_o) + \zeta_{\bullet}\sin(2\theta_{\bullet})\}/n^3$$

$$\xi_{11} = \{2048 \times (0.898)\sin(90^\circ) + 2048 \times (1 - 0.898)\sin(90^\circ) + 1024 \times \sin(0^\circ) + 1024 \times \sin(180^\circ)\}/4096 = 0.40$$

Noting that $\xi_{12} = 0$ for $\theta_{\pm} = \pm 45^\circ$.

Hence this Pseudo Quasi-Homogeneous Quasi-Isotropic laminate is defined by the extensional lamination parameters $(\xi_1, \xi_2) = (0, 0)$ and bending lamination parameters $(\xi_9, \xi_{10}, \xi_{11}) = (0, 0, 0.4)$.

4. Results and Discussion

Table 3(a) summarizes the definitive list of *Bending-Twisting* coupled laminate configurations, arranged according to sub-sequence symmetry, and expressed as a percentage of the total for each ply number grouping. Ply number groupings, $n = 4, 5$ and 6, contain only 1, 2 and 4 symmetric (*SS*) solutions, respectively, and have therefore been omitted. Details of sub-sequence symmetries for ply groupings for $n = 19$ ($\Sigma = 662,178$), 20 ($\Sigma = 606,046$) and 21 ($\Sigma = 6,172,510$) are also omitted, but contain 3.4% (22,760), 7.2% (43,406) and 1.4% (87,172) symmetric sequences, respectively.

The corresponding summary for fully uncoupled laminates is given in Table 3(b) for comparison. Together, these results demonstrate that a much larger design space exists for *Bending-Twisting* coupled laminates compared to their fully uncoupled counterparts, especially for the common symmetric designs, which dominate the design space for laminates with up to 12 plies. By contrast, there are no symmetric fully uncoupled laminates below 12 plies; the design space is instead dominated by anti-symmetric laminates.

Common design rules [13] suggest that anti-symmetric laminates eliminate *Bending-Twisting* coupling, which is supported by the absence of these results in Table 3(a). However, the same rules suggest that the coupling stiffness matrix [B] is non-zero, leading to thermal warping distortions in such designs, which is not the case for any of the designs presented in this article. Anti-symmetric laminates are discussed in more detail elsewhere [14]. By contrast, similar design rules suggest that symmetric laminates eliminate the coupling stiffness matrix [B], but introduce *Bending-Twisting* coupling, which is not supported by the results of Table 3(b) for *Simple* or uncoupled laminates. This summary of results therefore demonstrates that employing design rules based on laminate symmetry can lead to a substantial part of the design space being overlooked. This may be crucial in cases such as fuselage design, which are typically within the range $12 \leq n \leq 16$ plies, where the design space is dominated by other forms of sub-sequence symmetry.

Abridged listings of stacking sequences and non-dimensional parameters are given in Tables A8 – A13, representing each distinct form of sub-sequence symmetry found.

The numbers of Quasi-Isotropic laminates within the definitive list of *Bending-Twisting* coupled laminates are summarized in Table 4. These satisfy the requirements of Eqs (8) and (9), defining extensional isotropy and give rise to $\pi/3$ isotropy when $n_+ = n_- = n_o$, and a 60° spacing is employed between each of the three ply orientations, and to $\pi/4$ isotropy when $n_+ = n_- = n_o = n_\bullet$, and a 45° spacing is employed between each of the four ply orientations. Individual sequences within the abridged listings are marked with an asterisk if they possess Quasi-Isotropic properties.

Finally, Pseudo Quasi-Homogeneous ($\mathbf{A}_S\mathbf{B}_0\mathbf{D}_F$) laminates are introduced as a newly discovered, yet important laminate sub-set. Such laminates have concomitant orthotropic properties, i.e. matching orthotropic or isotropic stiffness in extension and bending, as defined by Eq. (10). However, because $A_{16} = A_{26} = 0$, hence $\xi_3 = \xi_4 = 0$, the effects of *Bending-Twisting* coupling are now isolated; the large numbers of laminate configurations sharing the same orthotropic extensional and bending stiffness properties possess a range of $D_{16} = D_{26} \neq 0$, hence $\xi_{11} = \xi_{12} \neq 0$. These configurations are summarised in Table 5 and listed in full in the electronic annex; grouped according to sub-sequence symmetry, number of plies, n , and descending order of lamination parameters $\xi_1 = \xi_9$, $\xi_2 = \xi_{10}$ and ξ_{11} , respectively, noting that $\xi_{12} = 0$ for the standard fibre orientations assumed, i.e., $\pm 45^\circ$, 0° and 90° .

4.1 Design space interrogation

For optimum design, ply angle dependent lamination parameters are often preferred, since these allow the stiffness terms to be expressed as linear variables within convenient bounds ($-1.0 \leq \xi_i \leq 1.0$). However, the optimized lamination parameters must then be matched to a corresponding laminate configuration within the feasible region. This process is challenging, but is aided by graphical representation of the lamination parameter design spaces, as illustrated in Figs 1 and 2 for symmetric (SS) and non-symmetric (NN) sub-sequence symmetries, identified in Table 3(a). The remaining sub-sequence symmetries are presented in Figs A9 – A12 and corresponding listings of Tables A8 – A13 of the electronic appendix. These are 2-dimensional spaces for extensional stiffness and 3-dimensional spaces for bending stiffness due to the presence of *Bending-Twisting* coupling, i.e. $\xi_{11} \neq 0$. Standard ply orientations ($\pm 45^\circ$, 0°

and 90°) have been chosen specifically because they have most relevance to current design practice, and also avoid the complication of presenting 4-dimensional data, which would be the case for general angle-ply orientations, i.e., $\pm\theta \neq \pm 45^\circ$.

Figure 1 illustrates the point cloud of individual laminate configurations for Non-symmetric angle- and cross-ply sub-sequences (NN) with $4 \leq n \leq 18$, listed in abridged form in Table A9 and corresponding to: (a) plan, (b) front elevation and (c) side elevation for the 3 dimensional bending stiffness design space and (d) front elevation for the 2-dimensional extensional stiffness design space, which is common to all the design space representations that follow. From the total of 124,556 configurations, there are only 107 unique solutions in terms of extensional stiffness, equating to 84,011 unique solutions for bending stiffness. There is a clear bias in the position of the lamination parameter point cloud towards the positive ξ_{11} region of the design space as a result of the first (surface) ply being set to $+45^\circ$; the point cloud would be mirrored about the ξ_{11} axis if the signs of the angle plies were switched.

Figure 2 presents the lamination parameter design spaces for Symmetric angle- and cross-ply sub-sequences (SS), with $4 \leq n \leq 18$, listed in abridged form in Table A13. These are the ubiquitous balanced and symmetric designs used almost exclusively in design practice. The 23,470 configurations are contained within the 146 unique lamination parameter points for extensional stiffness (ξ_1, ξ_2) and the 22,498 unique points within the 3-dimensional point cloud of lamination parameters for bending stiffness ($\xi_9, \xi_{10}, \xi_{11}$).

The results presented in this section demonstrate that whilst balanced and symmetric laminates gives rise to *Bending-Twisting* coupling, they account for less than 3% of the

total design space for laminates with up to 21 plies. However, in terms of the number of unique points within the design spaces of Figs 1 and 2, symmetric (*SS*) laminates represent 41% of the design space for extensional stiffness and 14% for bending stiffness, compared to non-symmetric (*NN*) laminates with 30% and 72%, respectively.

4.2 Interpretation of Lamination parameter design spaces

The results Figs 1 and 2 can be interpreted in a number of ways for the purposes of laminate design. The annotated lamination parameter design space of Fig. 3(a) indicates that stacking sequences corresponding to the points $(-1, 1)$, $(0, -1)$ or $(1, 1)$, contain, respectively, 90° plies, $\pm 45^\circ$ plies or 0° plies only. It can therefore be readily appreciated that points lying along the edge of the triangular feasible region defined by the line drawn between $(\xi_1, \xi_2) = (0, -1)$ and $(1, 1)$ correspond to laminates with 0 and $\pm 45^\circ$ plies only, whereas those along the line between $(0, -1)$ and $(-1, 1)$ consist of $\pm 45^\circ$ and 90° plies only. The Quasi-Isotropic laminate corresponds to $(\xi_1, \xi_2) = (0, 0)$.

Practical design rules are often based on ply percentages [6], which can be mapped onto the lamination parameter design space as illustrated on Fig. 3(a) to help with interpretation of the results. These rules often restrict the design space to the central triangular region indicated by bold lines; other sources [13] suggest the extended region shown with broken lines.

Ply percentages are only generally applicable to the design of in-plane properties. However, Fig. 3(b) presents results for Quasi-Homogenous laminates, listed elsewhere [1] with $8 \leq n \leq 21$ plies, which now permit the mapping of ply percentages onto the lamination parameter design space for bending stiffness (ξ_9, ξ_{10}) , which explains the rationale behind the axis labels of Fig. 3(a) and (b); the lamination parameters for

extensional and bending stiffness are identical for Quasi-Homogenous laminates, i.e. $(\xi_1, \xi_2) = (\xi_9, \xi_{10})$. Using the closed form buckling solution:

$$N_{x,\infty} = \pi^2 \left[D_{11} \left[\frac{1}{\lambda} \right]^2 + 2(D_{12} + 2D_{66}) \frac{1}{b^2} + D_{22} \left[\frac{1}{b^4} \right] \lambda^2 \right] \quad (23)$$

where λ is the buckling half-wavelength, exact buckling factor results, $k_{x,\infty}$ ($= N_{x,\infty} b^2 / \pi^2 D_{110}$), can be generated at each of the 15 equally spaced grid points across the lamination parameter design space of Fig. 3(b), from which the 4th order polynomial:

$$k_{x,\infty} = 4.000 - 1.049\xi_{10} - 1.217\xi_9^2 + 0.340\xi_{10}\xi_9^2 - 0.360\xi_9^4 - 0.034\xi_{10}^2\xi_9^2 \quad (24)$$

is then readily derived. D_{110} corresponds to the first of Eq. (21) with $(\xi_9, \xi_{10}) = (0, 0)$, representing the Isotropic laminate, giving rise to the classical buckling factor result, $k_{x,\infty} = 4.00$, using Eq. (24). This equation is used to generate compression buckling contours for the infinitely long plate with simply supported edges, which are mapped onto the lamination parameter design space of Fig. 3(c).

Note that the number of significant figures in the coefficients of Eq. (24) have been reduced, but are sufficient to maintain a buckling factor accurate to 2 decimal places.

The top corners of the triangular region, representing laminates with 90° or 0° degree plies only, have buckling factor $k_{x,\infty} = 1.68$ (with buckling half-waves $b/\lambda = 1.94 = (D_{22}/D_{11})^{1/4}$ and $\lambda/b = 1.94$, respectively), whereas the bottom corner, representing laminates with $\pm 45^\circ$ plies only, has buckling factor $k_{x,\infty} = 5.05$ (with buckling half-wave $\lambda = b$). By ignoring the effect of *Bending-Twisting* coupling designers are effectively using this contour map, which is applicable only to fully uncoupled laminates, i.e. ξ_{11} (and ξ_{12}) = 0.

The mapping of ply percentages to buckling factor contours for *Bending-Twisting* coupled laminates is only possible when *Extension-Shearing* coupling is present and Quasi-Homogeneous properties exist, as is clear from Fig. 3(d); for *Bending-Twisting* coupled laminates, ξ_3 (and ξ_4) = 0 hence $\xi_3 \neq \xi_{11}$. The restriction is further demonstrated in Fig. 4, containing the lamination parameter point cloud for Pseudo Quasi-Homogenous laminates. Here the orthotropic lamination parameter of Fig. 4(b) are matched as in Fig. 3(c), i.e., $\xi_1 = \xi_9$, and $\xi_2 = \xi_{10}$. However, $\xi_3 = 0$ for this class of laminate, hence ξ_3 and ξ_{11} cannot be paired in Fig. 4(a) and (c). Figure 4(a) and (c) serve only to illustrate the range of ξ_{11} , relating to the magnitude of *Bending-Twisting* coupling, for each orthotropic lamination parameter point (ξ_9, ξ_{10}) in Fig. 4(b).

The concept of Quasi-Homogenous properties is further explained by the polar plots of Fig. 5. Here, the lamination parameters are illustrated with respect to off-axis material alignment, β . The Quasi-Homogeneous laminate $[+/-2/+/-/+2/-]_s$ of Fig. 5(a) has identical lamination parameters in both extension ($\xi_1 - \xi_4$) and bending ($\xi_9 - \xi_{12}$) for all off-axis orientations $0 < \beta < 360^\circ$; the non-zero lamination parameter ξ_4 (ξ_{12}) gives rise to *Extension-Shearing* (*Bending-Twisting*) coupling, i.e. $A_{16}, A_{26} (D_{16}, D_{26}) \neq 0$, which would be expected for off-axis alignment of any orthotropic laminate. By contrast, the Pseudo Quasi-Homogeneous laminate $[+4/-4]_s$ of Fig. 5(b) exhibits differences between extension and bending due to the presence of *Bending-Twisting* coupling, i.e., $\xi_{11} = 0.75$ when the material and structural axes are coincident ($\beta = 0$), hence $\xi_3 (= 0) \neq \xi_{11}$ as expected. However, the orthotropic stiffness properties are paired only for orthogonal alignments, i.e., $\beta = 0, 90, \dots$, etc. Nevertheless, the Pseudo Quasi-Homogenous laminates illustrated in Figure 4 are an important sub-group, which permit the effect of

increasing *Bending-Twisting* coupling magnitude, or ξ_{11} , to be studied, with orthotropic properties from across the design space of Figure 4(b). Complete laminate listings are therefore provided in the electronic annex for Pseudo Quasi-Homogeneous laminates within the range $12 \leq n \leq 16$.

5. Effect of Bending-Twisting coupling on compression buckling strength

Ignoring the effects of *Bending-Twisting* coupling continues to be broadly justified on the basis that the effects dissipate for laminates with a large number of plies. However, buckling strength is strongly influenced by such coupling in thin laminates; compression buckling strength is overestimated (unsafe) if the effects of *Bending-Twisting* coupling are ignored.

Note that the results presented in this section represent continuous plates, supported at regular plate length intervals, a , and whilst compression buckling results for isotropic plates are the same as those for isolated plates with simply supported edges, mode interaction, due to *Bending-Twisting* coupling, will generally result in an increase in buckling strength compared to the isolated plate.

5.1 Details of analysis and modelling

Two analysis procedures are adopted for calculation of the new results presented. Continuous and infinitely long plate results are obtained using the panel buckling analysis and optimum design code VICONOPT [15], which is based on the stiffness matrix method with exact flat plate theory; it can be described as an exact infinite strip theory. An ABAQUS Finite Element analysis [16] is undertaken to establish the simply supported and clamped results corresponding to isolated plates.

VICONOPT is based on the earlier programs VIPASA and VICON. VIPASA (Vibration and Instability of Plate Assemblies with Shear and Anisotropy) theory assumes that the mode of buckling varies sinusoidally in the longitudinal direction with half-wavelength λ . This type of analysis was used only to generate the asymptotic values for Fig. 6, representing the infinitely long plate. VICON (VIPASA with CONstraints) theory uses Lagrangian multipliers to impose point constraints, so that rectangular boundaries can be accurately represented when the composite material possesses *Bending-Twisting* coupling; skewed nodal lines are known to result in this case, even for compression loaded plates. The analysis assumes that the deflections of the plate assembly can be expressed as a Fourier series, in which suitable combinations of half wavelengths are now coupled, in order to satisfy the point constraints. Thus results are for an infinitely long plate assembly, with supports repeating at panel length intervals, a . Clamped conditions can be enforced by coupling wavelengths that satisfy zero rotation, as well as displacement, at the point constraint locations; hence the infinitely long plate assembly degenerates to the equivalent isolated plate assembly in such cases. Results from the ABAQUS and VICONOPT match in these cases.

The ABAQUS finite element analysis used a thin plate element (S8R5), with plate dimensions of $300\text{mm} \times 300\text{mm}$, together with a 16-ply laminate, of total thickness $H = (n \times t = 16 \times 0.1397\text{mm} =) 2.24\text{mm}$, ensure that the results are representative of the thin plate solution. A high degree of convergence is achieved using 30×30 elements for the square plate ($a/b = 1.0$) and maintained by adjusting the number of elements with respect to changes in aspect-ratio, e.g. 45×30 elements for $a/b = 1.5$, etc. By contrast, 30 strips were used in the VICONOPT analysis.

5.2 Garland Curves

Lamination parameters are used in the labelling of the Garland curves for compression buckling factor, $k_x (= N_x b^2 / \pi^2 D_{\text{Iso}})$, presented across a range of aspect ratios (a/b) in Fig.

6. The lamination parameter $-0.5 \leq \xi_{11} \leq 0.5$ is a measure of the magnitude of *Bending-Twisting* coupling for Pseudo Quasi-homogeneous Quasi-Isotropic laminates in Fig. 6(a), with $(\xi_1, \xi_2) = (0, 0)$ and $(\xi_9, \xi_{10}) = (0, 0)$; the bounds do however vary with $\xi_{10} (= \xi_2)$ up to a maximum of $-1.0 \leq \xi_{11} \leq 1.0$ when $\xi_{10} = -1.0$, which correspond to the Angle-ply laminate designs in Fig. 6(b).

Comparisons are made against an equivalent fully uncoupled isotropic ($\mathbf{A}_I \mathbf{B}_0 \mathbf{D}_I$) laminate datum and the *Bending-Twisting* coupled ($\mathbf{A}_I \mathbf{B}_0 \mathbf{D}_F$) laminate derived in Sections 3.1 and 3.4, where all elements of the \mathbf{ABD} matrix are identical except for D_{16} and D_{26} , and which are zero only in the $\mathbf{A}_I \mathbf{B}_0 \mathbf{D}_I$ laminate. This comparison serves to isolate the effects of *Bending-Twisting* coupling, i.e. D_{16} and D_{26} .

Note that only the curves corresponding to $\xi_{11} = 0$ on Fig. 6(a) can be obtained from the closed form buckling solution of Eq. (23) for the infinitely long plate, or:

$$N_x = \pi^2 \left[D_{11} \left[\frac{m}{a} \right]^2 + 2(D_{12} + 2D_{66}) \frac{1}{b^2} + D_{22} \left[\frac{1}{b^4} \left[\left[\frac{a}{m} \right]^2 \right] \right] \right] \quad (25)$$

for the finite length plate, where m is the integer number of half-wavelengths within the plate length, a . A single half-wavelength is assumed across the plate width, b . Buckling loads are over-predicted (i.e., unsafe) whenever *Bending-Twisting* coupling is present, since D_{16} and D_{26} are not accounted for in Eqs (23) or (25); the magnitude of the over-prediction increases with increasing $\xi_{11} \equiv D_{16} = D_{26}$.

Discrete ABAQUS results on Fig. 6(a), for the isolated plate, are superimposed for comparison. They represent the 16 ply laminate $[+/\bigcirc/\bullet/-/\bullet/+2/\bigcirc]_S$ with $\xi_{11} = 0.4$ and demonstrate clear differences between the continuous and isolated plate cases. The Garland curves for the continuous plate results demonstrate the pronounced feature of descending curves, with increasing aspect ratio (a/b), resulting from *Bending-Twisting* coupling, which are barely detectable in the isolated plate result, for which there is a 0.6% reduction in buckling factor, k_x , between aspect ratio $a/b = 1.0$ and 2.0 , compared to 3.9% for the continuous plate case.

Descending curves are a common feature in isotropic skew plates [17], for both isolated and continuous cases, which provides a good analogy since *Bending-Twisting* coupling ($\xi_{11} > 0$) gives rise to skewed nodal lines in the buckling mode shapes, as illustrated in Fig. 7(a) and (b) for infinitely long plates.

The asymptotes on Fig. 6(a) represent $k_{x,\infty}$ for the infinitely long plate, and reveal bounds on buckling strength reductions of up to 16% for Pseudo Quasi-Homogeneous, Quasi-Isotropic laminates with simple supports; noting that the reduction for practical rather than hypothetical designs is up to 10%, which corresponds to the 16 ply laminate $[+/\bigcirc/\bullet/-/\bullet/+2/\bigcirc]_S$ with $\xi_{11} = 0.4$.

Descending curves are also pronounced in the isolated plate corresponding to the 16 ply laminate $[+4/-4]_S$ with $\xi_{11} = 0.75$, illustrated in Fig. 6(b). Here, the reduction is 4.2% in buckling factor, k_x , between aspect ratios $a/b = 1.0$ and 2.0 . The asymptotes, representing $k_{x,\infty}$, reveal bounds on buckling strength reductions of up to 57% for Pseudo Quasi-Homogeneous, Angle-ply laminates with simple supports. However, bounds on practical designs reveal a 29% reduction.

It should be noted that whilst non-symmetric (*NN*) laminates have by far the highest number of solutions within the feasible design spaces presented in Figs (9) – (2), the degree of *Bending-Twisting* coupling is limited to $\xi_{11} \leq 0.65$. The most significant degree of *Bending-Twisting* coupling, and hence reduction in buckling strength, occurs in symmetric *SS* laminates for which $\xi_{11} \leq 0.75$.

A final set of buckling curves are presented in Fig. 8 to test the hypothesis that continuous plates degenerate into isolated plates when edges are clamped, hence the ABAQUS results [18] for the isotropic plate, i.e. $\xi_{11} = 0.0$, as well as the Pseudo Quasi-Homogeneous, Quasi-Isotropic laminate with $\xi_{11} = 0.4$ are in agreement. Asymptotes, representing $k_{x,\infty}$, for the infinitely long plate with clamped edges are also given and reveal a hypothetical buckling strength reduction of up to 14% below the fully isotropic laminate. However, bounds on practical designs reveal an 8% reduction.

Note that the equivalent Isotropic (**A₁B₀D₁**) laminate datum configuration was chosen specifically to allow convergence of the ABAQUS and VICONOPT analyses to be verified against the closed form buckling solution of Eqs. (23) and (25). The properties used in the modelling were: $E_{\text{Iso}} = E_1 = E_2 = 61.673\text{GPa}$, $\nu_{\text{Iso}} = 0.326$ and $G_{\text{Iso}} = 23.262\text{GPa}$, from which $D_{\text{Iso}} = E_{\text{Iso}}H^3/(1 - \nu_{\text{Iso}}^2)$ follows.

6. Laminate Selection

Studies on the failure of composite laminates feature in the so called World-Wide Failure Exercises. The third in this series [19] is concerned with the assessment of current predictive capabilities for damage in composite laminates, including delamination, stacking sequence effects, etc., and provide details of the rationale behind the selection of a series of benchmark configurations for assessment of these damage

mechanisms. Of particular relevance in the context of the current article are the four Quasi-Isotropic laminate configurations chosen, with stacking sequences and corresponding lamination parameters given in Table 6.

Configurations (1) – (3) of Table 6 show alternative ‘balanced and symmetric’ stacking sequences representing $\pi/4$ Quasi-Isotropic laminates, defined for the assessment of changes in damage initiation and progression behaviour, but are unusual in the fact that configurations (1) and (2) have 0° outer surface plies, which is not common design practice. Neither possess significant *Bending-Twisting* coupling and are also out with the design space, based on ply percentages, adopted in common design practice, see Fig. 3(c). Configuration (3) sits on the boundary of what is acceptable design practice for orthotropic stiffness properties and on the boundary of the feasible region of the design space in terms of *Bending-Twisting* coupling magnitude, for which there are no known design guidelines. It therefore represents a lower bound solution for compression buckling strength with respect to the equivalent orthotropic laminate, with $\xi_{11} = 0$. Configuration (4) is defined for the purpose of investigating flexural response but represents a $\pi/3$ Quasi-Isotropic laminate, which is seldom used in design practice. However, because $\xi_9 \approx \xi_{10} \approx 0$, it is similar in nature to the Pseudo Quasi-homogeneous configurations presented here with $\pi/4$ isotropy and in fact possesses a similar magnitude of *Bending-Twisting* coupling to the laminate $[+/\text{O}/\bullet/+\bullet/-_2/\text{O}]_s$ used in the buckling assessments of Fig. 6, representing a lower-bound buckling solution.

It is important to note that many studies on flexural behavior, e.g., buckling, post-buckling, low velocity impact response, etc., continue to adopt *Bending-Twisting* coupled laminates as the preferred benchmark configuration, but few consider the effects of the coupling response. It is therefore arguably more difficult for the

composite laminate designer to apply the lessons learned in such studies when faced with different laminate designs.

This article has therefore presented a set of *Bending-Twisting* coupled configurations, which offer an alternative set of benchmark laminates for future studies. These benchmark configurations all contain angle plies on the top surface of the laminate, which is in keeping with common damage tolerance heuristics of placing ‘sacrificial’ angle plies on exposed surfaces. However, they also contain sequences with different ply orientations on the protected surface. Indeed, the question of whether ‘sacrificial’ angle plies are necessary on both surfaces of the laminate does not seem to have been previously addressed; perhaps due to the continuing misconception that stacking sequence symmetry is a requirement for uncoupled behaviour. Nevertheless, these laminate configurations become important in common design practice if they are interpreted as the symmetric half of the laminate rather than the total stacking sequence as presented here.

7. Conclusions

The definitive list of laminate stacking sequences for *Bending-Twisting* coupling has been developed for up to 21 plies. It has been shown to contain many forms of non-symmetric angle-ply and cross-ply sub-sequences, yet all configurations can be manufactured flat under a standard elevated temperature curing process by virtue of the decoupled nature between in-plane and out-of-plane behaviour. Indeed, the common balanced and symmetric design rule, normally assumed necessary to achieve this warp free condition, accounts for less than 3% of the design space within this range of ply number groupings investigated.

The definitive list has also been shown to contain $\pi/3$ and $\pi/4$ Quasi-Isotropic Laminates, which are sub-sets of *Bending-Twisting* coupled laminates, and are commonly adopted as benchmark designs. However Pseudo Quasi-Homogeneous ($\mathbf{A}_s\mathbf{B}_0\mathbf{D}_F$) laminates, including those with Quasi-Isotropic properties, have been introduced as an alternative set of benchmark configurations, since their concomitant orthotropic stiffness properties allow the effects of *Bending-Twisting* coupling to be studied in isolation.

Comparisons of the compression buckling response of Pseudo Quasi-Homogeneous laminates reveal that *Bending-Twisting* coupling results in reduced buckling strength of up to 10% for practical designs with Quasi-Isotropic properties and up to 29% for Angle-ply only configurations; these compare to theoretical bounds of 16% and 59%, respectively.

Acknowledgements

The Newton Research Collaboration Programme (NRCP1516/4/50) is gratefully acknowledged for supporting the concluding part of this research.

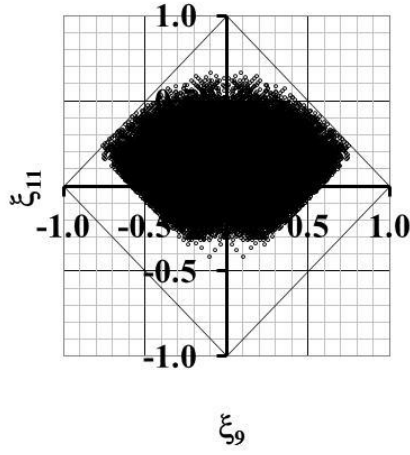
References

1. York, C. B. Unified approach to the characterization of coupled composite laminates: benchmark configurations and special cases. *Journal of Aerospace Engineering* 2010;23:219-242.
2. York, C. B. On Extension-Shearing coupled laminates. *Composite Structures*, 2015;120:472-482.

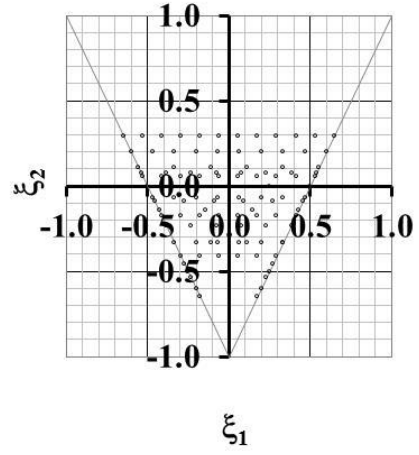
3. York, C. B. Characterization of non-symmetric forms of fully orthotropic laminates. *J. Aircraft* 2009;46:1114-1125.
4. Jones, R. M. *Mechanics of Composite Materials*. Taylor & Francis, London, 1999.
5. Engineering Sciences Data Unit. Stiffnesses of laminated plates. ESDU Item No. 94003, IHS, 1994.
6. Bailie, J. A., Ley, R. P. and Pasricha, A. A summary and review of composite laminate design guidelines. Task 22, NASA Contract NAS1-19347, 1997.
7. Irisarri, F.-X., Lasseigne, A., Leroy, F.-H. and Le Riche, R. Optimal design of laminated composite structures with ply drops using stacking sequence tables. *Composite Structures* 2014;107:559-569.
8. Nemeth, M. P. Importance of anisotropy on buckling of compression-loaded symmetric composite plates. *AIAA Journal*, 1986;24:1831-1835.
9. Herencia, J. E., Weaver, P. M. and Friswell, M. I. Closed-form solutions for buckling of long anisotropic plates with various boundary conditions under axial compression. *Journal of Engineering Mechanics* 2010;136:1105-1114.
10. York, C. B. and Almeida, S. F. M. Effect of bending-twisting coupling on the compression and shear buckling strength of infinitely long plates. *Composite Structures*, Submitted for possible publication.
11. Engineering Sciences Data Unit. Laminate stacking sequences for special orthotropy (Application to fibre reinforced composites). ESDU Item No. 82013, IHS, 1982.
12. Tsai, S.W., Hahn, H.T. *Introduction to composite materials*. Technomic Publishing Co. Inc., Lancaster, 1980.

13. Niu, M. C. Composite Airframe Structures, 3rd Edition. Connilit Press, Hong Kong. 2000.
14. Li, D., and York, C. B. Bounds on the natural frequencies of laminated rectangular plates with extension-twisting (and shearing-bending) coupling. Composite Structures. 2015;131:37-46.
15. Williams, F. W. Kennedy, D. Butler, R. and Anderson, M. S. VICONOPT: Program for exact vibration and buckling analysis or design of prismatic plate assemblies. AIAA J. 1991;29:1927-1928.
16. ABAQUS/Standard, Version 6.12. Dassault Systèmes Simulia Corp., 2012.
17. Huyton, P., and York, C.B. Buckling of skew plates with continuity or rotational edge restraint. Journal of Aerospace Engineering, 2001;14:92-101.
18. York, C. B. Elastic buckling design curves for isotropic rectangular plates with continuity or elastic edge restraint against rotation. Aeronautical Journal, 2000;104:175-182.
19. Kaddour, A. S., Hinton M. J., Li, S. and Smith, P. A. Damage prediction in polymer composites: Update of Part A of the Third World-Wide Failure Exercise (WWFE-III). Proceedings of the 17th International Conference on Composite Materials, Paper No. F12:7, Edinburgh, Scotland. 2009.

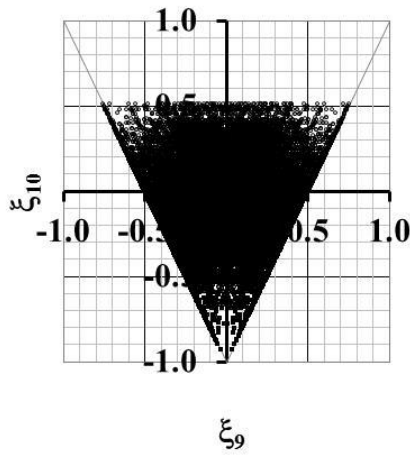
Figures



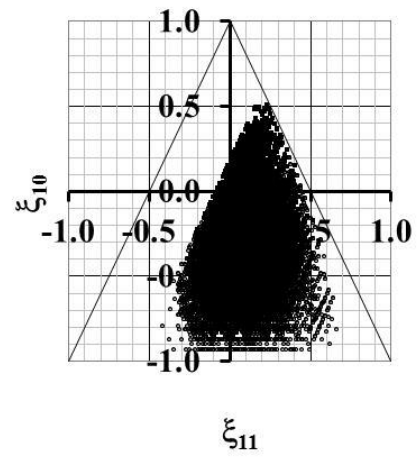
(a)



(d)

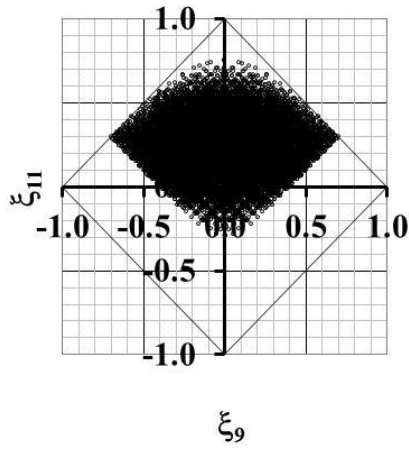


(b)

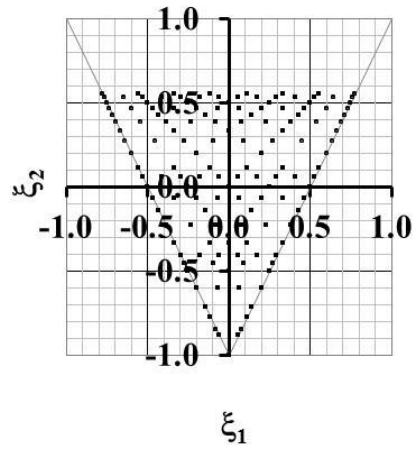


(c)

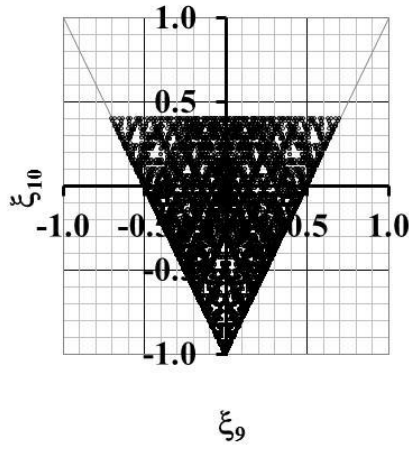
Figure 1



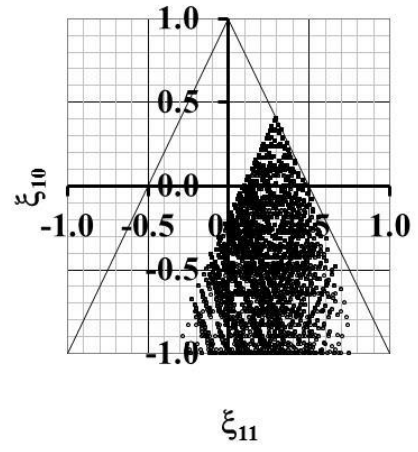
(a)



(d)

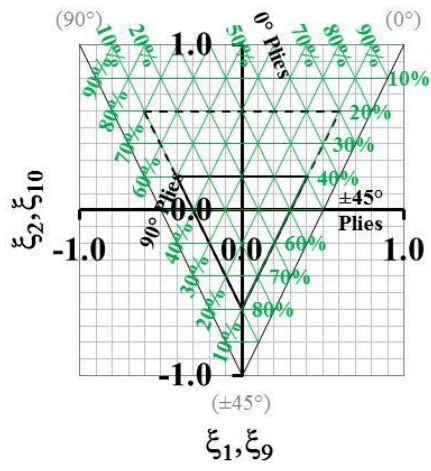


(b)

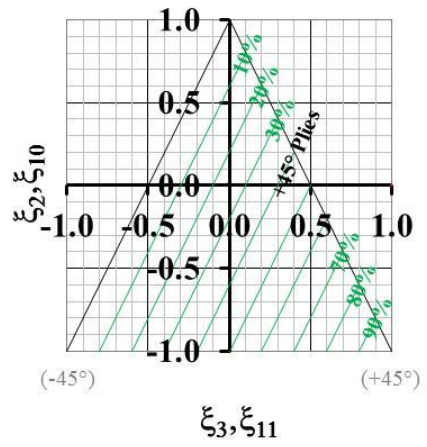


(c)

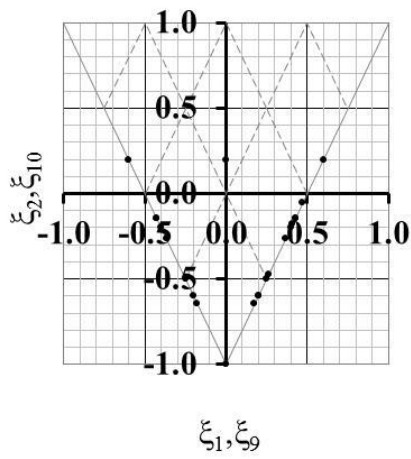
Figure 2



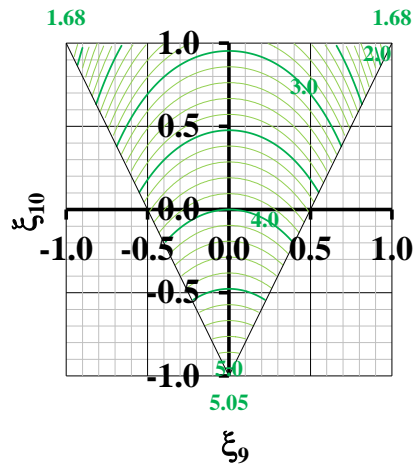
(a)



(d)

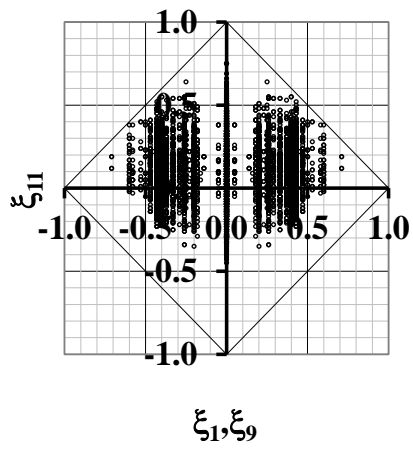


(b)

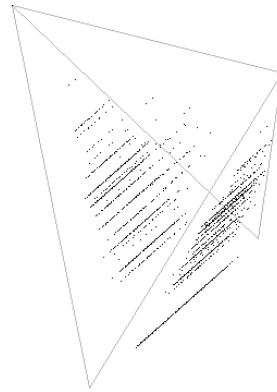


(c)

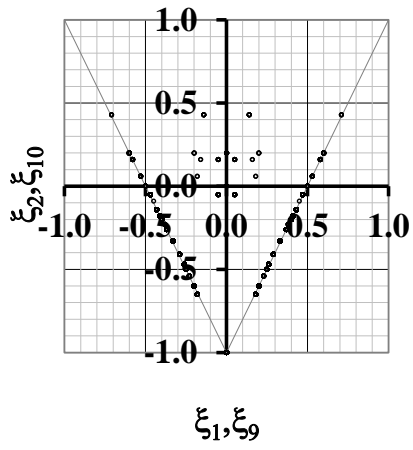
Figure 3



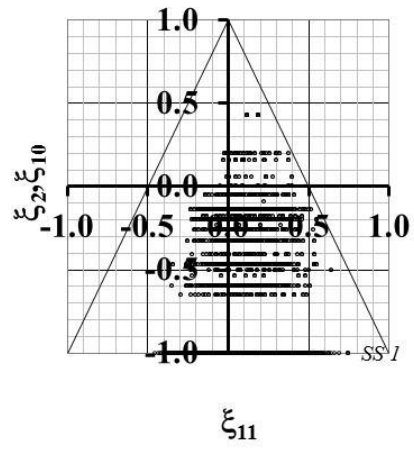
(a)



(d)

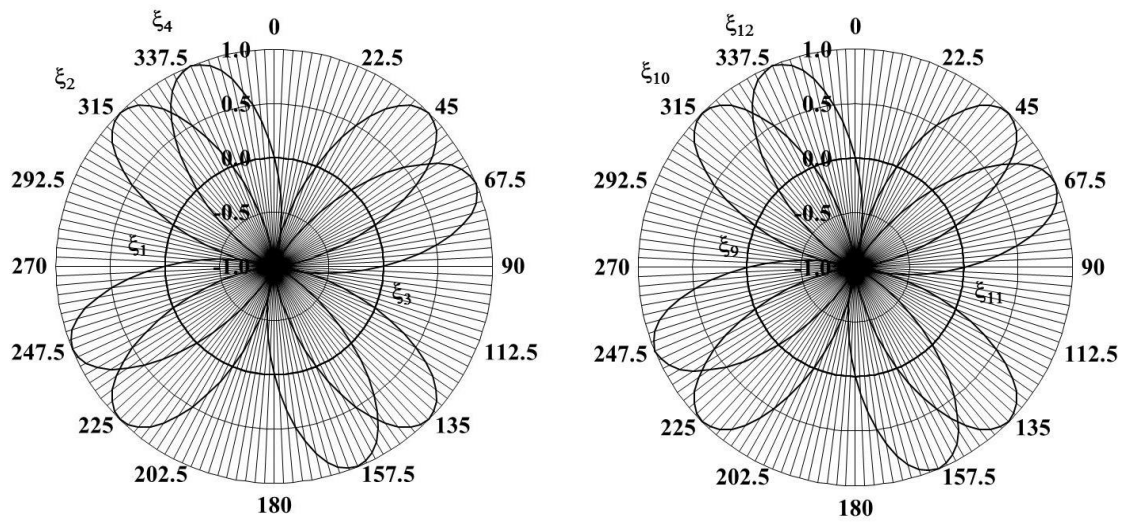


(b)

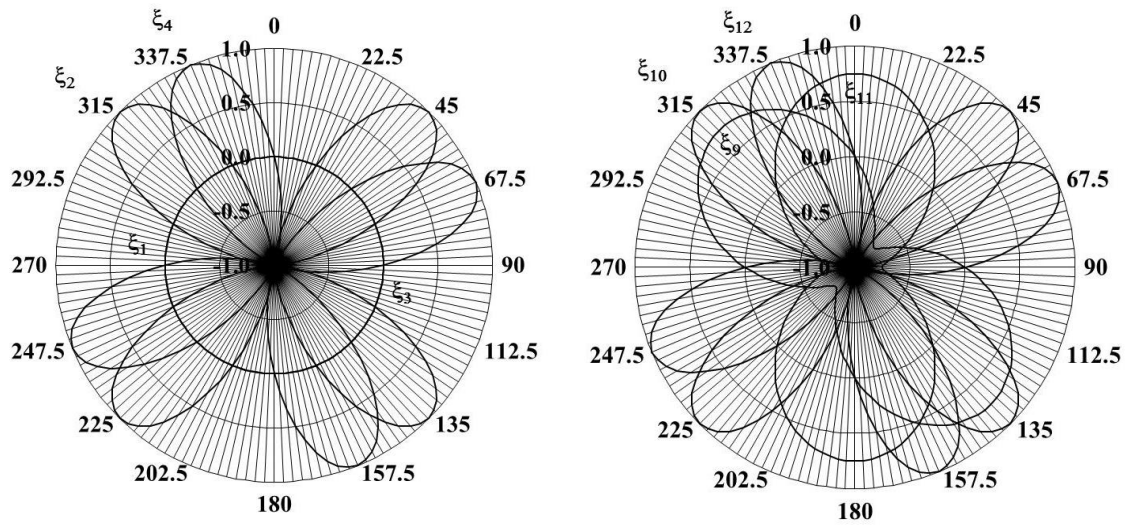


(c)

Figure 4

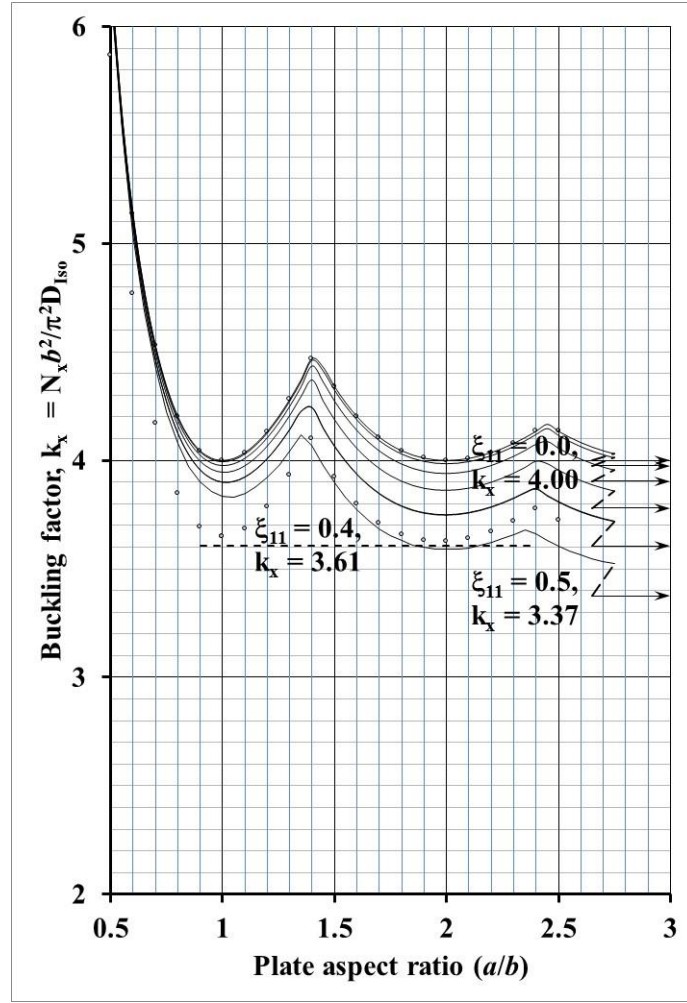


(a)



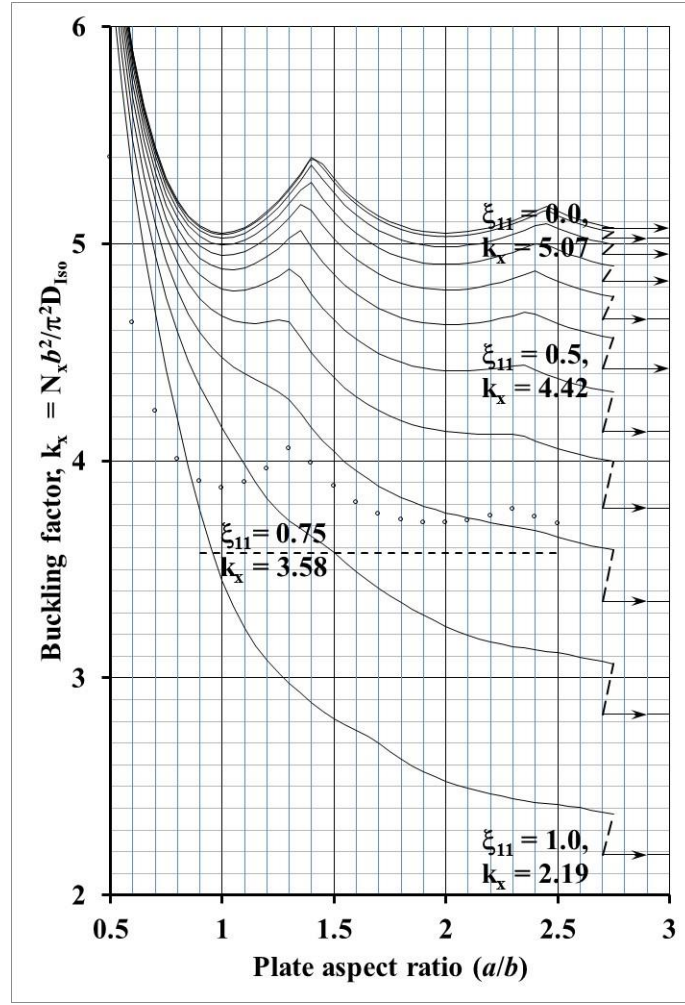
(b)

Figure 5



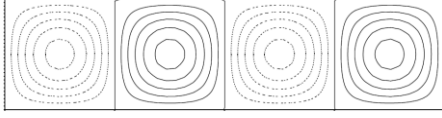
(a)

Figure 6

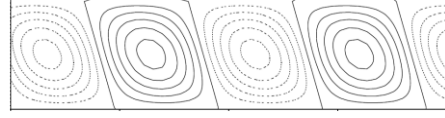


(b)

Figure 6



(a) $\xi_{11} = 0.0$, $k_{x,\infty} = 4.00$ and $\lambda = b$



(b) $\xi_{11} = 0.5$, $k_{x,\infty} = 3.37$ and $\lambda = (286/300)b$

Figure 7

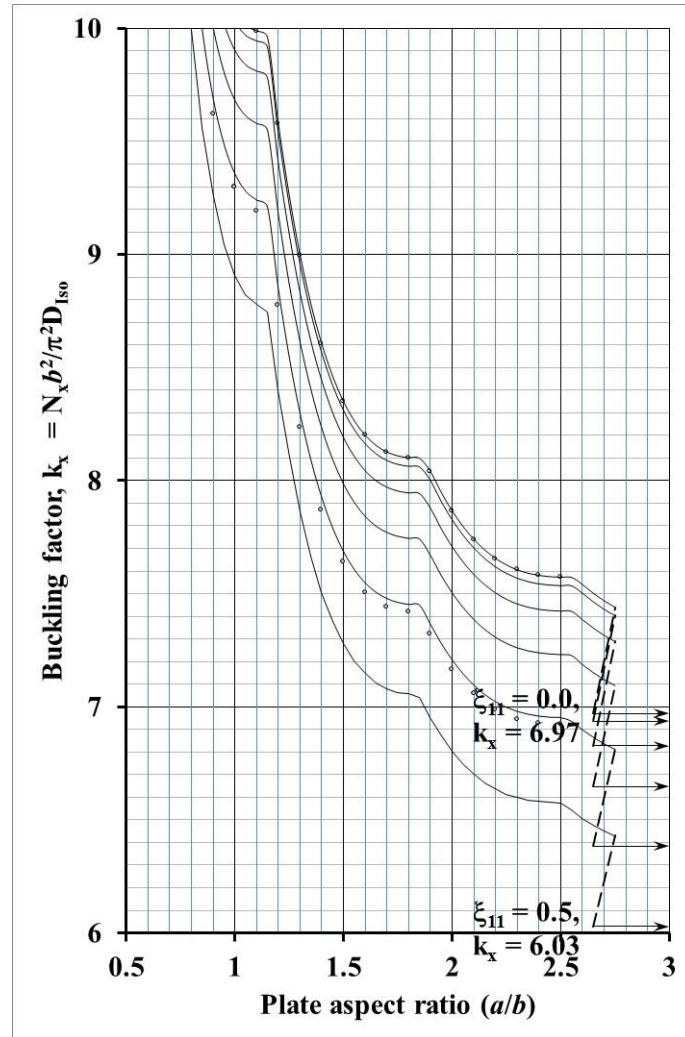


Figure 8

Figure Captions

Figure 1 – Lamination parameter design spaces for the *Bending-Twisting* coupled laminates with $4 \leq n \leq 18$, listed in abridged form in Table A9, with Non-symmetric angle-ply and Non-symmetric cross-ply sub-sequences (*NN*), corresponding to: (a) plan, (b) front elevation and (c) side elevation for bending stiffness and; (d) extensional stiffness.

Figure 2 – Lamination parameter design spaces for the *Bending-Twisting* coupled laminates with $4 \leq n \leq 18$, listed in abridged form in Table A13, with Symmetric angle-ply and Symmetric cross-ply sub-sequences (*SS*), corresponding to: (a) plan, (b) front elevation and (c) side elevation for bending stiffness and; (d) extensional stiffness.

Figure 3 – Lamination parameter design space for: (a) ply percentages, indicating the sub-region used in practical design; (b) Quasi-Homogeneous ($A_S B_0 D_S$) laminates, i.e. $\xi_1 = \xi_9$ and $\xi_2 = \xi_{10}$, corresponding to the sequence configurations listed in Ref. [1] with $8 \leq n \leq 21$ plies, and indicating the 15 grid points used in the derivation of the 4th order polynomial of Eq. (24) used to generate the: (d) compression buckling contours, $k_{x,\infty}$, for infinitely long plates with simply supported edges and; (b) mapping of relative angle-ply percentages for Quasi-Homogeneous ($A_F B_0 D_F$) laminates, i.e., $\xi_3 = \xi_{11}$.

Figure 4 – Pseudo Quasi-Homogeneous ($A_S B_0 D_F$) laminate design space, i.e. $\xi_1 = \xi_9$ and $\xi_2 = \xi_{10}$, for laminates with 4, 8, $11 \leq n \leq 21$ plies, corresponding to third angle orthographic projection of: (a) plan view; (b) front elevation and; (c) side elevation for bending stiffness. The Isometric view (d) is shown to aid interpretation of the point cloud data.

Figure 5 – Polar plots of lamination parameter variation with off-axis material alignment, β , for: (a) Quasi-Homogeneous ($\xi_{11} = 0$) laminate $[+/-2/+/-/+2/-]_S$ and; (b)

Pseudo Quasi-Homogeneous ($\xi_{11} = 0.75$) laminate $[+4/-4]_s$, corresponding to $\xi_9 = 0$ and $\xi_{10} = -1.0$ on Fig. 4.

Figure 6 – Compression buckling factor curves for continuous plates with: (a) Quasi-Isotropic laminates $(\xi_9, \xi_{10}) = (0,0)$ and $\xi_{11} = 0, 0.1, 0.2, 0.3, 0.4$ and 0.5 and; (b) Angle-ply laminates $(\xi_9, \xi_{10}) = (0,-1.0)$ and $\xi_{11} = 0, 0.1, \dots, 0.9$ and 1.0 . Discrete ABAQUS results for isolated plates with isotropic material after Ref. [18], i.e., $\xi_{11} = 0$, and *Bending-Twisting* coupled laminates with $\xi_{11} = 0.4$ and 0.75 , representing stacking sequences $[+/\bigcirc/\bullet/+\bullet/-2/\bigcirc]_s$ and $[+4/-4]_s$, respectively, are provided for comparison.

Figure 7 – Compression buckling mode shape comparisons for the infinitely long plate with simply supported edges, corresponding to Pseudo Quasi-Homogeneous Quasi-Isotropic laminates with: (a) $\xi_{11} = 0.0$ and (b) $\xi_{11} = 0.5$. Plate width b intervals are indicated along the panel edge.

Figure 8 – Compression buckling factor curves for clamped plate results with Quasi-Isotropic laminates $(\xi_9, \xi_{10}) = (0,0)$ and $\xi_{11} = 0, 0.1, 0.2, 0.3, 0.4$ and 0.5 . Asymptotes represent the infinitely long plate results are indicated together with the bounding values for k_x . Discrete ABAQUS results for isolated plates with isotropic material after Ref. [18], i.e., $\xi_{11} = 0$, and *Bending-Twisting* coupled laminates with $\xi_{11} = 0.4$, representing stacking sequences $[+/\bigcirc/\bullet/+\bullet/-2/\bigcirc]_s$, is provided for comparison.

Tables

Table 1 – Unrestrained thermal (contraction) response of square, initially flat, composite laminates. Stacking sequence configurations containing cross- and angle-ply sub-sequences are representative of the minimum ply number grouping of each class of laminate.

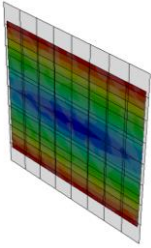
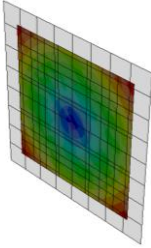
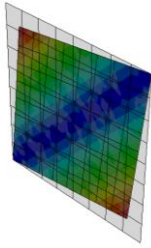
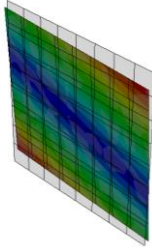
Uncoupled in Extension (A_S)		Extension-Shearing (A_F)	
Uncoupled in Bending (D_S)	Bending-Twisting (D_F)	Bending-Twisting (D_F)	Uncoupled in Bending (D_S)
$A_S B_0 D_S$ [+/-2/O/+2/-] _T	$A_S B_0 D_F$ [+/-/-/+] _T	$A_F B_0 D_F$ [+/ ₊] _T	$A_F B_0 D_S$ [±/O/-/O/-3/O/-3/O/+] _T
			
<i>Simple laminate</i>	<u><i>B-T</i></u>	<u><i>E-S;B-T</i></u>	<u><i>E-S</i></u>

Table 2 – Calculation procedure for the non-dimensional parameters for an $\mathbf{A}_S\mathbf{B}_0\mathbf{D}_F$ laminates.

Ply	θ	A				B				D			
		$A\Sigma_+$	$A\Sigma_-$	$A\Sigma_\circ$	$A\Sigma_\bullet$	$B\Sigma_+$	$B\Sigma_-$	$B\Sigma_\circ$	$B\Sigma_\bullet$	$D\Sigma_+$	$D\Sigma_-$	$D\Sigma_\circ$	$D\Sigma_\bullet$
		$(z_k - z_{k-1})$			$(z_k^2 - z_{k-1}^2)$				$(z_k^3 - z_{k-1}^3)$				
		<u>4</u>	<u>4</u>	<u>4</u>	<u>4</u>	<u>0</u>	<u>0</u>	<u>0</u>	<u>0</u>	<u>460</u>	<u>52</u>	<u>256</u>	<u>256</u>
1	+	1	→	1		-15	→	-15		169	→	169	
2	○	1			1	-13	→		-13	127	→		127
3	●	1				-11	→		-11	91	→		91
4	+	1	→	1		-9	→	-9		61	→	61	
5	●	1			1	-7	→		-7	37	→		37
6	-	1	→	1		-5	→	-5		19	→	19	
7	-	1	→	1		-3	→	-3		7	→	7	
8	○	1			1	-1	→		-1	1	→		1
9	○	1			1	1	→		1	1	→		1
10	-	1	→	1		3	→	3		7	→	7	
11	-	1	→	1		5	→	5		19	→	19	
12	●	1			1	7	→		7	37	→		37
13	+	1	→	1		9	→	9		61	→	61	
14	●	1			1	11	→		11	91	→		91
15	○	1			1	13	→		13	127	→		127
16	+	1	→	1		15	→	15		169	→	169	

Table 3 – Design space (%) comparisons for each sub-symmetric grouping for: (a) *Bending-Twisting* coupled ($\mathbf{A}_S\mathbf{B}_0\mathbf{D}_F$) laminates and; (b) Fully uncoupled ($\mathbf{A}_S\mathbf{B}_0\mathbf{D}_S$) or *Simple* laminates. The total number of solutions to which the percentages relate, are given in the final row.

(a)												
n	7	8	9	10	11	12	13	14	15	16	17	18
NC	-	-	-	-	-	-	-	-	-	-	0.1%	-
NN	-	-	16.7%	-	35.8%	20.0%	52.1%	32.0%	68.0%	54.0%	79.9%	69.5%
NS	-	-	-	-	7.5%	6.2%	10.8%	11.2%	10.5%	11.8%	8.0%	10.3%
SC	-	-	-	-	3.8%	2.8%	0.9%	-	0.9%	1.1%	0.3%	-
SN	-	-	-	-	-	-	4.8%	4.8%	4.3%	4.0%	3.8%	4.7%
SS	100%	100%	83.3%	100%	52.8%	71.0%	31.4%	52.0%	16.3%	29.1%	7.9%	15.5%
Σ	8	15	36	56	212	290	1,336	1,500	9,666	10,210	75,540	73,068

(b)												
n	7	8	9	10	11	12	13	14	15	16	17	18
AC	-	-	-	-	-	-	-	-	6.7%	3.3%	4.6%	-
AN	-	-	-	-	-	-	-	-	6.7%	-	12.7%	8.2%
AS	100%	100%	100%	100%	100%	84.0%	100%	86.4%	80.0%	74.4%	54.7%	58.3%
NN	-	-	-	-	-	-	-	-	5.6%	11.9%	24.0%	24.6%
NS	-	-	-	-	-	-	-	-	-	0.6%	0.7%	1.5%
SC	-	-	-	-	-	-	-	-	-	0.6%	0.2%	-
SN	-	-	-	-	-	-	-	-	-	-	0.4%	0.5%
SS	-	-	-	-	-	16.0%	-	13.6%	1.1%	9.2%	2.7%	6.9%
Σ	2	1	6	6	24	25	84	88	360	360	1,832	1,603

Table 4 – Design space occupied by $\pi/3$ Quasi-Isotropic laminates for the various forms of sub-sequence symmetries, including total number (Σ) of configurations, for each ply number grouping. Ply number groupings ($n =$) 8 and 16 represent $\pi/4$ Quasi-Isotropic laminates.

n	4	5	6	7	8	9	10	11	12	13	14	15	16	17	18
NN	-	-	-	-	-	6	-	-	58	-	-	1,064	1,524	-	14,826
NS	-	-	-	-	-	-	-	-	-	-	-	144	-	-	1,104
SC	-	-	-	-	-	-	-	-	-	-	-	-	100	-	-
SN	-	-	-	-	-	-	-	-	-	-	-	-	-	-	-
SS	-	-	4	-	6	-	-	-	58	-	-	-	624	-	1,102
Σ	-	-	4	-	6	6	-	-	116	-	-	1,208	2,248	-	17,032

Table 5 – Design space occupied by Pseudo Quasi-Homogeneous laminates for $11 \leq n \leq 21$ ply *Bending-Twisting* coupled ($\mathbf{A}_s\mathbf{B}_0\mathbf{D}_F$) laminates corresponding to the various forms of sub-sequence symmetries, including total number (Σ) of configurations, for each ply number grouping. The single solution for $n = 4$, i.e., $[+/-]_s$, the three solutions for $n = 8$, i.e., $[+/-/-/+]_s$, $[+/-/+/-]_s$ and $[+ /+ /-/-]_s$, are not presented.

n	11	12	13	14	15	16	17	18	19	20	21
NC	-	-	-	-	-	-	-	-	-	-	-
NN	2	-	44	-	100	32	314	544	1,480	1,710	1,680
NS	-	18	-	-	-	270	128	-	20	2,590	32
SC	-	-	-	-	-	-	-	-	-	6	-
SN	-	-	-	-	-	-	-	-	-	-	-
SS	-	10	-	6	-	86	-	-	20	152	36
Σ	2	28	44	6	100	388	442	544	1,520	4,458	1,748

Table 6 – Benchmark configurations for damage assessment, after Ref. [19].

Stacking Sequence Configuration		ξ_9	ξ_{10}	ξ_{11}	ξ_{12}
(1)	$[0^\circ/90^\circ/-45^\circ/+45^\circ]_S$	0.28	0.75	-0.09	0.00
(2)	$[0^\circ/-45^\circ/+45^\circ/90^\circ]_S$	0.56	0.19	0.19	0.00
(3)	$[45^\circ/0^\circ/90^\circ/-45^\circ]_S$	0.19	-0.19	0.56	0.00
(4)	$[+30^\circ/90^\circ/-30^\circ/90^\circ]_S$	0.03	-0.03	0.41	0.41

Table 7 – Transformed reduced stiffness, Q'_{ij} (N/mm²), for IM7/8552 carbon-fiber/epoxy with $\theta = -45^\circ, 45^\circ, 0^\circ$ and 90° .

θ	Q'_{11}	Q'_{12}	Q'_{16}	Q'_{22}	Q'_{26}	Q'_{66}
-45	50,894	40,554	-37,791	50,894	-37,791	41,355
45	50,894	40,554	37,791	50,894	37,791	41,355
0	162,660	4,369	0	11,497	0	5,170
90	11,497	4,369	0	162,660	0	5,170

Electronic Appendix

This electronic appendix to the main article on *Bending-Twisting* coupled laminates contains:

A proof for non-dimensional design constraints;

Abridged listings of stacking sequences and non-dimensional parameters, which are given in Tables A8 – A13, and represent each distinct form of sub-sequence symmetry found;

Third angle orthographic projections of the 3-dimensional design space for bending stiffness lamination parameters ($\xi_9, \xi_{10}, \xi_{11}$) and 2-dimensional extensional stiffness lamination parameters (ξ_1, ξ_2), when standard ply angles $0^\circ, \pm 45^\circ$ and 90° are adopted and;

Pseudo quasi-homogeneous laminate stacking sequence listings for practical fuselage thickness, i.e. $12 \leq n \leq 16$ plies.

A1. Proof for non-dimensional design constraints

Elements of the stiffness matrices are related to lamination parameters and laminate invariants, originally conceived by Tsai and Hahn [12], through the following equations:

$$\begin{aligned}
 A_{11} &= \{U_1 + \xi_1 U_2 + \xi_2 U_3\} \times H \\
 A_{12} &= A_{21} = \{-\xi_2 U_3 + U_4\} \times H \\
 A_{16} &= A_{61} = \{\xi_3 U_2/2 + \xi_4 U_3\} \times H \\
 A_{22} &= \{U_1 - \xi_1 U_2 + \xi_2 U_3\} \times H \\
 A_{26} &= A_{62} = \{\xi_3 U_2/2 - \xi_4 U_3\} \times H \\
 A_{66} &= \{-\xi_2 U_3 + U_5\} \times H
 \end{aligned} \tag{A1}$$

$$\begin{aligned}
 B_{11} &= \{\xi_5 U_2 + \xi_6 U_3\} \times H^2/4 \\
 B_{12} &= B_{21} = \{-\xi_6 U_3\} \times H^2/4 \\
 B_{16} &= B_{61} = \{\xi_7 U_2/2 + \xi_8 U_3\} \times H^2/4 \\
 B_{22} &= \{-\xi_5 U_2 + \xi_6 U_3\} \times H^2/4 \\
 B_{26} &= B_{62} = \{\xi_7 U_2/2 - \xi_8 U_3\} \times H^2/4 \\
 B_{66} &= \{-\xi_6 U_3\} \times H^2/4 = 0
 \end{aligned} \tag{A2}$$

$$\begin{aligned}
 D_{11} &= \{U_1 + \xi_9 U_2 + \xi_{10} U_3\} \times H^3/12 \\
 D_{12} &= D_{21} = \{U_4 - \xi_{10} U_3\} \times H^3/12 \\
 D_{16} &= D_{61} = \{\xi_{11} U_2/2 + \xi_{12} U_3\} \times H^3/12 \\
 D_{22} &= \{U_1 - \xi_9 U_2 + \xi_{10} U_3\} \times H^3/12 \\
 D_{26} &= D_{62} = \{\xi_{11} U_2/2 - \xi_{12} U_3\} \times H^3/12 \\
 D_{66} &= \{-\xi_{10} U_3 + U_5\} \times H^3/12
 \end{aligned} \tag{A3}$$

where the U_i are calculated from the reduced stiffness terms, Q_{ij} , of Eq. (22) in the main body of the article.

These ply orientation dependent lamination parameters are related to the non-dimensional parameters for the A, B and D matrices through the following expressions:

$$\begin{aligned}
 \xi_1 &= \{n_+ \cos(2\theta_+) + n_- \cos(2\theta_-) + n_o \cos(2\theta_o) + n_\bullet \cos(2\theta_\bullet)\}/n \\
 \xi_2 &= \{n_+ \cos(4\theta_+) + n_- \cos(4\theta_-) + n_o \cos(4\theta_o) + n_\bullet \cos(4\theta_\bullet)\}/n
 \end{aligned} \tag{A4}$$

$$\xi_3 = \{n_+\sin(2\theta_+) + n_-\sin(2\theta_-) + n_o\sin(2\theta_o) + n_\bullet\sin(2\theta_\bullet)\}/n$$

$$\xi_4 = \{n_+\sin(4\theta_+) + n_-\sin(4\theta_-) + n_o\sin(4\theta_o) + n_\bullet\sin(4\theta_\bullet)\}/n$$

$$\xi_5 = \{\chi_+\cos(2\theta_+) + \chi_-\cos(2\theta_-) + \chi_o\cos(2\theta_o) + \chi_\bullet\cos(2\theta_\bullet)\}/n^2$$

$$\xi_6 = \{\chi_+\cos(4\theta_+) + \chi_-\cos(4\theta_-) + \chi_o\cos(4\theta_o) + \chi_\bullet\cos(4\theta_\bullet)\}/n^2$$

$$\xi_7 = \{\chi_+\sin(2\theta_+) + \chi_-\sin(2\theta_-) + \chi_o\sin(2\theta_o) + \chi_\bullet\sin(2\theta_\bullet)\}/n^2$$

$$\xi_8 = \{\chi_+\sin(4\theta_+) + \chi_-\sin(4\theta_-) + \chi_o\sin(4\theta_o) + \chi_\bullet\sin(4\theta_\bullet)\}/n^2$$

(A5)

$$\xi_9 = \{\zeta_+\cos(2\theta_+) + \zeta_-\cos(2\theta_-) + \zeta_o\cos(2\theta_o) + \zeta_\bullet\cos(2\theta_\bullet)\}/n^3$$

$$\xi_{10} = \{\zeta_+\cos(4\theta_+) + \zeta_-\cos(4\theta_-) + \zeta_o\cos(4\theta_o) + \zeta_\bullet\cos(4\theta_\bullet)\}/n^3$$

$$\xi_{11} = \{\zeta_+\sin(2\theta_+) + \zeta_-\sin(2\theta_-) + \zeta_o\sin(2\theta_o) + \zeta_\bullet\sin(2\theta_\bullet)\}/n^3$$

$$\xi_{12} = \{\zeta_+\sin(4\theta_+) + \zeta_-\sin(4\theta_-) + \zeta_o\sin(4\theta_o) + \zeta_\bullet\sin(4\theta_\bullet)\}/n^3$$

(A6)

For *Bending-Twisting* coupled ($A_S B_0 D_F$) laminates, the elements of the stiffness matrices should satisfy the following constraints:

$$A_{16} = A_{26} = 0$$

$$B_{ij} = 0$$

$$D_{16}, D_{26} \neq 0$$

(A7)

Inserting the constraints of Eq. (A7) into Eqs (A4) - (A6) gives:

$$A_{16} = A_{26} = 0 \quad \rightarrow \xi_3 = \xi_4 = 0$$

$$B_{ij} = 0 \quad \rightarrow \xi_5 = \xi_6 = \xi_7 = \xi_8 = 0$$

$$D_{16}, D_{26} \neq 0 \quad \rightarrow \xi_{11}, \xi_{12} \neq 0$$

(A8)

The lamination parameters for $A_S B_0 D_S$ laminates should therefore satisfy the following constraints:

$$\xi_3 = \xi_4 = 0$$

$$\xi_5 = \xi_6 = \xi_7 = \xi_8 = 0$$

$$\xi_{11}, \xi_{12} \neq 0$$

(A9)

Applying the lamination parameter constraints of Eq. (A9) to the lamination parameters of Eqs (A4) – (A6), for laminates containing 0° and 90° cross plies and angle plies with arbitrary orientations θ° , gives:

$$\begin{aligned}
\xi_3 &= \{n_+\sin(2\theta_+) + n_-\sin(2\theta_-) + n_0\sin(2 \times 0) + n_{90^\circ}\sin(2 \times 90)\}/n \\
\xi_3 &= \{n_+\sin(2\theta_+) + n_-\sin(2\theta_-)\}/n = 0 \quad \rightarrow n_+ = n_- \\
\xi_4 &= \{n_+\sin(4\theta_+) + n_-\sin(4\theta_-) + n_0\sin(4 \times 0) + n_{90^\circ}\sin(4 \times 90)\}/n \\
\xi_4 &= \{n_+\sin(4\theta_+) + n_-\sin(4\theta_-)\}/n = 0 \quad \rightarrow n_+ = n_-
\end{aligned} \tag{A10}$$

$$\begin{aligned}
\xi_5 &= \{\chi_+\cos(2\theta_+) + \chi_-\cos(2\theta_-) + \chi_0\cos(2 \times 0) + \chi_{90}\cos(2 \times 90)\}/n^2 \\
&\{(\chi_+ + \chi_-)\cos(2\theta_+) + \chi_0 - \chi_{90}\}/n^2 = 0 \quad \rightarrow (\chi_+ + \chi_-)\cos(2\theta_+) + \chi_0 - \chi_{90} = 0 \\
\xi_6 &= \{\chi_+\cos(4\theta_+) + \chi_-\cos(4\theta_-) + \chi_0\cos(4 \times 0) + \chi_{90}\cos(4 \times 90)\}/n^2 \\
&\{(\chi_+ + \chi_-)\cos(4\theta_+) + \chi_0 + \chi_{90}\}/n^2 = 0 \quad \rightarrow (\chi_+ + \chi_-)\cos(4\theta_+) + \chi_0 + \chi_{90} = 0 \\
\xi_7 &= \{\chi_+\sin(2\theta_+) + \chi_-\sin(2\theta_-) + \chi_0\sin(2 \times 0) + \chi_{90}\sin(2 \times 90)\}/n^2 \\
&(\chi_+ + \chi_-)\sin(2\theta_-)/n^2 = 0 \quad \rightarrow \chi_+ = \chi_- = 0 \\
\xi_8 &= \{\chi_+\sin(4\theta_+) + \chi_-\sin(4\theta_-) + \chi_0\sin(4 \times 0) + \chi_{90}\sin(4 \times 90)\}/n^2 \\
&(\chi_+ + \chi_-)\sin(4\theta_-)/n^2 = 0 \quad \rightarrow \chi_+ = \chi_- = 0
\end{aligned} \tag{A11}$$

$$\begin{aligned}
\xi_{11} &= \{\zeta_+\sin(2\theta_+) + \zeta_-\sin(2\theta_-) + \zeta_0\sin(2 \times 0) + \zeta_{90^\circ}\sin(2 \times 90)\}/n \\
\xi_{11} &= (\zeta_+ - \zeta_-)\sin(2\theta_+)/n^3 \neq 0 \quad \rightarrow (\zeta_+ - \zeta_-) \neq 0 \\
\xi_{12} &= \{\zeta_+\sin(4\theta_+) + \zeta_-\sin(4\theta_-) + \zeta_0\sin(4 \times 0) + \zeta_{90^\circ}\sin(4 \times 90)\}/n^3 \\
\xi_{12} &= (\zeta_+ - \zeta_-)\sin(4\theta_+)/n^3 \neq 0 \quad \rightarrow (\zeta_+ - \zeta_-) \neq 0
\end{aligned} \tag{A12}$$

Therefore, $A_5B_0D_F$ laminates should satisfy the following non-dimensional parameter constraints when angle-ply (+/-) can be assigned any arbitrary orientation, $0 < \theta < 90^\circ$, and the cross-ply (\bigcirc/\bullet , representing $0^\circ/90^\circ$) can be interchanged:

$$\begin{aligned}
n_+ &= n_- \\
\chi_+ &= \chi_- = 0 \\
\chi_0 &= \chi_{90} = 0 \\
\zeta_+, \zeta_- &\neq 0
\end{aligned} \tag{A13}$$

A2. Abridged Stacking sequence listings

Abridged listings of stacking sequences and non-dimensional parameters are given in Tables A8 – A13, representing each distinct form of sub-sequence symmetry found. As adopted in the listings [3,11] for *Simple* or uncoupled laminates, the stacking sequence configurations with *Bending-Twisting* coupling are ordered in terms of ascending numbers of plies, n , or bending stiffness parameter ζ ($= n^3$), which are in turn ordered by ascending value of the bending stiffness parameter for the angle plies ($\zeta_{\pm} = \zeta_+ + \zeta_-$). This is a logic approach for design, given that compression buckling strength increases directly with increasing ζ_{\pm} . For *Bending-Twisting* coupled laminates, a ratio (ζ_+/ζ_{\pm}) of the bending stiffness parameters for angle plies is introduced. Sequences with the same ζ ($= n^3$) are ordered in descending order of $|(\zeta_+/\zeta_{\pm}) - (\zeta_-/\zeta_{\pm})|$ to reflect the increasing compression buckling strength that these designs possess as they approach their uncoupled ($|(\zeta_+/\zeta_{\pm}) - (\zeta_-/\zeta_{\pm})| = 0$) counterparts. Finally sequences are ordered in descending order of $|(\zeta_o/(\zeta_o + \zeta_{\bullet}) - (\zeta_{\bullet}/(\zeta_o + \zeta_{\bullet}))|$, representing the relative difference in bending stiffness of cross-ply sub-sequences; this is introduced for laminates with matching ζ and $|(\zeta_+/\zeta_{\pm}) - (\zeta_-/\zeta_{\pm})|$, since compression buckling strength of infinitely long plates is maximised when $\zeta_o/(\zeta_o + \zeta_{\bullet}) = (\zeta_{\bullet}/(\zeta_o + \zeta_{\bullet}))$. The numbering of sequences within each sub-symmetric form, described in the previous section, may therefore be readily extended for laminates with higher ply number groupings.

Table A8 – Stacking sequences for *NC* laminates with Non-symmetric angle-ply and Cross-symmetric cross-ply sub-sequences with $n = 17$.

Ref.	Sequence	n	n_{\pm}	n_o	ζ_{\pm}	ζ_o	ζ_+/ζ_{\pm} (%)
<i>NC 1</i>	+ ● ● - - + + ● ● ○ - - + + ○ ● +	17	10	4	2842	1036	70.3
:	:	:	:	:	:	:	:
<i>NC 104</i>	+ + - - ○ ● - ● ○ ○ + ○ ● - + + -	17	10	4	4282	316	56.7

Table A9 – Stacking sequences for *NN* laminates with Non-symmetric angle-ply and Non-symmetric cross-ply sub-sequences with $9 \leq n \leq 18$. Reference numbers marked with an asterisk (*) are quasi-isotropic.

Ref.	Sequence	n	n_{\pm}	n_o	ζ_{\pm}	ζ_o	ζ_+/ζ_{\pm} (%)
<i>NN 1*</i>	+ ● - ● - + - + ●	9	6	0	414	0	76.1
:	:	:	:	:	:	:	:
<i>NN 6*</i>	+ ○ - - + ○ ○ - +	9	6	3	558	171	69.4
<i>NN 7</i>	+ ● ● ● - - - + + ● ●	11	6	0	486	0	94.4
:	:	:	:	:	:	:	:
<i>NN 82</i>	+ - - ○ ○ + + - ○ + -	11	8	3	1160	171	43.8
<i>NN 83*</i>	+ ● ● + - - - - ● + + ●	12	8	0	896	0	92.9
:	:	:	:	:	:	:	:

<i>NN 140*</i>	+ - - ○ ○ + ○ + - ○ + -	12 8 4 1472 256 43.5
<i>NN 141</i>	+ ● ● ● ● - - - + ● + ● ●	13 6 0 702 0 96.2
:	:	:
<i>NN 836</i>	+ - - ○ + + - ○ ○ - + + -	13 10 3 2026 171 48.8
<i>NN 837</i>	+ ● ● ● - + - - ● - + + ● ●	14 8 0 1088 0 85.3
:	:	:
<i>NN 1316</i>	+ - - ○ ○ + ● ● ○ + - ○ + -	14 8 4 2240 496 43.6
<i>NN 1317</i>	+ ● ● ● ● ● - - - ● + + ● ● ●	15 6 0 918 0 97.1
:	:	:
<i>NN 7886</i>	+ - + - - ○ ○ + - + ○ + - + -	15 12 3 3204 171 48.9
<i>NN 7887</i>	+ ● ● ● ● - - + ● - - + + ● ● ●	16 8 0 1280 0 83.8
:	:	:
<i>NN 13398</i>	+ + - - - ○ ○ - ○ + + ○ + + - -	16 12 4 3840 256 49.4
<i>NN 13399</i>	+ ● ● ● ● ● - - - ● + ● + ● ● ●	17 6 0 1206 0 97.8
:	:	:
<i>NN 73754</i>	+ - - + + - ○ ○ - + - ○ + + - + -	17 14 3 4742 171 49.7
<i>NN 73755</i>	+ ● ● ● ● ● - - ● + - - + + ● ● ● ●	18 8 0 1472 0 85.9
:	:	:
<i>NN 124556</i>	+ - - + ○ - + ○ ● ● + ○ ○ - - + - +	18 12 4 5328 496 50.9

Table A10 – Stacking sequences for *NS* laminates with Non-symmetric angle-ply and Symmetric cross-ply sub-sequences with $11 \leq n \leq 18$. Reference numbers marked with an asterisk (*) are quasi-isotropic.

Ref.	Sequence	n	n_{\pm}	n_o	ζ_{\pm}	ζ_o	ζ_{+}/ζ_{\pm} (%)
<i>NS 1</i>	+ - + - + ● - - - + +	11	10	0	1330	0	68.9
:	:	:	:	:	:	:	:
<i>NS 16</i>	+ - + - - ○ + - + + -	11	10	1	1330	1	54.5
<i>NS 17</i>	+ - + + - - - + - - + +	12	12	0	1728	0	70.8
:	:	:	:	:	:	:	:
<i>NS 34</i>	+ - - + + - - + - + + -	12	12	0	1728	0	51.4
<i>NS 35</i>	+ ● - + - + ● - - - + ● +	13	10	0	1594	0	74.1
:	:	:	:	:	:	:	:
<i>NS 178</i>	+ - - + + - ○ - + - + + -	13	12	1	2196	1	51.6
<i>NS 179</i>	+ ● - + + - - - + - - + ● +	14	12	0	2016	0	75.0
:	:	:	:	:	:	:	:
<i>NS 346</i>	+ - - + + - ○ ○ - + - + + -	14	12	2	2736	8	51.8
<i>NS 347*</i>	+ ● ● - + - + ● - - - + ● ● +	15	10	0	1906	0	78.3
:	:	:	:	:	:	:	:
<i>NS 1362</i>	+ - + - - - + ○ + + + - - - +	15	14	1	3374	1	49.3
<i>NS 1363</i>	+ ● ● - + + - - - + - - + ● ● +	16	12	0	2352	0	78.6

:	:
<i>NS 2568</i>	+ + - - - - + - + + - + - + - 16 16 0 4096 0 50.6
<i>NS 2569</i>	+ ● ● ● - + - + ● - - - + ● ● ● + 17 10 0 2266 0 81.8
:	:
<i>NS 8620</i>	+ - - + + - + - ○ - - + + + - + - 17 16 1 4912 1 51.0
<i>NS 8621*</i>	+ ● ● ● - + + - - - + - - + ● ● ● + 18 12 0 2736 0 81.6
:	:
<i>NS 16116</i>	+ - + - - - + + ○ ○ + - + - + - - + 18 16 2 5824 8 49.6

Table A11 – Stacking sequences for *SC* laminates with Symmetric angle-ply and Cross-symmetric cross-ply sub-sequences with $11 \leq n \leq 17$. Reference numbers marked with an asterisk (*) are quasi-isotropic.

Ref.	Sequence	n	n_{\pm}	n_0	ζ_{\pm}	ζ_0	ζ_{+}/ζ_{\pm} (%)
<i>SC 1</i>	+ ● ○ - ○ ● ● - ● ○ +	11	4	3	700	315	86.0
:	:	:	:	:	:	:	:
<i>SC 8</i>	+ - ● ○ ○ ○ ● ● ○ - +	11	4	4	988	172	60.9
<i>SC 9</i>	+ ● ○ ○ ● - - ○ ● ● ○ +	12	4	4	736	496	98.9
:	:	:	:	:	:	:	:
<i>SC 16</i>	+ - ● ○ ○ ● ○ ● ● ○ - +	12	4	4	1216	256	59.9
<i>SC 17</i>	+ ● ○ ○ ● - ● - ○ ● ● ○ +	13	4	4	892	652	97.1
:	:	:	:	:	:	:	:
<i>SC 28</i>	+ - ● ○ ○ ● ○ ○ ● ● ○ - +	13	4	5	1468	365	59.0
<i>SC 29</i>	+ ● ○ ● ○ ○ - ● - ● ● ○ ● ○ +	15	4	5	1204	1085	97.8
:	:	:	:	:	:	:	:
<i>SC 112</i>	+ - - + ● ○ ○ ○ ○ ● ● ○ + - - +	15	8	4	3032	172	51.6
<i>SC 113</i>	+ ● ● ○ ○ ○ ○ - - ● ● ● ● ○ ○ +	16	4	6	1360	1368	99.4
:	:	:	:	:	:	:	:
<i>SC 226*</i>	+ - - + ● ○ ○ ● ○ ● ● ○ + - - +	16	8	4	3584	256	51.3
<i>SC 227</i>	+ ● ○ ● ○ ○ - ● ● ○ - ● ● ○ ● ○ +	17	4	6	1636	1638	94.0
:	:	:	:	:	:	:	:
<i>SC 426</i>	+ - - + ● ○ ○ ● ○ ○ ● ● ○ + - - +	17	8	5	4184	365	51.1

Table A12 – Stacking sequences for *SN* laminates with Symmetric angle-ply and Non-symmetric cross-ply sub-sequences with $13 \leq n \leq 18$.

Ref.	Sequence	n	n_{\pm}	n_0	ζ_{\pm}	ζ_0	ζ_{+}/ζ_{\pm} (%)
<i>SN 1</i>	+ ● ● ○ ○ - ● - ● ● ● ○ +	13	4	3	892	459	97.1
:	:	:	:	:	:	:	:
<i>SN 64</i>	+ - ● ○ ○ ○ ● ● ○ ● ○ - +	13	4	5	1468	413	59.0
<i>SN 65</i>	+ ● ○ ● ● ○ - - ● ○ ○ ● ● +	14	4	4	1024	496	99.2

:		:
<i>SN 136</i>	+ - ● ○ ○ ● ○ ○ ○ ● ● ○ - +	14 4 6 1744 504 58.3
<i>SN 137</i>	+ ● ○ ● ● ● - ● - ○ ○ ● ● ● +	15 4 3 1204 459 97.8
:		:
<i>SN 552</i>	+ - ● ○ ○ ● ○ ● ○ ○ ● ● ○ - +	15 4 6 2044 678 57.6
<i>SN 553</i>	+ ● ● ○ ● ● ○ - - ● ○ ○ ● ● ● +	16 4 4 1360 496 99.4
:		:
<i>SN 960</i>	+ - ● ○ ○ ● ○ ● ● ○ ○ ● ● ○ - +	16 4 6 2368 888 57.1
<i>SN 961</i>	+ ● ● ○ ● ● ● - ● - ○ ○ ● ● ● ● +	17 4 3 1564 459 98.3
:		:
<i>SN 3832</i>	+ - - + ● ○ ○ ○ ● ● ○ ● ○ + - - +	17 8 5 4184 413 51.1
<i>SN 3833</i>	+ ● ● ● ○ ● ● ○ - - ● ○ ○ ● ● ● ● +	18 4 4 1744 496 99.5
:		:
<i>SN 7272</i>	+ - - + ● ○ ○ ● ● ● ○ ● ● ● ○ + - - +	18 8 4 4832 496 51.0

Table A13 – Stacking sequences for *SS* laminates with Symmetric angle-ply and Symmetric cross-ply sub-sequences with $4 \leq n \leq 18$. Reference numbers marks with an asterisk (*) are quasi-isotropic.

Ref.	Sequence	n	n_{\pm}	n_o	ζ_{\pm}	ζ_o	ζ_{+}/ζ_{\pm} (%)
<i>SS 1</i>	+ - - +	4	4	0	64	0	87.5
<i>SS 2</i>	+ - ● - +	5	4	0	124	0	79.0
<i>SS 3</i>	+ - ○ - +	5	4	1	124	1	79.0
<i>SS 4*</i>	+ ● - - ● +	6	4	0	160	0	95.0
:		:					
<i>SS 7*</i>	+ - ○ ○ - +	6	4	2	208	8	73.1
<i>SS 8</i>	+ ● - ● - ● +	7	4	0	244	0	89.3
:		:					
<i>SS 15</i>	+ - ○ ● ○ - +	7	4	2	316	26	69.0
<i>SS 16</i>	+ ● ● - - ● ● +	8	4	0	304	0	97.4
:		:					
<i>SS 30</i>	+ - - + + - - +	8	8	0	512	0	59.4
<i>SS 31</i>	+ ● ● - ● - ● ● +	9	4	0	412	0	93.7
:		:					
<i>SS 60</i>	+ - - + ○ + - - +	9	8	1	728	1	56.6
<i>SS 61</i>	+ ● ● ● - - ● ● ● +	10	4	0	496	0	98.4
:		:					
<i>SS 116</i>	+ - - + ○ ○ + - - +	10	8	2	992	8	54.8
<i>SS 117</i>	+ ● ● ● - ● - ● ● ● +	11	4	0	628	0	95.9
:		:					
<i>SS 228</i>	+ - - + ○ ● ○ + - - +	11	8	2	1304	26	53.7
<i>SS 229</i>	+ ● ● ● ● - - ● ● ● ● +	12	4	0	736	0	98.9

SS 434																																																																																																																																																																																																																																																																																																																																																																																																																																																																																																																																																																																																																																																																																																																																																																																																																																																																																																																																																																																																																																																																																																																																																																																																																																																																																																																																																																																																																																																																																																																															</
--------	--	--	--	--	--	--	--	--	--	--	--	--	--	--	--	--	--	--	--	--	--	--	--	--	--	--	--	--	--	--	--	--	--	--	--	--	--	--	--	--	--	--	--	--	--	--	--	--	--	--	--	--	--	--	--	--	--	--	--	--	--	--	--	--	--	--	--	--	--	--	--	--	--	--	--	--	--	--	--	--	--	--	--	--	--	--	--	--	--	--	--	--	--	--	--	--	--	--	--	--	--	--	--	--	--	--	--	--	--	--	--	--	--	--	--	--	--	--	--	--	--	--	--	--	--	--	--	--	--	--	--	--	--	--	--	--	--	--	--	--	--	--	--	--	--	--	--	--	--	--	--	--	--	--	--	--	--	--	--	--	--	--	--	--	--	--	--	--	--	--	--	--	--	--	--	--	--	--	--	--	--	--	--	--	--	--	--	--	--	--	--	--	--	--	--	--	--	--	--	--	--	--	--	--	--	--	--	--	--	--	--	--	--	--	--	--	--	--	--	--	--	--	--	--	--	--	--	--	--	--	--	--	--	--	--	--	--	--	--	--	--	--	--	--	--	--	--	--	--	--	--	--	--	--	--	--	--	--	--	--	--	--	--	--	--	--	--	--	--	--	--	--	--	--	--	--	--	--	--	--	--	--	--	--	--	--	--	--	--	--	--	--	--	--	--	--	--	--	--	--	--	--	--	--	--	--	--	--	--	--	--	--	--	--	--	--	--	--	--	--	--	--	--	--	--	--	--	--	--	--	--	--	--	--	--	--	--	--	--	--	--	--	--	--	--	--	--	--	--	--	--	--	--	--	--	--	--	--	--	--	--	--	--	--	--	--	--	--	--	--	--	--	--	--	--	--	--	--	--	--	--	--	--	--	--	--	--	--	--	--	--	--	--	--	--	--	--	--	--	--	--	--	--	--	--	--	--	--	--	--	--	--	--	--	--	--	--	--	--	--	--	--	--	--	--	--	--	--	--	--	--	--	--	--	--	--	--	--	--	--	--	--	--	--	--	--	--	--	--	--	--	--	--	--	--	--	--	--	--	--	--	--	--	--	--	--	--	--	--	--	--	--	--	--	--	--	--	--	--	--	--	--	--	--	--	--	--	--	--	--	--	--	--	--	--	--	--	--	--	--	--	--	--	--	--	--	--	--	--	--	--	--	--	--	--	--	--	--	--	--	--	--	--	--	--	--	--	--	--	--	--	--	--	--	--	--	--	--	--	--	--	--	--	--	--	--	--	--	--	--	--	--	--	--	--	--	--	--	--	--	--	--	--	--	--	--	--	--	--	--	--	--	--	--	--	--	--	--	--	--	--	--	--	--	--	--	--	--	--	--	--	--	--	--	--	--	--	--	--	--	--	--	--	--	--	--	--	--	--	--	--	--	--	--	--	--	--	--	--	--	--	--	--	--	--	--	--	--	--	--	--	--	--	--	--	--	--	--	--	--	--	--	--	--	--	--	--	--	--	--	--	--	--	--	--	--	--	--	--	--	--	--	--	--	--	--	--	--	--	--	--	--	--	--	--	--	--	--	--	--	--	--	--	--	--	--	--	--	--	--	--	--	--	--	--	--	--	--	--	--	--	--	--	--	--	--	--	--	--	--	--	--	--	--	--	--	--	--	--	--	--	--	--	--	--	--	--	--	--	--	--	--	--	--	--	--	--	--	--	--	--	--	--	--	--	--	--	--	--	--	--	--	--	--	--	--	--	--	--	--	--	--	--	--	--	--	--	--	--	--	--	--	--	--	--	--	--	--	--	--	--	--	--	--	--	--	--	--	--	--	--	--	--	--	--	--	--	--	--	--	--	--	--	--	--	--	--	--	--	--	--	--	--	--	--	--	--	--	--	--	--	--	--	--	--	--	--	--	--	--	--	--	--	--	--	--	--	--	--	--	--	--	--	--	--	--	--	--	--	--	--	--	--	--	--	--	--	--	--	--	--	--	--	--	--	--	--	--	--	--	--	--	--	--	--	--	--	--	--	--	--	--	--	--	--	--	--	--	--	--	--	--	--	--	--	--	--	--	--	--	--	--	--	--	--	--	--	--	--	--	--	--	--	--	--	--	--	--	--	--	--	--	--	--	--	--	--	--	--	--	--	--	--	--	--	--	--	--	--	--	--	--	--	--	--	--	--	--	--	--	--	--	--	--	--	--	--	--	--	--	--	--	--	--	--	--	--	--	--	--	--	--	--	--	--	--	--	--	--	--	--	--	--	--	--	--	--	--	--	--	--	--	--	--	--	--	--	--	--	--	--	--	--	--	--	--	--	--	--	--	--	--	--	--	--	--	--	--	--	--	--	--	--	--	--	--	--	--	--	--	--	--	--	--	--	--	--	--	--	--	--	--	--	--	--	--	--	--	--	--	--	--	--	--	--	--	--	--	--	--	--	--	--	--	--	--	--	--	--	--	--	--	--	--	--	--	--	--	--	--	--	--	--	--	--	--	--	--	--	--	--	--	--	--	--	--	--	--	--	--	--	--	--	--	--	--	--	--	--	--	--	--	--	--	--	--	--	--	--	--	--	--	--	--	--	--	--	--	--	--	--	--	--	--	--	--	--	--	--	--	--	--	--	--	--	--	--	--	--	--	--	--	--	--	--	--	--	--	--	--	--	--	--	--	--	--	--	--	--	--	--	--	--	--	--	--	--	--	--	--	--	--	--	--	--	--	--	--	--	--	--	--	--	--	--	--	--	--	--	--	--	--	--	--	--	--	--	--	--	--	--	--	--	--	--	--	--	--	--	--	--	--	--	--	--	--	--	--	--	--	--	--	--	--	--	--	--	--	--	--	--	--	--	--	--	--	--	--	--	--	--	--	--	--	--	--	--	--	--	--	--	--	--	--	--	--	--	--	--	--	--	--	--	--	--	--	--	--	--	--	--	--	--	--	--	--	--	--	--	--	--	--	--	--	--	--	--	--	--	--	--	--	--	--	--	--	--	--	--	--	--	--	--	--	--	--	--	--	--	--	--	--	--	--	--	--	--	--	--	--	--	--	--	--	--	--	--	--	--	--	--	--	--	--	--	--	--	--	--	--	--	--	--	--	--	--	--	--	--	--	--	--	--	--	--	--	--	--	--	--	--	--	--	--	--	--	--	--	--	--	--	--	--	--	--	--	--	--	--	--	--	--	--	--	--	--	--	--	--	--	--	--	--	--	--	--	--	--	--	--	--	--	--	--	--	--	--	--	--	--	--	--	--	--	--	--	--	--	--	--	--	--	--	--	--	--	--	--	--	--	--	--	--	--	--	--	--	--	--	--	--	--	--	--	--	--	--	--	--	--	--	--	--	--	--	--	--	--	--	--	----

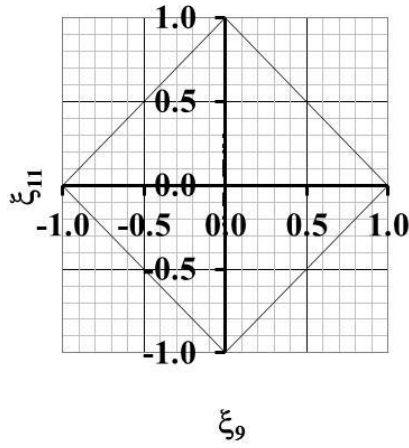
A3. Lamination parameter design spaces

The figures presented in this section represent third angle orthographic projections of the 3-dimensional design space for bending stiffness lamination parameters ($\xi_9, \xi_{10}, \xi_{11}$) and 2-dimensional extensional stiffness lamination parameters (ξ_1, ξ_2), when standard ply angles 0° , $\pm 45^\circ$ and 90° are adopted. Sequences for each ply number grouping are summarised according to ply number grouping and sub-sequence symmetry in Table A1.

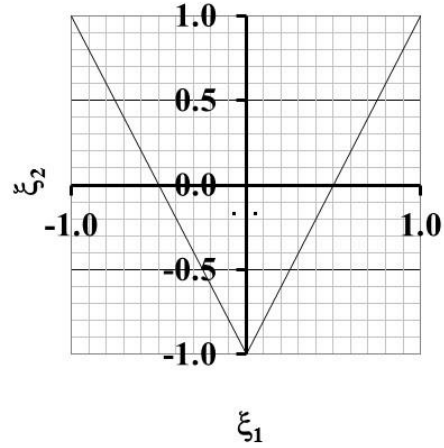
Table A1 – Design space occupied by the various forms of sub-sequence symmetries, including total number (Σ) of configurations, for each ply number grouping. Details for ply groupings for $n = 19$ ($\Sigma = 662,178$), 20 ($\Sigma = 606,046$) and 21 ($\Sigma = 6,172,510$) are not presented, but contain 22,760, 43,406 and 87,172 symmetric sequences, respectively.

n	4	5	6	7	8	9	10	11	12	13	14	15	16	17	18
<i>NC</i>	-	-	-	-	-	-	-	-	-	-	-	-	-	104	-
<i>NN</i>	-	-	-	-	-	6	-	76	58	696	480	6,570	5,512	60,356	50,802
<i>NS</i>	-	-	-	-	-	-	-	16	18	144	168	1,016	1,206	6,052	7,496
<i>SC</i>	-	-	-	-	-	-	-	8	8	12	-	84	114	200	-
<i>SN</i>	-	-	-	-	-	-	-	-	-	64	72	416	408	2,872	3,440
<i>SS</i>	1	2	4	8	15	30	56	112	206	420	780	1,580	2,970	5,956	11,330
Σ	1	2	4	8	15	36	56	212	290	1,336	1,500	9,666	10,210	75,540	73,068

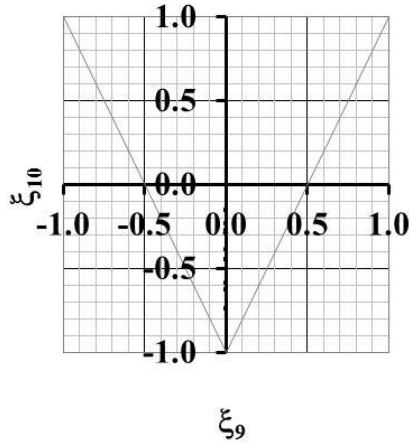
Figure A9 presents the lamination parameter design spaces for Non-symmetric angle-ply and Cross-symmetric cross-ply sub-sequences (*NC*), corresponding to: (a) plan, (b) front elevation and (c) side elevation for the 3 dimensional bending stiffness design space and (d) front elevation for the 2-dimensional extensional stiffness design space, which is common to all the design space representations that follow. For this form of sub-symmetry, solutions are possible only for ply number grouping $n = 17$ within the range $4 \leq n \leq 18$, which correspond to the listing of Table A8. The point cloud represents a total of 104 laminate configurations, of which only two unique points exist on the lamination parameter design space for extensional stiffness ($\xi_1 = \pm 0.06$ and $\xi_2 = -0.18$) and only 40 unique points are present for bending stiffness; each point representing either 4 or 8 alternative designs sharing the same stiffness properties. All configurations feature a cross ply at the laminate mid-plane, i.e. on the plane of symmetry, which renders $n_{\circ} \neq n_{\bullet}$, despite the cross symmetric nature of the designs, hence $\xi_1 \neq 0$ on Fig. A9 (d). However the bending stiffness parameters $\zeta_{\circ} = \zeta_{\bullet}$, hence $\xi_9 = 0$ on Fig. A9(a) and (b).



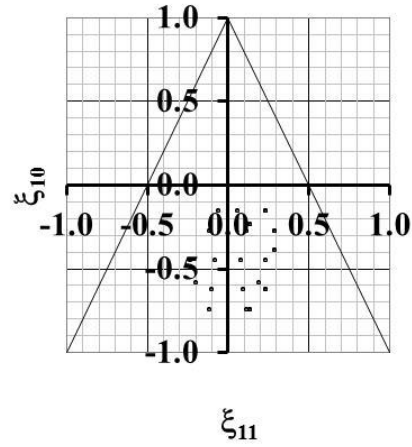
(a)



(d)



(b)



(c)

Figure A9 – Lamination parameter design spaces for the *Bending-Twisting* coupled laminates with $n = 17$, listed in abridged form in Table A8, with Non-symmetric angle-ply and Cross-symmetric cross-ply sub-sequences (*NC*), corresponding to: (a) plan, (b) front elevation and (c) side elevation for bending stiffness and; (d) extensional stiffness.

Figure A10 contains the solutions for Non-symmetric angle-ply and Symmetric cross-ply sub-sequences (NN) with $11 \leq n \leq 18$, listed in abridged form in Table A10. Of the 16,116 configurations, there are only 50 unique extensional stiffness properties leading to 10,325 unique bending stiffness properties. Horizontal strings of lamination parameter points are visible in Fig. A10(c), which arise from the symmetric nature of the cross-ply sub-sequences, which have a tendency to pin the orthogonal stiffness properties to a specific (ξ_9, ξ_{10}) coordinate; the variation in ξ_{11} about each (ξ_9, ξ_{10}) coordinate set is the result of as many as 130 different non-symmetry angle-ply sub-sequences. This is an important discovery, since it allows the isolated effects of *Bending-Twisting* coupling to be assessed for different regions within the feasible design space.

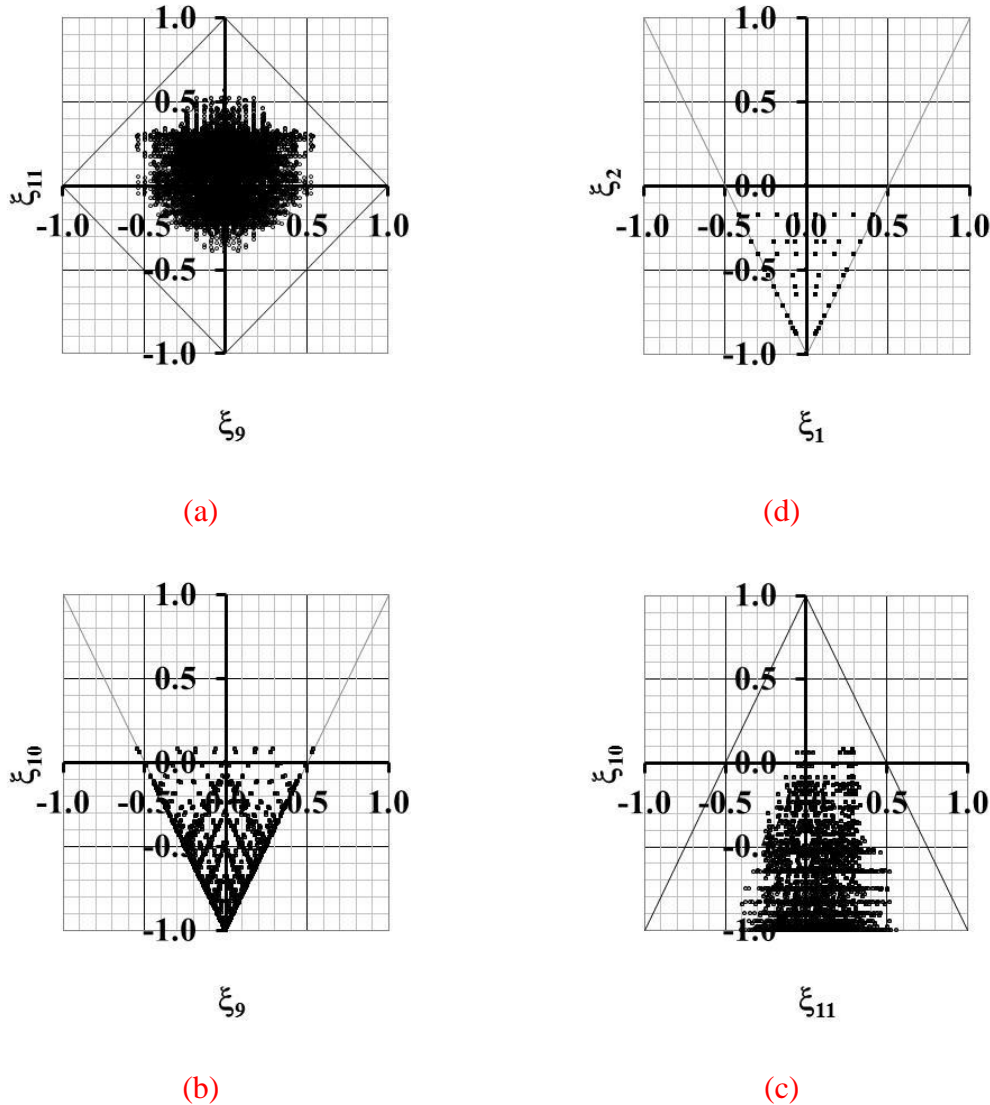


Figure A10 – Lamination parameter design spaces for the *Bending-Twisting* coupled laminates with $11 \leq n \leq 18$, listed in abridged form in Table A10, with Non-symmetric angle-ply and Symmetric cross-ply sub-sequences (NS), corresponding to: (a) plan, (b) front elevation and (c) side elevation for bending stiffness and; (d) extensional stiffness.

Figure A11 presents the lamination parameter design spaces for Symmetric angle-ply and Cross-symmetric cross-ply sub-sequences (SC), with $11 \leq n \leq 17$, listed in abridged form in Table A11. The design spaces possess similar patterns to those seen in Fig. A9 for NC designs. However, even ply number groupings result in $\xi_1 = 0$, with $\xi_2 = 0, 0.33$ and 0.5 . From a total of 426 configurations, only 15 unique co-ordinate points exist in the extensional lamination parameter design space, which give rise to the 206 unique points in bending.

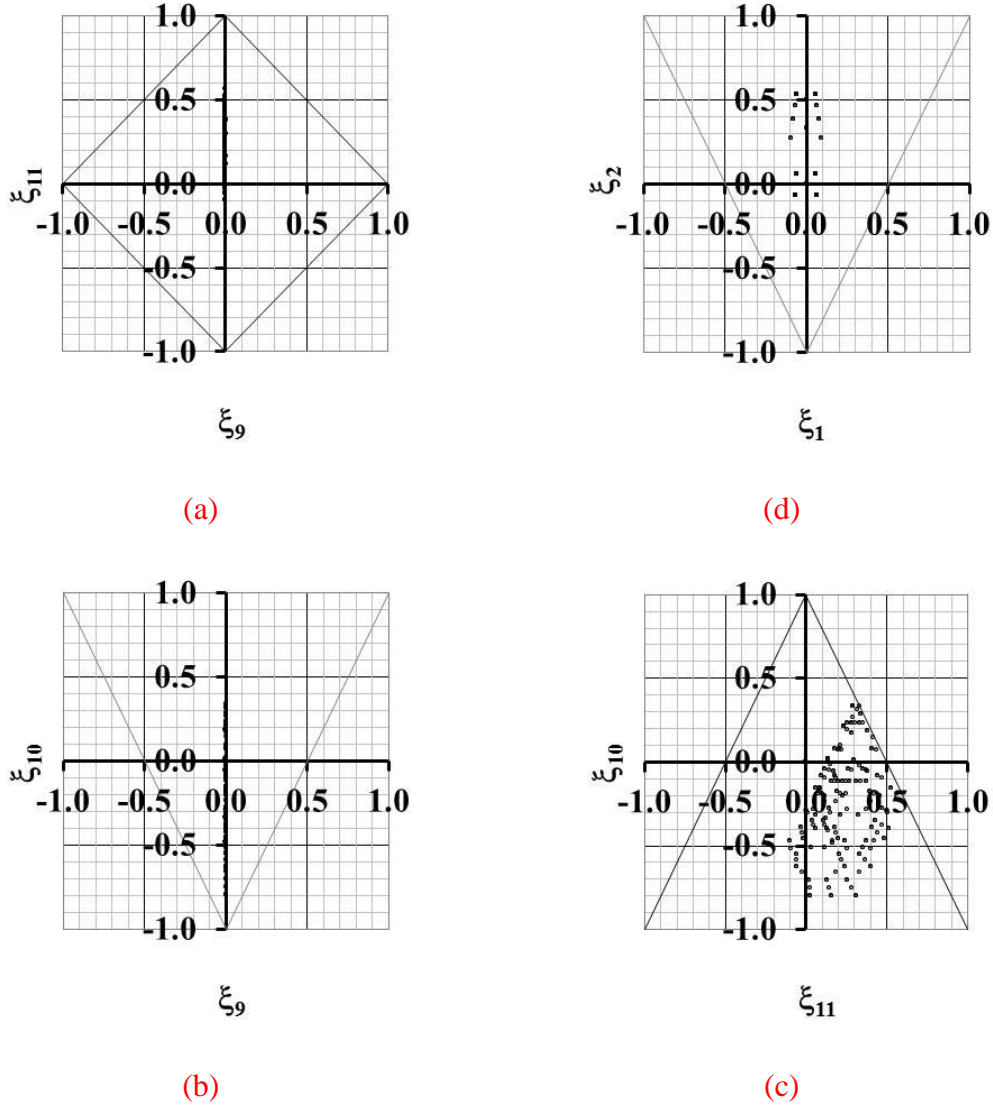


Figure A11 – Lamination parameter design spaces for the *Bending-Twisting* coupled laminates with $11 \leq n \leq 17$, listed in abridged form in Table A11, with Symmetric angle-ply and Cross-symmetric cross-ply sub-sequences (SC), corresponding to: (a) plan, (b) front elevation and (c) side elevation for bending stiffness and; (d) extensional stiffness.

Figure A12 presents the lamination parameter design spaces for Symmetric angle-ply and Non-symmetric cross-ply sub-sequences (SN), with $13 \leq n \leq 18$, listed in abridged form in Table A12. The 7,272 configurations are contained within the 33 unique lamination parameter points for extensional stiffness (ξ_1, ξ_2) and the 3,244 unique points within the 3-dimensional point cloud of lamination parameters for bending stiffness ($\xi_9, \xi_{10}, \xi_{11}$).

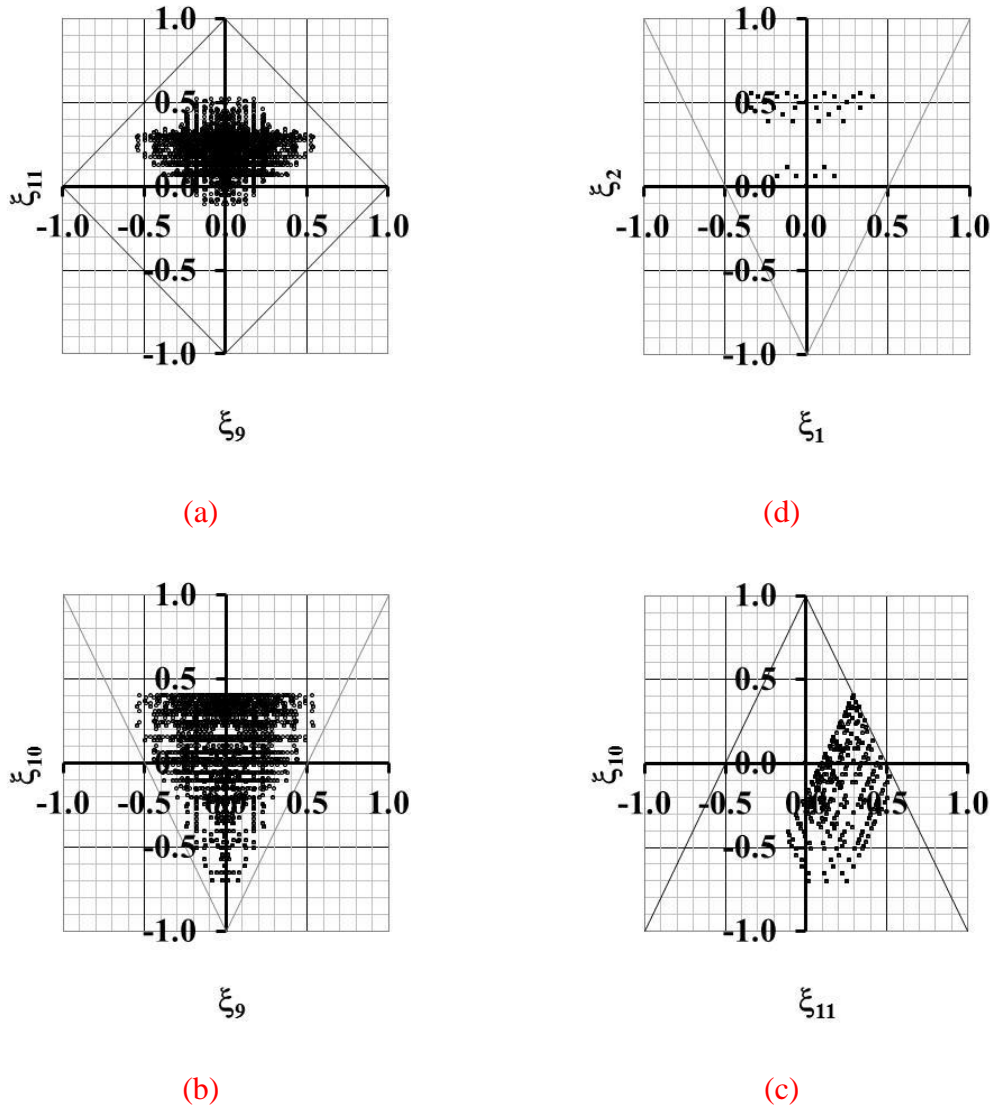


Figure A12 – Lamination parameter design spaces for the *Bending-Twisting* coupled laminates with $13 \leq n \leq 18$, listed in abridged form in Table A12, with Symmetric angle-ply and Non-symmetric cross-ply sub-sequences (SN), corresponding to: (a) plan, (b) front elevation and (c) side elevation for bending stiffness and; (d) extensional stiffness.

A4. Pseudo Quasi-Homogeneous Laminate Configurations

This section provides the laminates stacking sequence listings for practical fuselage thickness, i.e. $12 \leq n \leq 16$ plies. These configurations make up the lamination parameter design space of Fig. 4 of the main article, corresponding to standard laminates with $\pm 45^\circ$, 0° and 90° in place of the symbols \pm , \bigcirc and \bullet , respectively, hence $\xi_{12} = 0$. They are listed in order of increasing ply number grouping and then in descending order of lamination parameters $\xi_1 = \xi_9$, $\xi_2 = \xi_{10}$ and ξ_{11} , respectively; sequences approaching $\xi_9 = 0.00$, $\xi_{10} = -1.00$ and $\xi_{11} = 0.00$, possess the highest compression buckling factor, $k_{x,\infty}$.

Table A2 – Stacking sequences for Pseudo Quasi-Homogeneous ($\mathbf{A}_S\mathbf{B}_0\mathbf{D}_F$) laminates, illustrated on Fig.4, with $12 \leq n \leq 16$ plies, corresponding to: (a) *NN* configurations with Non-symmetric angle-ply and cross-ply sub-sequences; (b) *NS* configurations with Non-symmetric angle-ply and Symmetric cross-ply sub-sequences and;(c) *SS* configurations with Symmetric angle-ply and cross-ply sub-sequences.

(a)									
Ref.	Sequence							n	$\xi_1 = \xi_9$ $\xi_2 = \xi_{10}$ ξ_{11}
<i>NN</i> 3	+	\bigcirc	-	+	\bigcirc	\bigcirc	-	13	0.38 -0.23 0.33
<i>NN</i> 4	+	-	\bigcirc	\bigcirc	\bigcirc	+	-	13	0.38 -0.23 0.20
<i>NN</i> 5	+	\bigcirc	\bigcirc	-	-	+	-	13	0.38 -0.23 0.20
<i>NN</i> 6	+	\bigcirc	-	-	\bigcirc	\bigcirc	+	13	0.38 -0.23 0.07
<i>NN</i> 7	+	\bigcirc	\bigcirc	-	-	-	+	13	0.38 -0.23 0.07
<i>NN</i> 8	+	-	\bigcirc	\bigcirc	\bigcirc	-	-	13	0.38 -0.23 -0.07
<i>NN</i> 9	+	\bigcirc	+	-	-	+	-	13	0.23 -0.54 0.48
<i>NN</i> 10	+	+	\bigcirc	-	-	\bigcirc	+	13	0.23 -0.54 0.48
<i>NN</i> 11	+	\bigcirc	-	+	+	-	-	13	0.23 -0.54 0.44
<i>NN</i> 12	+	+	\bigcirc	-	-	\bigcirc	+	13	0.23 -0.54 0.44
<i>NN</i> 13	+	-	\bigcirc	+	-	\bigcirc	+	13	0.23 -0.54 0.22
<i>NN</i> 14	+	\bigcirc	-	+	-	-	+	13	0.23 -0.54 0.22
<i>NN</i> 15	+	\bigcirc	+	-	-	-	-	13	0.23 -0.54 0.22
<i>NN</i> 16	+	-	\bigcirc	+	-	\bigcirc	+	13	0.23 -0.54 0.17
<i>NN</i> 17	+	\bigcirc	-	-	+	+	-	13	0.23 -0.54 0.17
<i>NN</i> 18	+	-	\bigcirc	-	+	\bigcirc	+	13	0.23 -0.54 0.11
<i>NN</i> 19	+	\bigcirc	-	-	+	-	+	13	0.23 -0.54 0.11
<i>NN</i> 20	+	\bigcirc	-	-	+	-	+	13	0.23 -0.54 0.04
<i>NN</i> 21	+	-	\bigcirc	+	-	\bigcirc	-	13	0.23 -0.54 0.04
<i>NN</i> 22	+	\bigcirc	-	-	-	+	-	13	0.23 -0.54 -0.04
<i>NN</i> 23	+	-	\bigcirc	-	+	\bigcirc	-	13	0.23 -0.54 -0.04
<i>NN</i> 24	+	-	\bigcirc	-	-	\bigcirc	-	13	0.23 -0.54 -0.22

<i>NN 25</i>	+	+	●	-	-	●	-	+	-	-	+	●	+	13	-0.23	-0.54	0.48
<i>NN 26</i>	+	●	+	-	-	+	-	●	-	-	●	+	+	13	-0.23	-0.54	0.48
<i>NN 27</i>	+	+	●	-	-	●	-	-	+	+	-	●	+	13	-0.23	-0.54	0.44
<i>NN 28</i>	+	●	-	+	+	-	-	●	-	-	●	+	+	13	-0.23	-0.54	0.44
<i>NN 29</i>	+	●	-	+	-	-	+	●	-	+	●	-	+	13	-0.23	-0.54	0.22
<i>NN 30</i>	+	●	+	-	-	-	-	●	+	+	●	+	-	13	-0.23	-0.54	0.22
<i>NN 31</i>	+	-	●	+	-	●	+	-	-	+	-	●	+	13	-0.23	-0.54	0.22
<i>NN 32</i>	+	●	-	-	+	+	-	●	-	+	●	-	+	13	-0.23	-0.54	0.17
<i>NN 33</i>	+	-	●	+	-	●	-	+	+	-	-	●	+	13	-0.23	-0.54	0.17
<i>NN 34</i>	+	●	-	-	+	-	+	●	+	-	●	-	+	13	-0.23	-0.54	0.11
<i>NN 35</i>	+	-	●	-	+	●	+	-	+	-	-	●	+	13	-0.23	-0.54	0.11
<i>NN 36</i>	+	-	●	+	-	●	-	-	+	+	+	●	-	13	-0.23	-0.54	0.04
<i>NN 37</i>	+	●	-	-	+	-	+	●	-	+	●	+	-	13	-0.23	-0.54	0.04
<i>NN 38</i>	+	-	●	-	+	●	-	+	-	+	+	●	-	13	-0.23	-0.54	-0.04
<i>NN 39</i>	+	●	-	-	-	+	+	●	+	-	●	+	-	13	-0.23	-0.54	-0.04
<i>NN 40</i>	+	-	●	-	-	●	+	+	+	+	-	●	-	13	-0.23	-0.54	-0.22
<i>NN 41</i>	+	●	-	+	●	●	-	-	●	-	+	+	●	13	-0.38	-0.23	0.33
<i>NN 42</i>	+	●	●	-	-	+	-	+	●	●	●	-	+	13	-0.38	-0.23	0.20
<i>NN 43</i>	+	-	●	●	●	+	-	+	-	-	●	●	+	13	-0.38	-0.23	0.20
<i>NN 44</i>	+	●	●	-	-	-	+	+	●	●	●	+	-	13	-0.38	-0.23	0.07
<i>NN 45</i>	+	●	-	-	●	●	+	+	●	-	-	+	●	13	-0.38	-0.23	0.07
<i>NN 46</i>	+	-	●	●	●	-	-	+	+	+	●	●	-	13	-0.38	-0.23	-0.07
<i>NN 47</i>	+	○	○	○	-	○	○	+	-	-	○	○	○	15	0.60	0.20	0.30
<i>NN 48</i>	+	○	○	○	○	-	+	+	○	○	-	○	○	15	0.60	0.20	0.30
<i>NN 49</i>	+	○	○	○	-	○	○	○	+	○	○	-	○	15	0.60	0.20	0.21
<i>NN 50</i>	+	○	○	○	-	-	○	○	○	○	+	+	-	15	0.60	0.20	0.13
<i>NN 51</i>	+	○	+	+	-	-	-	-	○	+	○	-	+	15	0.20	-0.60	0.51
<i>NN 52</i>	+	+	-	○	+	○	-	-	-	-	+	+	○	15	0.20	-0.60	0.51
<i>NN 53</i>	+	-	+	○	+	○	-	-	-	+	-	+	○	15	0.20	-0.60	0.38
<i>NN 54</i>	+	○	+	-	+	-	-	-	○	+	○	+	-	15	0.20	-0.60	0.38
<i>NN 55</i>	+	○	+	-	-	+	-	+	○	-	○	-	+	15	0.20	-0.60	0.37
<i>NN 56</i>	+	+	-	○	-	○	+	-	+	-	-	+	○	15	0.20	-0.60	0.37
<i>NN 57</i>	+	○	-	+	+	-	-	+	○	-	○	-	+	15	0.20	-0.60	0.34
<i>NN 58</i>	+	○	+	-	-	-	+	-	○	-	○	-	+	15	0.20	-0.60	0.34
<i>NN 59</i>	+	+	-	○	-	○	-	+	+	-	-	+	○	15	0.20	-0.60	0.34
<i>NN 60</i>	+	+	-	○	-	○	+	-	-	-	+	+	-	15	0.20	-0.60	0.34

<i>NN 61</i>	+ ○ - + - + -	+	- ○ - ○ - + +	15	0.20	-0.60	0.30
<i>NN 62</i>	+ + - ○ - ○ -	+	- + - + - ○ +	15	0.20	-0.60	0.30
<i>NN 63</i>	+ - + ○ - ○ +	-	+ - - - + ○ +	15	0.20	-0.60	0.27
<i>NN 64</i>	+ ○ + - - - +	-	+ ○ - ○ + - +	15	0.20	-0.60	0.27
<i>NN 65</i>	+ ○ - - + + +	-	- ○ - ○ - + +	15	0.20	-0.60	0.26
<i>NN 66</i>	+ + - ○ - ○ -	-	+ + + - - ○ +	15	0.20	-0.60	0.26
<i>NN 67</i>	+ ○ + - - + -	-	- ○ + ○ + + -	15	0.20	-0.60	0.26
<i>NN 68</i>	+ - + ○ - ○ +	-	- + - + - ○ +	15	0.20	-0.60	0.23
<i>NN 69</i>	+ ○ - + - + -	-	+ ○ - ○ + - +	15	0.20	-0.60	0.23
<i>NN 70</i>	+ ○ - + + - -	-	- ○ + ○ + + -	15	0.20	-0.60	0.23
<i>NN 71</i>	+ - + ○ - ○ -	+	+ - - + - ○ +	15	0.20	-0.60	0.20
<i>NN 72</i>	+ ○ - + - - +	+	- ○ - ○ + - +	15	0.20	-0.60	0.20
<i>NN 73</i>	+ - + ○ - ○ -	+	- + + - - ○ +	15	0.20	-0.60	0.17
<i>NN 74</i>	+ ○ - - + + -	+	- ○ - ○ + - +	15	0.20	-0.60	0.17
<i>NN 75</i>	+ ○ + - - - -	+	+ ○ - ○ + + -	15	0.20	-0.60	0.17
<i>NN 76</i>	+ + - ○ - ○ -	-	+ - + + + ○ -	15	0.20	-0.60	0.17
<i>NN 77</i>	+ ○ - + - - +	-	+ ○ - ○ + + -	15	0.20	-0.60	0.11
<i>NN 78</i>	+ - - ○ + ○ +	+	- - - + - ○ +	15	0.20	-0.60	0.09
<i>NN 79</i>	+ ○ - + - - -	+	+ ○ + ○ - - +	15	0.20	-0.60	0.09
<i>NN 80</i>	+ ○ - - + + -	-	+ ○ - ○ + + -	15	0.20	-0.60	0.09
<i>NN 81</i>	+ - + ○ - ○ -	+	- - + + + ○ -	15	0.20	-0.60	0.09
<i>NN 82</i>	+ ○ - - + - +	+	- ○ - ○ + + -	15	0.20	-0.60	0.06
<i>NN 83</i>	+ - + ○ - ○ -	-	+ + - + + ○ -	15	0.20	-0.60	0.06
<i>NN 84</i>	+ - - ○ + ○ +	-	+ - + - - ○ +	15	0.20	-0.60	0.04
<i>NN 85</i>	+ ○ - - + - +	-	+ ○ + ○ - - +	15	0.20	-0.60	0.04
<i>NN 86</i>	+ ○ - - + - -	+	+ ○ + ○ - + -	15	0.20	-0.60	-0.06
<i>NN 87</i>	+ - - ○ + ○ +	-	- + - + + ○ -	15	0.20	-0.60	-0.06
<i>NN 88</i>	+ ○ - - - + +	-	+ ○ + ○ - + -	15	0.20	-0.60	-0.09
<i>NN 89</i>	+ - - ○ + ○ -	+	+ - - + + ○ -	15	0.20	-0.60	-0.09
<i>NN 90</i>	+ - - ○ + ○ -	+	- + + - + ○ -	15	0.20	-0.60	-0.11
<i>NN 91</i>	+ - - ○ + ○ -	-	+ + + + - ○ -	15	0.20	-0.60	-0.17
<i>NN 92</i>	+ ○ - - - + -	+	+ ○ + ○ + - -	15	0.20	-0.60	-0.17
<i>NN 93</i>	+ - - ○ - ○ +	+	+ + - - + ○ -	15	0.20	-0.60	-0.23
<i>NN 94</i>	+ - - ○ - ○ +	+	+ - + + - ○ -	15	0.20	-0.60	-0.26
<i>NN 95</i>	+ ● ○ ○ ○ - -	+	○ ● - ● ○ ○ +	15	0.20	0.20	0.30
<i>NN 96</i>	+ ○ ○ ● - ● ○	+	- - ○ ○ ○ ● +	15	0.20	0.20	0.30
<i>NN 97</i>	+ ● ● ○ - ○ ●	+	- - ● ● ● ○ +	15	-0.20	0.20	0.30
<i>NN 98</i>	+ ○ ● ● ● - -	+	● ○ - ○ ● ● +	15	-0.20	0.20	0.30

NN 99	+	●	+	+	-	-	-	-	-	●	+	●	-	+	+	15	-0.20	-0.60	0.51	
NN 100	+	+	-	●	+	●	-	-	-	-	+	+	●	+		15	-0.20	-0.60	0.51	
NN 101	+	●	+	-	+	-	-	-	-	●	+	●	+	-	+	15	-0.20	-0.60	0.38	
NN 102	+	-	+	●	+	●	-	-	-	+	-	+	●	+		15	-0.20	-0.60	0.38	
NN 103	+	●	+	-	-	+	-	-	+	●	-	●	-	+	+	15	-0.20	-0.60	0.37	
NN 104	+	+	-	●	-	●	+	-	-	+	-	-	+	●	+	15	-0.20	-0.60	0.37	
NN 105	+	●	-	+	+	-	-	-	+	●	-	●	-	+	+	15	-0.20	-0.60	0.34	
NN 106	+	●	+	-	-	-	+	+	-	●	-	●	-	+	+	15	-0.20	-0.60	0.34	
NN 107	+	+	-	●	-	●	-	+	+	-	-	-	+	●	+	15	-0.20	-0.60	0.34	
NN 108	+	+	-	●	-	●	+	-	-	-	+	+	-	●	+	15	-0.20	-0.60	0.34	
NN 109	+	●	-	+	-	+	-	+	-	●	-	●	-	+	+	15	-0.20	-0.60	0.30	
NN 110	+	+	-	●	-	●	-	+	-	+	-	+	-	●	+	15	-0.20	-0.60	0.30	
NN 111	+	●	+	-	-	-	+	-	+	●	-	●	+	-	+	15	-0.20	-0.60	0.27	
NN 112	+	-	+	●	-	●	+	-	+	-	-	-	+	●	+	15	-0.20	-0.60	0.27	
NN 113	+	●	-	-	+	+	+	-	-	●	-	●	-	+	+	15	-0.20	-0.60	0.26	
NN 114	+	●	+	-	-	+	-	-	-	●	+	●	+	+	-	15	-0.20	-0.60	0.26	
NN 115	+	+	-	●	-	●	-	-	+	+	+	+	-	-	●	+	15	-0.20	-0.60	0.26
NN 116	+	●	-	+	-	+	-	-	+	●	-	●	+	-	+	15	-0.20	-0.60	0.23	
NN 117	+	●	-	+	+	-	-	-	-	●	+	●	+	+	-	15	-0.20	-0.60	0.23	
NN 118	+	-	+	●	-	●	+	-	-	+	-	+	-	●	+	15	-0.20	-0.60	0.23	
NN 119	+	●	-	+	-	-	+	+	-	●	-	●	+	-	+	15	-0.20	-0.60	0.20	
NN 120	+	-	+	●	-	●	-	+	+	-	-	+	-	●	+	15	-0.20	-0.60	0.20	
NN 121	+	●	-	-	+	+	-	+	-	●	-	●	+	-	+	15	-0.20	-0.60	0.17	
NN 122	+	+	-	●	-	●	-	-	+	-	+	+	+	●	-	15	-0.20	-0.60	0.17	
NN 123	+	●	+	-	-	-	-	+	+	●	-	●	+	+	-	15	-0.20	-0.60	0.17	
NN 124	+	-	+	●	-	●	-	+	-	+	+	-	-	●	+	15	-0.20	-0.60	0.17	
NN 125	+	●	-	+	-	-	+	-	+	●	-	●	+	+	-	15	-0.20	-0.60	0.11	
NN 126	+	●	-	+	-	-	-	+	+	●	+	●	-	-	+	15	-0.20	-0.60	0.09	
NN 127	+	-	+	●	-	●	-	+	-	-	+	+	+	●	-	15	-0.20	-0.60	0.09	
NN 128	+	●	-	-	+	+	-	-	+	●	-	●	+	+	-	15	-0.20	-0.60	0.09	
NN 129	+	-	-	●	+	●	+	+	-	-	-	+	-	●	+	15	-0.20	-0.60	0.09	
NN 130	+	-	+	●	-	●	-	-	+	+	-	+	+	●	-	15	-0.20	-0.60	0.06	
NN 131	+	●	-	-	+	-	+	+	-	●	-	●	+	+	-	15	-0.20	-0.60	0.06	
NN 132	+	●	-	-	+	-	+	-	+	●	+	●	-	-	+	15	-0.20	-0.60	0.04	
NN 133	+	-	-	●	+	●	+	-	+	-	+	-	-	●	+	15	-0.20	-0.60	0.04	
NN 134	+	-	-	●	+	●	+	-	-	+	-	+	+	●	-	15	-0.20	-0.60	-0.06	
NN 135	+	●	-	-	+	-	-	+	+	●	+	●	-	+	-	15	-0.20	-0.60	-0.06	
NN 136	+	-	-	●	+	●	-	+	+	-	-	+	+	●	-	15	-0.20	-0.60	-0.09	
NN 137	+	●	-	-	-	+	+	-	+	●	+	●	-	+	-	15	-0.20	-0.60	-0.09	
NN 138	+	-	-	●	+	●	-	+	-	+	+	-	+	●	-	15	-0.20	-0.60	-0.11	

<i>NN 139</i>	+ - - ● + ● - -	-	+ + + + - ● -	15	-0.20	-0.60	-0.17
<i>NN 140</i>	+ ● - - - + -	+	+ ● + ● + - -	15	-0.20	-0.60	-0.17
<i>NN 141</i>	+ - - ● - ● +	+	+ + - - + ● -	15	-0.20	-0.60	-0.23
<i>NN 142</i>	+ - - ● - ● +	+	+ - + + - ● -	15	-0.20	-0.60	-0.26
<i>NN 143</i>	+ ● ● ● - ● ●	+	- - ● ● ● ● +	15	-0.60	0.20	0.30
<i>NN 144</i>	+ ● ● ● ● - -	+	● ● - ● ● ● +	15	-0.60	0.20	0.30
<i>NN 145</i>	+ ● ● ● - ● -	●	+ ● ● - ● + ●	15	-0.60	0.20	0.21
<i>NN 146</i>	+ ● ● ● - - ●	●	● ● + + - ● ●	15	-0.60	0.20	0.13
<i>NN 147</i>	+ ○ ○ + - ○ ○ -	○	- - ○ ○ + + ○	16	0.50	0.00	0.38
<i>NN 148</i>	+ ○ ○ + ○ - - ○	-	○ ○ - ○ + + ○	16	0.50	0.00	0.38
<i>NN 149</i>	+ ○ - ○ ○ + ○ ○	-	- + - ○ ○ ○ +	16	0.50	0.00	0.23
<i>NN 150</i>	+ ○ ○ ○ - + - -	○	○ ○ + ○ ○ - ○ +	16	0.50	0.00	0.23
<i>NN 151</i>	+ ○ - ○ ○ + ○ -	○	- ○ + - ○ + ○	16	0.50	0.00	0.19
<i>NN 152</i>	+ ○ ○ - ○ + - ○	-	○ ○ + ○ - + ○	16	0.50	0.00	0.19
<i>NN 153</i>	+ ○ - ○ ○ - ○ +	○	+ ○ - - ○ + ○	16	0.50	0.00	0.09
<i>NN 154</i>	+ ○ ○ - - ○ ○ +	○	+ - ○ ○ - + ○	16	0.50	0.00	0.09
<i>NN 155</i>	+ - ○ ○ ○ ○ + -	○	○ ○ - + - + ○ ○	16	0.50	0.00	0.09
<i>NN 156</i>	+ ○ ○ - ○ - + ○	-	○ ○ + ○ + - ○	16	0.50	0.00	0.09
<i>NN 157</i>	+ - ○ ○ ○ ○ - +	○	○ ○ + - - + ○ ○	16	0.50	0.00	0.05
<i>NN 158</i>	+ ○ ○ - - ○ ○ +	○	- + ○ ○ + - ○	16	0.50	0.00	0.05
<i>NN 159</i>	+ ○ ○ ○ - - - +	○	○ ○ + ○ ○ + ○ -	16	0.50	0.00	0.05
<i>NN 160</i>	+ - ○ ○ ○ ○ - +	○	○ ○ - + + - ○ ○	16	0.50	0.00	0.02
<i>NN 161</i>	+ ○ - ○ ○ - ○ +	○	- ○ + + ○ - ○	16	0.50	0.00	0.02
<i>NN 162</i>	+ ○ - ○ ○ - ○ ○	-	+ + + ○ ○ ○ -	16	0.50	0.00	-0.05
<i>NN 163</i>	+ ● ● + - ● ● -	●	- - ● ● + + ●	16	-0.50	0.00	0.38
<i>NN 164</i>	+ ● ● + ● - - ●	-	● ● - ● + + ●	16	-0.50	0.00	0.38
<i>NN 165</i>	+ ● - ● ● + ● ●	-	- + - ● ● ● +	16	-0.50	0.00	0.23
<i>NN 166</i>	+ ● ● ● - + - -	●	● ● + ● ● - ● +	16	-0.50	0.00	0.23
<i>NN 167</i>	+ ● - ● ● + ● -	●	- ● + - ● + ●	16	-0.50	0.00	0.19
<i>NN 168</i>	+ ● ● - ● + - ●	-	● ● + ● - + ●	16	-0.50	0.00	0.19
<i>NN 169</i>	+ - ● ● ● ● + -	●	● ● - + - + ● ●	16	-0.50	0.00	0.09
<i>NN 170</i>	+ ● - ● ● - ● +	●	+ ● - - ● + ●	16	-0.50	0.00	0.09
<i>NN 171</i>	+ ● ● - - ● ● +	●	+ - ● ● - + ●	16	-0.50	0.00	0.09
<i>NN 172</i>	+ ● ● - ● - + ●	-	● ● + ● + - ●	16	-0.50	0.00	0.09
<i>NN 173</i>	+ ● ● ● - - - +	●	● ● + ● ● + ● -	16	-0.50	0.00	0.05
<i>NN 174</i>	+ - ● ● ● ● - +	●	● ● + - - + ● ●	16	-0.50	0.00	0.05
<i>NN 175</i>	+ ● ● - - ● ● +	●	- + ● ● + - ●	16	-0.50	0.00	0.05

<i>NN 176</i>	+ - ● ● ● ● - + ● ● - + + - ● ●	16	-0.50	0.00	0.02
<i>NN 177</i>	+ ● - ● ● - ● + ● - ● + + ● - ●	16	-0.50	0.00	0.02
<i>NN 178</i>	+ ● - ● ● - ● ● - + + + ● ● ● -	16	-0.50	0.00	-0.05

(b)

Ref.	Sequence	n	$\xi_1 = \xi_9$	$\xi_2 = \xi_{10}$	ξ_{11}
<i>NS 1</i>	+ - + + - - - + - - + +	12	0.00	-1.00	0.42
<i>NS 2</i>	+ + - - + - - - + + - +	12	0.00	-1.00	0.42
<i>NS 3</i>	+ - + - + - + - - - + +	12	0.00	-1.00	0.33
<i>NS 4</i>	+ + - - - + - + - + - +	12	0.00	-1.00	0.33
<i>NS 5</i>	+ - - + + + - - - - + +	12	0.00	-1.00	0.25
<i>NS 6</i>	+ + - - - - + + + - - +	12	0.00	-1.00	0.25
<i>NS 7</i>	+ + - - - + - - + + + -	12	0.00	-1.00	0.25
<i>NS 8</i>	+ + - - - - + + - + + -	12	0.00	-1.00	0.19
<i>NS 9</i>	+ - + - + - - - + + + -	12	0.00	-1.00	0.17
<i>NS 10</i>	+ - - + + - + - - + - +	12	0.00	-1.00	0.14
<i>NS 11</i>	+ - + - - + - + + - - +	12	0.00	-1.00	0.14
<i>NS 12</i>	+ - + - - + - + - + + -	12	0.00	-1.00	0.08
<i>NS 13</i>	+ - - + + - - + - + + -	12	0.00	-1.00	0.03
<i>NS 14</i>	+ - - + - + + - - + + -	12	0.00	-1.00	-0.03
<i>NS 15</i>	+ - - + - + - + + - + -	12	0.00	-1.00	-0.08
<i>NS 16</i>	+ - - - + + + - + - + -	12	0.00	-1.00	-0.17
<i>NS 17</i>	+ - - + - - + + + + - -	12	0.00	-1.00	-0.19
<i>NS 18</i>	+ - - - + + - + + + - -	12	0.00	-1.00	-0.25
<i>NS 19</i>	+ - ○ + ○ + - - + - - ○ - ○ + +	16	0.25	-0.50	0.32
<i>NS 20</i>	+ ○ - + + - - ○ ○ - + - - + ○ +	16	0.25	-0.50	0.32
<i>NS 21</i>	+ ○ + - - + - ○ ○ - - + + - ○ +	16	0.25	-0.50	0.32
<i>NS 22</i>	+ + ○ - ○ - - + - - + ○ + ○ - +	16	0.25	-0.50	0.32
<i>NS 23</i>	+ - ○ + ○ - + + - - - ○ - ○ + +	16	0.25	-0.50	0.29
<i>NS 24</i>	+ + ○ - ○ - - - + + - ○ + ○ - +	16	0.25	-0.50	0.29
<i>NS 25</i>	+ ○ - + - + - ○ ○ + - - - + ○ +	16	0.25	-0.50	0.26
<i>NS 26</i>	+ ○ + - - - + ○ ○ - + - + - ○ +	16	0.25	-0.50	0.26
<i>NS 27</i>	+ + ○ - ○ - - - + - + ○ + ○ + -	16	0.25	-0.50	0.23
<i>NS 28</i>	+ ○ - - + + - ○ ○ + - - + - ○ +	16	0.25	-0.50	0.15
<i>NS 29</i>	+ ○ - + - - + ○ ○ - + + - - ○ +	16	0.25	-0.50	0.15
<i>NS 30</i>	+ - ○ + ○ - + - - - + ○ + ○ + -	16	0.25	-0.50	0.12
<i>NS 31</i>	+ - ○ - ○ + + + - - - ○ + ○ - +	16	0.25	-0.50	0.08
<i>NS 32</i>	+ - ○ + ○ - - - + + + ○ - ○ - +	16	0.25	-0.50	0.08

<i>NS 33</i>	+ - ○ + ○ - - + - + - ○ + ○ + -	16	0.25	-0.50	0.08
<i>NS 34</i>	+ ○ - + - - + ○ ○ - - + + + ○ -	16	0.25	-0.50	0.08
<i>NS 35</i>	+ ○ - - + + - ○ ○ - - + + + ○ -	16	0.25	-0.50	0.06
<i>NS 36</i>	+ ○ + - - - ○ ○ + + + - + ○ -	16	0.25	-0.50	0.06
<i>NS 37</i>	+ ○ - - - + + ○ ○ + - - + + ○ -	16	0.25	-0.50	-0.06
<i>NS 38</i>	+ ○ - + - - - ○ ○ + + + + - ○ -	16	0.25	-0.50	-0.06
<i>NS 39</i>	+ - ○ - ○ + - + - + + ○ - ○ + -	16	0.25	-0.50	-0.08
<i>NS 40</i>	+ ○ - - - + + ○ ○ - + + - + ○ -	16	0.25	-0.50	-0.08
<i>NS 41</i>	+ - ○ - ○ - + + + - + ○ - ○ + -	16	0.25	-0.50	-0.12
<i>NS 42</i>	+ - ○ - ○ - + - + + + ○ + ○ - -	16	0.25	-0.50	-0.23
<i>NS 43</i>	+ + - + + - - - - - + - - + + +	16	0.00	-1.00	0.56
<i>NS 44</i>	+ + + - - + - - - - - + + - + +	16	0.00	-1.00	0.56
<i>NS 45</i>	+ + - + - + - - - - + - - - + + +	16	0.00	-1.00	0.50
<i>NS 46</i>	+ + + - - - + - - - + - + - + +	16	0.00	-1.00	0.50
<i>NS 47</i>	+ - + + + - - - - - + - - - + + +	16	0.00	-1.00	0.47
<i>NS 48</i>	+ + - + - - + - + - - - - + + +	16	0.00	-1.00	0.47
<i>NS 49</i>	+ + + - - - - + - - + - - + - + +	16	0.00	-1.00	0.47
<i>NS 50</i>	+ + + - - - + - - - - + + + - +	16	0.00	-1.00	0.47
<i>NS 51</i>	+ + - - + + - - + - - - - + + +	16	0.00	-1.00	0.45
<i>NS 52</i>	+ + + - - - - + - - + + - - + +	16	0.00	-1.00	0.45
<i>NS 53</i>	+ - + + + - - - - - + - + - + +	16	0.00	-1.00	0.43
<i>NS 54</i>	+ + - + - + - - - - - + + + - +	16	0.00	-1.00	0.43
<i>NS 55</i>	+ - + + - + - - + - - - - + + +	16	0.00	-1.00	0.42
<i>NS 56</i>	+ + - - + - + + - - - - - + + +	16	0.00	-1.00	0.42
<i>NS 57</i>	+ + + - - - - - + + - + - - + +	16	0.00	-1.00	0.42
<i>NS 58</i>	+ + + - - - - + - - + - + + - +	16	0.00	-1.00	0.42
<i>NS 59</i>	+ - + + - - + + - - - - - + + +	16	0.00	-1.00	0.40
<i>NS 60</i>	+ + - - + + - - - - + - - + - + +	16	0.00	-1.00	0.40
<i>NS 61</i>	+ + - + - - + - - - + + - - + +	16	0.00	-1.00	0.40
<i>NS 62</i>	+ + + - - - - - + + - - + + - +	16	0.00	-1.00	0.40
<i>NS 63</i>	+ - + - + + - + - - - - - + + +	16	0.00	-1.00	0.38
<i>NS 64</i>	+ - + + - + - - - - + - - + - + +	16	0.00	-1.00	0.38
<i>NS 65</i>	+ + - + - - + - - - + - + + - +	16	0.00	-1.00	0.38
<i>NS 66</i>	+ + + - - - - - + - + + - + - +	16	0.00	-1.00	0.38
<i>NS 67</i>	+ + + - - - - + - - - + + + + -	16	0.00	-1.00	0.38
<i>NS 68</i>	+ + - - + - + - + - - - - + - + +	16	0.00	-1.00	0.36
<i>NS 69</i>	+ + - + - - - + - - + - - - + +	16	0.00	-1.00	0.36
<i>NS 70</i>	+ - + + - + - - - - + + - - + +	16	0.00	-1.00	0.35
<i>NS 71</i>	+ + - - + + - - - - + - + + - +	16	0.00	-1.00	0.35

<i>NS 72</i>	+ - + + - - + -	+ - - - + - + +	16	0.00	-1.00	0.34
<i>NS 73</i>	+ + - + - - - +	- + - - + + - +	16	0.00	-1.00	0.34
<i>NS 74</i>	+ + + - - - - -	+ - + - + + + -	16	0.00	-1.00	0.34
<i>NS 75</i>	+ - - + + + + -	- - - - - + + +	16	0.00	-1.00	0.33
<i>NS 76</i>	+ + - - - + + +	- - - - + - + +	16	0.00	-1.00	0.33
<i>NS 77</i>	+ + - + - - - -	+ + + - - - + +	16	0.00	-1.00	0.33
<i>NS 78</i>	+ + + - - - - -	- + + + + - - +	16	0.00	-1.00	0.33
<i>NS 79</i>	+ + - + - - + -	- - - + + + + -	16	0.00	-1.00	0.33
<i>NS 80</i>	+ - + - + + - -	+ - - - + - + +	16	0.00	-1.00	0.32
<i>NS 81</i>	+ + - + - - - +	- - + + - + - +	16	0.00	-1.00	0.32
<i>NS 82</i>	+ - + + - - + -	- + - + - - + +	16	0.00	-1.00	0.30
<i>NS 83</i>	+ + - - + - + -	- + - - + + - +	16	0.00	-1.00	0.30
<i>NS 84</i>	+ + - - + + - -	- - - + + + + -	16	0.00	-1.00	0.30
<i>NS 85</i>	+ + + - - - - -	- + + + - + + -	16	0.00	-1.00	0.30
<i>NS 86</i>	+ - + - + - + +	- - - - + - + +	16	0.00	-1.00	0.29
<i>NS 87</i>	+ + - + - - - -	+ + - + - + - +	16	0.00	-1.00	0.29
<i>NS 88</i>	+ - + - + + - -	- + - + - - + +	16	0.00	-1.00	0.28
<i>NS 89</i>	+ - + + - - - +	+ - - + - - + +	16	0.00	-1.00	0.28
<i>NS 90</i>	+ + - - - + + -	+ - - + - - + +	16	0.00	-1.00	0.28
<i>NS 91</i>	+ + - - + - - +	- + + - - - + +	16	0.00	-1.00	0.28
<i>NS 92</i>	+ + - - + - - +	+ - - - + + - +	16	0.00	-1.00	0.28
<i>NS 93</i>	+ + - - + - + -	- - + + - + - +	16	0.00	-1.00	0.28
<i>NS 94</i>	+ - + + - + - -	- - - + + + + -	16	0.00	-1.00	0.28
<i>NS 95</i>	+ + - + - - - +	- - + - + + + -	16	0.00	-1.00	0.28
<i>NS 96</i>	+ - - + + + - +	- - - - + - + +	16	0.00	-1.00	0.26
<i>NS 97</i>	+ - + + - - - +	- + + - - - + +	16	0.00	-1.00	0.26
<i>NS 98</i>	+ - + - + + - -	- + - - + + - +	16	0.00	-1.00	0.26
<i>NS 99</i>	+ + - - - + + -	+ - - - + + - +	16	0.00	-1.00	0.26
<i>NS 100</i>	+ - + + - - + -	- - + + - + - +	16	0.00	-1.00	0.26
<i>NS 101</i>	+ + - + - - - -	+ - + + + - - +	16	0.00	-1.00	0.26
<i>NS 102</i>	+ + - + - - - -	+ + - - + + + -	16	0.00	-1.00	0.26
<i>NS 103</i>	+ - + - + - + -	+ - - + - - + +	16	0.00	-1.00	0.25
<i>NS 104</i>	+ + - - + - - +	- + - + - + - +	16	0.00	-1.00	0.25
<i>NS 105</i>	+ + - - + - + -	- - + - + + + -	16	0.00	-1.00	0.25
<i>NS 106</i>	+ + - + - - - -	+ - + + - + + -	16	0.00	-1.00	0.23
<i>NS 107</i>	+ - + - + - + -	- + + - - - + +	16	0.00	-1.00	0.22
<i>NS 108</i>	+ - + - + - + -	+ - - - + + - +	16	0.00	-1.00	0.22
<i>NS 109</i>	+ - + + - - - +	- + - + - + - +	16	0.00	-1.00	0.22
<i>NS 110</i>	+ + - - - + + -	- + - + - + - +	16	0.00	-1.00	0.22
<i>NS 111</i>	+ - + + - - + -	- - + - + + + -	16	0.00	-1.00	0.22
<i>NS 112</i>	+ - - + + + - -	+ - - + - - + +	16	0.00	-1.00	0.21

<i>NS 113</i>	+ - + - - + + +	- - - + - - + +	16	0.00	-1.00	0.21
<i>NS 114</i>	+ + - - + - - -	+ + + - - + - +	16	0.00	-1.00	0.21
<i>NS 115</i>	+ + - - + - - +	- - + + + - - +	16	0.00	-1.00	0.21
<i>NS 116</i>	+ + - - + - - +	- + - - + + + -	16	0.00	-1.00	0.21
<i>NS 117</i>	+ - + - + - - +	+ - + - - - + +	16	0.00	-1.00	0.20
<i>NS 118</i>	+ + - - - + - +	+ - - + - + - +	16	0.00	-1.00	0.20
<i>NS 119</i>	+ - + - + + - -	- - + - + + + -	16	0.00	-1.00	0.20
<i>NS 120</i>	+ - - + + - + +	- - - + - - + +	16	0.00	-1.00	0.19
<i>NS 121</i>	+ - - + + + - -	- + + - - - + +	16	0.00	-1.00	0.19
<i>NS 122</i>	+ - - + + + - -	+ - - - + + - +	16	0.00	-1.00	0.19
<i>NS 123</i>	+ - + - - + + +	- - - - + + - +	16	0.00	-1.00	0.19
<i>NS 124</i>	+ - + + - - - -	+ + + - - + - +	16	0.00	-1.00	0.19
<i>NS 125</i>	+ - + + - - - +	- - + + + - - +	16	0.00	-1.00	0.19
<i>NS 126</i>	+ + - - - + + -	- - + + + - - +	16	0.00	-1.00	0.19
<i>NS 127</i>	+ + - - + - - -	+ + - + + - - +	16	0.00	-1.00	0.19
<i>NS 128</i>	+ - + + - - - +	- + - - + + + -	16	0.00	-1.00	0.19
<i>NS 129</i>	+ + - - - + + -	- + - - + + + -	16	0.00	-1.00	0.19
<i>NS 130</i>	+ + - - + - - +	- - + + - + + -	16	0.00	-1.00	0.19
<i>NS 131</i>	+ + - + - - - -	- + + + + - + -	16	0.00	-1.00	0.19
<i>NS 132</i>	+ - + - - + + -	+ - + - - - + +	16	0.00	-1.00	0.18
<i>NS 133</i>	+ + - - - + - +	- + + - - + - +	16	0.00	-1.00	0.18
<i>NS 134</i>	+ - - + + - + +	- - - - + + - +	16	0.00	-1.00	0.16
<i>NS 135</i>	+ - + + - - - -	+ + - + + - - +	16	0.00	-1.00	0.16
<i>NS 136</i>	+ + - - - + - +	+ - - - + + + -	16	0.00	-1.00	0.16
<i>NS 137</i>	+ - + + - - - +	- - + + - + + -	16	0.00	-1.00	0.16
<i>NS 138</i>	+ + - - - + + -	- - + + - + + -	16	0.00	-1.00	0.16
<i>NS 139</i>	+ + - - + - - -	+ + - + - + + -	16	0.00	-1.00	0.16
<i>NS 140</i>	+ - - + + - + -	+ - + - - - + +	16	0.00	-1.00	0.15
<i>NS 141</i>	+ - - + + + - -	- + - + - + - +	16	0.00	-1.00	0.15
<i>NS 142</i>	+ - + - + - + -	- - + + + - - +	16	0.00	-1.00	0.15
<i>NS 143</i>	+ + - - - + - +	- + - + + - - +	16	0.00	-1.00	0.15
<i>NS 144</i>	+ - + - + - + -	- + - - + + + -	16	0.00	-1.00	0.15
<i>NS 145</i>	+ - + - - + - +	+ + - - - - + +	16	0.00	-1.00	0.14
<i>NS 146</i>	+ - + - - + + -	+ - - + - + - +	16	0.00	-1.00	0.14
<i>NS 147</i>	+ - + - + - - +	- + + - - + - +	16	0.00	-1.00	0.14
<i>NS 148</i>	+ + - - - - + +	+ - + - - + - +	16	0.00	-1.00	0.14
<i>NS 149</i>	+ - + + - - - -	+ + - + - + + -	16	0.00	-1.00	0.14
<i>NS 150</i>	+ - + - + - - +	+ - - - + + + -	16	0.00	-1.00	0.13
<i>NS 151</i>	+ - + - + - + -	- - + + - + + -	16	0.00	-1.00	0.13
<i>NS 152</i>	+ + - - - + - +	- + - + - + + -	16	0.00	-1.00	0.13
<i>NS 153</i>	+ + - - + - - -	+ - + + + - + -	16	0.00	-1.00	0.13

<i>NS 154</i>	+ - - + - + + +	- - + - - - + +	16	0.00	-1.00	0.12
<i>NS 155</i>	+ - - + + - - +	+ + - - - - + +	16	0.00	-1.00	0.12
<i>NS 156</i>	+ - - + + - + -	+ - - + - + - +	16	0.00	-1.00	0.12
<i>NS 157</i>	+ - + - + - - +	- + - + + - - +	16	0.00	-1.00	0.12
<i>NS 158</i>	+ + - - - - + +	+ - - + + - - +	16	0.00	-1.00	0.12
<i>NS 159</i>	+ + - - - + - -	+ + + - + - - +	16	0.00	-1.00	0.12
<i>NS 160</i>	+ - - + + + - -	- + - - + + + -	16	0.00	-1.00	0.12
<i>NS 161</i>	+ - + - - + + -	+ - - - + + + -	16	0.00	-1.00	0.11
<i>NS 162</i>	+ - + + - - - -	+ - + + + - + -	16	0.00	-1.00	0.11
<i>NS 163</i>	+ - - + - + + -	+ + - - - - + +	16	0.00	-1.00	0.09
<i>NS 164</i>	+ - - + + - + -	- + + - - + - +	16	0.00	-1.00	0.09
<i>NS 165</i>	+ - + - - + + -	- + - + + - - +	16	0.00	-1.00	0.09
<i>NS 166</i>	+ + - - - - + +	- + + - + - - +	16	0.00	-1.00	0.09
<i>NS 167</i>	+ - - + + + - -	- - + + - + + -	16	0.00	-1.00	0.09
<i>NS 168</i>	+ - + - + - - +	- + - + - + + -	16	0.00	-1.00	0.09
<i>NS 169</i>	+ + - - - - + +	+ - - + - + + -	16	0.00	-1.00	0.09
<i>NS 170</i>	+ + - - - + - -	+ + + - - + + -	16	0.00	-1.00	0.09
<i>NS 171</i>	+ + - - - + - +	- - + + + - + -	16	0.00	-1.00	0.09
<i>NS 172</i>	+ - - + - + + +	- - - + - + - +	16	0.00	-1.00	0.08
<i>NS 173</i>	+ - + - + - - -	+ + + - + - - +	16	0.00	-1.00	0.08
<i>NS 174</i>	+ - - + + - + -	+ - - - + + + -	16	0.00	-1.00	0.08
<i>NS 175</i>	+ - - + + - - +	+ - + - - + - +	16	0.00	-1.00	0.07
<i>NS 176</i>	+ - + - - + - +	+ - - + + - - +	16	0.00	-1.00	0.07
<i>NS 177</i>	+ - + - - + + -	- + - + - + + -	16	0.00	-1.00	0.07
<i>NS 178</i>	+ + - - - - + +	- + + - - + + -	16	0.00	-1.00	0.07
<i>NS 179</i>	+ + - - - + - -	+ + - + + - + -	16	0.00	-1.00	0.07
<i>NS 180</i>	+ + - - + - - -	- + + + + + - -	16	0.00	-1.00	0.07
<i>NS 181</i>	+ - + - + - - -	+ + + - - + + -	16	0.00	-1.00	0.06
<i>NS 182</i>	+ - + - + - - +	- - + + + - + -	16	0.00	-1.00	0.06
<i>NS 183</i>	+ - - - + + + +	- + - - - - + +	16	0.00	-1.00	0.05
<i>NS 184</i>	+ - - + - + + -	+ - + - - + - +	16	0.00	-1.00	0.05
<i>NS 185</i>	+ - + - - + - +	- + + - + - - +	16	0.00	-1.00	0.05
<i>NS 186</i>	+ + - - - - + -	+ + + + - - - +	16	0.00	-1.00	0.05
<i>NS 187</i>	+ - - + - + + +	- - - - + + + -	16	0.00	-1.00	0.05
<i>NS 188</i>	+ - - + + - + -	- + - + - + + -	16	0.00	-1.00	0.05
<i>NS 189</i>	+ - + - - + - +	+ - - + - + + -	16	0.00	-1.00	0.05
<i>NS 190</i>	+ + - - - - + +	- + - + + - + -	16	0.00	-1.00	0.05
<i>NS 191</i>	+ - + + - - - -	- + + + + + - -	16	0.00	-1.00	0.05
<i>NS 192</i>	+ - + - - + + -	- - + + + - + -	16	0.00	-1.00	0.04
<i>NS 193</i>	+ - + - + - - -	+ + - + + - + -	16	0.00	-1.00	0.04
<i>NS 194</i>	+ - - + - + + -	+ - - + + - - +	16	0.00	-1.00	0.02

<i>NS 195</i>	+ - - + + - - + - + + - + - - +	16	0.00	-1.00	0.02
<i>NS 196</i>	+ - - + + - - + + - - + - + + -	16	0.00	-1.00	0.02
<i>NS 197</i>	+ - + - - + - + - + + - - + + -	16	0.00	-1.00	0.02
<i>NS 198</i>	+ + - - - + - - + - + + + + - -	16	0.00	-1.00	0.02
<i>NS 199</i>	+ - - + - + - + + + - - - + - +	16	0.00	-1.00	0.01
<i>NS 200</i>	+ - + - - - + + + - + - + - - +	16	0.00	-1.00	0.01
<i>NS 201</i>	+ - - + + - + - - - + + + - + -	16	0.00	-1.00	0.01
<i>NS 202</i>	+ + - - - - + - + + + - + - + -	16	0.00	-1.00	0.01
<i>NS 203</i>	+ - + - - - + + + - + - - - + + -	16	0.00	-1.00	-0.01
<i>NS 204</i>	+ - + - + - - - + - + + + + - -	16	0.00	-1.00	-0.01
<i>NS 205</i>	+ - - - + + + - + + - - - + - +	16	0.00	-1.00	-0.02
<i>NS 206</i>	+ - - - + + + + - - - + + - - +	16	0.00	-1.00	-0.02
<i>NS 207</i>	+ - - + + - - - + + + + - - - +	16	0.00	-1.00	-0.02
<i>NS 208</i>	+ - + - - - + + - + + + - - - +	16	0.00	-1.00	-0.02
<i>NS 209</i>	+ - - + - + + - - + + - - + + -	16	0.00	-1.00	-0.02
<i>NS 210</i>	+ - - + + - - + - + - + + - + -	16	0.00	-1.00	-0.02
<i>NS 211</i>	+ + - - - - + - + + - + + + - -	16	0.00	-1.00	-0.02
<i>NS 212</i>	+ - + - - - + + + - - + + - + -	16	0.00	-1.00	-0.04
<i>NS 213</i>	+ - + - - + - - + + + - + - + -	16	0.00	-1.00	-0.04
<i>NS 214</i>	+ - - - + + + + - - - + - + + -	16	0.00	-1.00	-0.05
<i>NS 215</i>	+ - - + - + - + + - + - + - - + + -	16	0.00	-1.00	-0.05
<i>NS 216</i>	+ - - + - + + - - + - + + - + -	16	0.00	-1.00	-0.05
<i>NS 217</i>	+ + - - - - + + + + + - - + -	16	0.00	-1.00	-0.05
<i>NS 218</i>	+ - + - - + - + - - + + + + - -	16	0.00	-1.00	-0.05
<i>NS 219</i>	+ - - - + + + - + - + - + - - +	16	0.00	-1.00	-0.06
<i>NS 220</i>	+ - - + - + - + - + + + + - - - +	16	0.00	-1.00	-0.06
<i>NS 221</i>	+ - - + + - - - + + + - + - + -	16	0.00	-1.00	-0.06
<i>NS 222</i>	+ - + - - - + + - + + - + - + -	16	0.00	-1.00	-0.06
<i>NS 223</i>	+ - - + - + - + + - + - - + + - + -	16	0.00	-1.00	-0.07
<i>NS 224</i>	+ - - + + - - + - - + + + + - -	16	0.00	-1.00	-0.07
<i>NS 225</i>	+ - + - - + - - + + - + + + - -	16	0.00	-1.00	-0.07
<i>NS 226</i>	+ + - - - - + + + + - + + - -	16	0.00	-1.00	-0.07
<i>NS 227</i>	+ - - - + + + - + - + - - + + -	16	0.00	-1.00	-0.08
<i>NS 228</i>	+ - - - + + - + + + - - + - - +	16	0.00	-1.00	-0.09
<i>NS 229</i>	+ - - + - - + + + - + + - - - +	16	0.00	-1.00	-0.09
<i>NS 230</i>	+ - - + - - + + + + - - - + + -	16	0.00	-1.00	-0.09
<i>NS 231</i>	+ - - + - + - + - + + + - + -	16	0.00	-1.00	-0.09
<i>NS 232</i>	+ - - + - + + - - - + + + + - -	16	0.00	-1.00	-0.09
<i>NS 233</i>	+ - - + + - - - + + - + + + - -	16	0.00	-1.00	-0.09
<i>NS 234</i>	+ - + - - - + + - + - + + + - -	16	0.00	-1.00	-0.09

NS 235	+ - - - + + + - + - - + + - + -	16	0.00	-1.00	-0.11
NS 236	+ - + - - - + - + + + + - - + -	16	0.00	-1.00	-0.11
NS 237	+ - - - + + - + + + - - - + + -	16	0.00	-1.00	-0.12
NS 238	+ - - - + + + - - + + - + - + -	16	0.00	-1.00	-0.13
NS 239	+ - - + - - + + + - + - + - + -	16	0.00	-1.00	-0.13
NS 240	+ - - + - + - + - + - + + + - -	16	0.00	-1.00	-0.13
NS 241	+ - + - - - + - + + + - + + - -	16	0.00	-1.00	-0.13
NS 242	+ - - + - + - - + + + + - - + -	16	0.00	-1.00	-0.14
NS 243	+ - - - + + - + + - + - + - + -	16	0.00	-1.00	-0.15
NS 244	+ - - + - - + + - + + + - - + -	16	0.00	-1.00	-0.16
NS 245	+ - - - + + + - - + - + + + - -	16	0.00	-1.00	-0.16
NS 246	+ - - + - - + + + - - + + + - -	16	0.00	-1.00	-0.16
NS 247	+ - - + - + - - + + + - + + - -	16	0.00	-1.00	-0.16
NS 248	+ - - - + + - + - + + + - - + -	16	0.00	-1.00	-0.19
NS 249	+ - - - + + - + + - - + + + - -	16	0.00	-1.00	-0.19
NS 250	+ - - + - - + + - + + - + + - -	16	0.00	-1.00	-0.19
NS 251	+ - + - - - - + + + + - + - -	16	0.00	-1.00	-0.19
NS 252	+ - - - + - + + + + - - + - + -	16	0.00	-1.00	-0.20
NS 253	+ - - - + + - + - + + - + + - -	16	0.00	-1.00	-0.21
NS 254	+ - - - + - + + + - + + - - + -	16	0.00	-1.00	-0.22
NS 255	+ - - + - - + - + + + + - + - -	16	0.00	-1.00	-0.23
NS 256	+ - - - + - + + + - + - + + - -	16	0.00	-1.00	-0.25
NS 257	+ - - - + + - - + + + + - + - -	16	0.00	-1.00	-0.26
NS 258	+ - - - - + + + + + - + - - + -	16	0.00	-1.00	-0.28
NS 259	+ - - - + - + + - + + + - + - -	16	0.00	-1.00	-0.28
NS 260	+ - - - - + + + + + - - + + - -	16	0.00	-1.00	-0.30
NS 261	+ - - + - - - + + + + + - - -	16	0.00	-1.00	-0.30
NS 262	+ - - - - + + + + - + + - + - -	16	0.00	-1.00	-0.33
NS 263	+ - - - + - + - + + + + - - -	16	0.00	-1.00	-0.34
NS 264	+ - - - - + + + - + + + + - - -	16	0.00	-1.00	-0.38
NS 265	+ + ● - ● - - + - - + ● + ● - +	16	-0.25	-0.50	0.32
NS 266	+ ● - + + - - ● ● - + - - + ● +	16	-0.25	-0.50	0.32
NS 267	+ ● + - - + - ● ● - - + + - ● +	16	-0.25	-0.50	0.32
NS 268	+ - ● + ● + - - + - - ● - ● + +	16	-0.25	-0.50	0.32
NS 269	+ + ● - ● - - - + + - ● + ● - +	16	-0.25	-0.50	0.29
NS 270	+ - ● + ● - + + - - - ● - ● + +	16	-0.25	-0.50	0.29
NS 271	+ ● - + - + - ● ● + - - - + ● +	16	-0.25	-0.50	0.26
NS 272	+ ● + - - - + ● ● - + - + - ● +	16	-0.25	-0.50	0.26
NS 273	+ + ● - ● - - - + - + ● + ● + -	16	-0.25	-0.50	0.23
NS 274	+ ● - - + + - ● ● + - - + - ● +	16	-0.25	-0.50	0.15

<i>NS 275</i>	+ ● - + - - + ● ● - + + - - ● +	16	-0.25	-0.50	0.15
<i>NS 276</i>	+ - ● + ● - + - - - + ● + ● + -	16	-0.25	-0.50	0.12
<i>NS 277</i>	+ - ● - ● + + + - - - ● + ● - +	16	-0.25	-0.50	0.08
<i>NS 278</i>	+ - ● + ● - - - + + + ● - ● - +	16	-0.25	-0.50	0.08
<i>NS 279</i>	+ ● - + - - + ● ● - - + + + ● -	16	-0.25	-0.50	0.08
<i>NS 280</i>	+ - ● + ● - - + - + - ● + ● + -	16	-0.25	-0.50	0.08
<i>NS 281</i>	+ ● - - + + - ● ● - - + + + ● -	16	-0.25	-0.50	0.06
<i>NS 282</i>	+ ● + - - - - ● ● + + + - + ● -	16	-0.25	-0.50	0.06
<i>NS 283</i>	+ ● - - - + + ● ● + - - + + ● -	16	-0.25	-0.50	-0.06
<i>NS 284</i>	+ ● - + - - - ● ● + + + + - ● -	16	-0.25	-0.50	-0.06
<i>NS 285</i>	+ ● - - - + + ● ● - + + - + ● -	16	-0.25	-0.50	-0.08
<i>NS 286</i>	+ - ● - ● + - + - + + ● - ● + -	16	-0.25	-0.50	-0.08
<i>NS 287</i>	+ - ● - ● - + + + - + ● - ● + -	16	-0.25	-0.50	-0.12
<i>NS 288</i>	+ - ● - ● - + - + + + ● + ● - -	16	-0.25	-0.50	-0.23

(c)

Ref.	Sequence	n	$\xi_1 = \xi_9$	$\xi_2 = \xi_{10}$	ξ_{11}
<i>SS 5</i>	+ + + - - - - - + + +	12	0.00	-1.00	0.75
<i>SS 6</i>	+ + - + - - - - + - + +	12	0.00	-1.00	0.58
<i>SS 7</i>	+ + - - + - - + - - + +	12	0.00	-1.00	0.47
<i>SS 8</i>	+ + - - - + + - - - + +	12	0.00	-1.00	0.42
<i>SS 9</i>	+ - + + - - - - + + - +	12	0.00	-1.00	0.36
<i>SS 10</i>	+ - + - + - - + - + - +	12	0.00	-1.00	0.25
<i>SS 11</i>	+ - + - - + + - - + - +	12	0.00	-1.00	0.19
<i>SS 12</i>	+ - - + + - - + + - - +	12	0.00	-1.00	0.08
<i>SS 13</i>	+ - - + - + + - + - - +	12	0.00	-1.00	0.03
<i>SS 14</i>	+ - - - + + + + - - - +	12	0.00	-1.00	-0.08
<i>SS 15</i>	+ ○ + ○ ○ - - - - ○ ○ + ○ +	14	0.43	-0.14	0.52
<i>SS 16</i>	+ ○ - ○ ○ + - - + ○ ○ - ○ +	14	0.43	-0.14	0.21
<i>SS 17</i>	+ ○ - ○ ○ - + + - ○ ○ - ○ +	14	0.43	-0.14	0.17
<i>SS 18</i>	+ ● + ● ● - - - - ● ● + ● +	14	-0.43	-0.14	0.52
<i>SS 19</i>	+ ● - ● ● + - - + ● ● - ● +	14	-0.43	-0.14	0.21
<i>SS 20</i>	+ ● - ● ● - + + - ● ● - ● +	14	-0.43	-0.14	0.17
<i>SS 21</i>	+ ○ ○ + ○ - - ○ ○ - - ○ + ○ ○ +	16	0.50	0.00	0.40
<i>SS 22</i>	+ ○ ○ - ○ + - ○ ○ - + ○ - ○ ○ +	16	0.50	0.00	0.23
<i>SS 23</i>	+ ○ ○ - ○ - + ○ ○ + - ○ - ○ ○ +	16	0.50	0.00	0.19

SS 24	++○+○--- -- --○+○++	16	0.25	-0.50	0.64
SS 25	+○++-- --○ ○-- --++○+	16	0.25	-0.50	0.50
SS 26	++○-○+- -- --+○-○++	16	0.25	-0.50	0.48
SS 27	++○-○-+- --+-○-○++	16	0.25	-0.50	0.43
SS 28	++○-○--+++- --○-○++	16	0.25	-0.50	0.41
SS 29	+○+-+-- --○ ○-- ++-+○+	16	0.25	-0.50	0.41
SS 30	+○+- --+-○ ○-+- --+○+	16	0.25	-0.50	0.34
SS 31	+○+- --+-○ ○+- --+○+	16	0.25	-0.50	0.29
SS 32	+○-++-- --○ ○-- ++-○+	16	0.25	-0.50	0.29
SS 33	+○-+-+-- --○ ○-+-+--○+	16	0.25	-0.50	0.22
SS 34	+--○+○+- -- --+○+○-+	16	0.25	-0.50	0.22
SS 35	+○-+- --+○ ○+- --+--○+	16	0.25	-0.50	0.18
SS 36	+--○+○-+- --+-○+○-+	16	0.25	-0.50	0.18
SS 37	+--○+○--+++- --+○+○-+	16	0.25	-0.50	0.15
SS 38	+○--+++-○ ○-++--○+	16	0.25	-0.50	0.13
SS 39	+○--+++-○ ○+-+--○+	16	0.25	-0.50	0.08
SS 40	+○---++○ ○++-- --○+	16	0.25	-0.50	0.01
SS 41	+--○-○++- --++○-○-+	16	0.25	-0.50	0.01
SS 42	+--○-○+-+ +-+○-○-+	16	0.25	-0.50	-0.01
SS 43	+--○-○-++ ++-○-○-+	16	0.25	-0.50	-0.06
SS 44	++++-- -- -- --++++	16	0.00	-1.00	0.75
SS 45	+++-+-- -- -- +-++	16	0.00	-1.00	0.66
SS 46	+++-+-- -- +--++	16	0.00	-1.00	0.59
SS 47	+++-+-- --+- --++	16	0.00	-1.00	0.54
SS 48	++-++-- -- -- ++-++	16	0.00	-1.00	0.54
SS 49	+++-+-- --+ +- --++	16	0.00	-1.00	0.52
SS 50	++-+-+-- --+ -+-++	16	0.00	-1.00	0.47
SS 51	++-+-+-- --+- -+-++	16	0.00	-1.00	0.42
SS 52	++-+-+-- --+ -+-++	16	0.00	-1.00	0.40
SS 53	+--++++-- -- --+++	16	0.00	-1.00	0.40
SS 54	++-+++- --+ +- --++	16	0.00	-1.00	0.38
SS 55	++-+++- --+ -+-++	16	0.00	-1.00	0.33
SS 56	+--+++++- --+ -++	16	0.00	-1.00	0.33
SS 57	++-+++- --+ -+-++	16	0.00	-1.00	0.30
SS 58	+--++++- --+ -++	16	0.00	-1.00	0.28
SS 59	++- --+++- --+ --++	16	0.00	-1.00	0.26
SS 60	+--++++- --+ -++	16	0.00	-1.00	0.26
SS 61	++- --+++- --+ --++	16	0.00	-1.00	0.23
SS 62	+--++++- --+ -++	16	0.00	-1.00	0.23

SS 63	++-- --++ ++-- --++ ++	16	0.00	-1.00	0.19
SS 64	+ - + - + - + - - + - + - +	16	0.00	-1.00	0.19
SS 65	+ - + - + - - + + - - + - +	16	0.00	-1.00	0.16
SS 66	+ - + - - + + - - + + - +	16	0.00	-1.00	0.12
SS 67	+ - - + + + - - - - + + - +	16	0.00	-1.00	0.12
SS 68	+ - + - - + - + + - + - - +	16	0.00	-1.00	0.09
SS 69	+ - - + + - + - - + - + + -	16	0.00	-1.00	0.07
SS 70	+ - + - - - + + + + - - + - +	16	0.00	-1.00	0.05
SS 71	+ - - + + - - + + - - + + - - +	16	0.00	-1.00	0.05
SS 72	+ - - + - + - + + - + - + - - +	16	0.00	-1.00	-0.02
SS 73	+ - - + - - + + + + - - + - - +	16	0.00	-1.00	-0.07
SS 74	+ - - - + + + - - + + + - - - +	16	0.00	-1.00	-0.09
SS 75	+ - - - + + - + + - + + - - - +	16	0.00	-1.00	-0.12
SS 76	+ - - - + - + + + + - + - - - +	16	0.00	-1.00	-0.16
SS 77	+ - - - - + + + + + + - - - - +	16	0.00	-1.00	-0.23
SS 78	+ ○ ● + ● - - ○ ○ - - ● + ● ○ +	16	0.00	0.00	0.40
SS 79	+ ● ○ + ○ - - ● ● - - ○ + ○ ● +	16	0.00	0.00	0.40
SS 80	+ ○ ● - ● + - ○ ○ - + ● - ● ○ +	16	0.00	0.00	0.23
SS 81	+ ● ○ - ○ + - ● ● - + ○ - ○ ● +	16	0.00	0.00	0.23
SS 82	+ ○ ● - ● - + ○ ○ + - ● - ● ○ +	16	0.00	0.00	0.19
SS 83	+ ● ○ - ○ - + ● ● + - ○ - ○ ● +	16	0.00	0.00	0.19
SS 84	++ ● + ● - - - - - - ● + ● + +	16	-0.25	-0.50	0.64
SS 85	+ ● + + - - - ● ● - - - + + ● +	16	-0.25	-0.50	0.50
SS 86	++ ● - ● + - - - - + ● - ● + +	16	-0.25	-0.50	0.48
SS 87	++ ● - ● - + - - + - ● - ● + +	16	-0.25	-0.50	0.43
SS 88	+ ● + - + - - ● ● - - + - + ● +	16	-0.25	-0.50	0.41
SS 89	++ ● - ● - - + + - - ● - ● + +	16	-0.25	-0.50	0.41
SS 90	+ ● + - - + - ● ● - + - - + ● +	16	-0.25	-0.50	0.34
SS 91	+ ● + - - - + ● ● + - - - + ● +	16	-0.25	-0.50	0.29
SS 92	+ ● - + + - - ● ● - - + + - ● +	16	-0.25	-0.50	0.29
SS 93	+ - ● + ● + - - - - + ● + ● - +	16	-0.25	-0.50	0.22
SS 94	+ ● - + - + - ● ● - + - + - ● +	16	-0.25	-0.50	0.22
SS 95	+ - ● + ● - + - - + - ● + ● - +	16	-0.25	-0.50	0.18
SS 96	+ ● - + - - + ● ● + - - + - ● +	16	-0.25	-0.50	0.18
SS 97	+ - ● + ● - - + + - - ● + ● - +	16	-0.25	-0.50	0.15
SS 98	+ ● - - + + - ● ● - + + - - ● +	16	-0.25	-0.50	0.13
SS 99	+ ● - - + - + ● ● + - + - - ● +	16	-0.25	-0.50	0.08
SS 100	+ - ● - ● + + - - + + ● - ● - +	16	-0.25	-0.50	0.01

<i>SS 101</i>	+	●	-	-	-	+	+	●	●	+	+	-	-	-	●	+	16	-0.25	-0.50	0.01
<i>SS 102</i>	+	-	●	-	●	+	-	+	+	-	+	●	-	●	-	+	16	-0.25	-0.50	-0.01
<i>SS 103</i>	+	-	●	-	●	-	+	+	+	+	-	●	-	●	-	+	16	-0.25	-0.50	-0.06
<i>SS 104</i>	+	●	●	+	●	-	-	●	●	-	-	●	+	●	●	+	16	-0.50	0.00	0.40
<i>SS 105</i>	+	●	●	-	●	+	-	●	●	-	+	●	-	●	●	+	16	-0.50	0.00	0.23
<i>SS 106</i>	+	●	●	-	●	-	+	●	●	+	-	●	-	●	●	+	16	-0.50	0.00	0.19
